UNIVERSITEIT VAN PRETORIA
UNIVERSITY OF PRETORIA
YUNIBESITHI YA PRETORIA
Denkleiers • Leading Minds • Dikgopolo tša Dihlalefi

Assessing the *in vitro* efficacy of *in silico* designed compounds targeting the malarial Q_i site of cytochrome bc_1

by

Laura Damadeu Kouemo

A dissertation submitted in fulfilment for a requirement for the degree

Magister Scientiae

in

Pharmacology

in the

Faculty of Health Science at the

University of Pretoria

2018

SUPERVISOR: Prof AD Cromarty (Department of Pharmacology, UP)

CO-SUPERVISOR: Prof L Birkholtz (Department of Biochemistry, Genetics and Microbiology, UP)

Dr. A Stander (Department of Physiology, UP)

ACKNOWLEDGEMENTS

I would like to acknowledge and give thanks to the following people for their assistance and technical expertise in various aspects.

The almighty God for His constant provision, strength, guidance, and love. Damadeu meaning love God.

Thanks to the UP ISMC MRC, Department of Biochemistry, Department of physiology and the Department of Pharmacology, University of Pretoria for their facilities and funding.

Thanks to the NRF Master Innovative Scholarship for their funding.

To my supervisors Prof Duncan Cromarty, Prof Lyn-Marie Birkholtz and Dr. Andre Stander for the discipline, guidance, and knowledge during my master studies in their respective departments. I would have never been the great scientist I am today without your supervision. I would like to thank Dr. Dina Coetzee, Dr. Bianca Brider, Ms. Mariska Naude, Mrs. Mariette Van der Walt, Mrs, Janette Ridder, Ms Sindi Nondaba and others for their technical advice in malaria parasite culturing and assays. Ms Margo Nell for culturing HepG2 cells for hepatotoxicity testing.

To Mrs. Kim Sheva and Ms. Channel Pillay for their advice and guidance. I will not have made it up to this point without your assistance.

My parents, Kouemo Pierre and Christine for allowing me to further my studies, and for their compassion, kindness and patience towards the completion of this degree.

My sisters, Sylviane, Isoline, Gaelle, Djougwa Kouemo Patricia and Ngamo Kouemo Rolenne thank you all for the patience and your words of encouragement.

My guardian Dr. Gabila Nubong and his wife Barbara for their moral support, spiritual guidance, and strength. My lovely aunt Veronique thanks for your moral support and kindness. To my nephews Kouemo Livingstone, Elako Kingsley, Tchamadeu Jamel-Owen, Fankam Landry and my lovely niece Fankam Blessing thanks for their moral support. Olga Kolle and Oceane Tchuem thanks for your listening ears and moral support.

To my friends Bongikile, Zelie, Ruth, Esther, Sweetness, Percy, Lesedi, Walters, Desmond, Donald, Max, Murielle, Dikeledi, Vuyelwa, Shamiso, Ewura, Banda, Mariska, Shey, Keith, Alicia and others for their support, advice and kindness.

DECLARATION OF ORIGINALITY

University of Pretoria

Faculty of Health Science
Department of Pharmacology

Full name: **Laura Damadeu Kouemo** Student number: **15142622**

Title of work: Assessing the *in vitro* efficacy of *in silico* designed compounds targeting the malarial Q_i site of cytochrome bc_1

Declaration:

1. I understand what plagiarism entails and am aware of the University's policy in this regard.
2. I declare that this thesis is my own, original work. Where someone else's work was used (whether from a printed source, the internet or any other source due acknowledgement was given and reference was made according to departmental requirements.
3. I did not make use of another student's previous work and submit it as my own.
4. I did not allow and will not allow anyone to copy my work with the intention of presenting it as his or her own work.

Signature: _____ Date: 01/08/2018

CONFERENCE PROCEEDINGS

The results of this dissertation have been presented as a poster titled “Assessing the *in vitro* efficacy of *in silico* designed compounds targeting the malarial Q_i site of cytochrome bc1” (1, 2 and 3) and oral presentations titled “3-phenylpyridin-4(1H)-one derivatives targeting the cytochrome bc_1 Q_i site shows antiplasmodial activity” (4, 5 and 6) at the following International and national conferences:

1. 2nd South African Malaria Research Conference (MOMR) at the University of Pretoria’s Groenkloof Campus (31st July - 2nd August 2016)
2. Health Science Faculty day 2016 (23rd August - 24th August 2016)
3. All Africa Congress on Pharmacology and Pharmacy 2016 (5th October - 8th October 2016)
4. 3rd South African Malaria Research Conference (MOMR) (7th November- 9th November 2017)
5. Health Science Faculty Day (22nd August – 23rd August 2017)
6. The South Africa Annual Pharmacology Conference (SAPHARM) (2nd October - 3rd October 2017)

SUMMARY

Plasmodium falciparum is the causative agent of the most commonly fatal form of malaria in Africa with annual deaths of more than 300 000. The rapid development and spread of antimalarial drug resistance by the parasite have stimulated research into the development of new drug classes. Target-based drug discovery have been used as a prominent and efficient tool to identify lead drugs. Reports suggest that selectively inhibiting the parasite mitochondrial electron transport could be a potential treatment effective at multi-stages of the parasite life cycle. Inhibitors of cytochrome *bc$_1$ (*Cyt *bc$_1$)*, an essential inner mitochondrial membrane protein that drives ATP synthesis in the mitochondria are claimed to be lethal to apicomplexan species including *Plasmodium*. The emergence of resistance to atovaquone, a Cyt *bc$_1$* complex Q_o site inhibitor, casts doubt over the long-term efficacy of new drugs targeting these mitochondrial proteins. Many aspects of potential drugs must be investigated to assess the suitability of new emerging drugs targeting the mitochondrion.

In silico target-based drug design methods using Autodock vina were used to design compounds that would theoretically bind to and inhibit the Q_i site of Cyt *bc$_1$* of the *P. falciparum*. The potential candidate compounds were selected from compounds defined by Gamo et al., (2010) and tested using *in silico* docking experiments. Homology models were developed and modified to improve their drug-likeness according to the Lipinski rule, QED parameters and synthesised by Wuxi App Tec. This study assessed the antiproliferative activity of six candidate compounds on *P. falciparum* parasites *in vitro* following *in silico* compound docking and drug likeness assessment. Initial *in vitro* screening data was obtained for the test compounds at 1 and 5 µM over 96 h and full dose-response curves was performed for compounds showing >70% proliferation inhibition at 1 µM against the 3D7 strain. Four of the test compounds, EE1, EE3, EE5 and EE7 gave IC_{50} values of 89 nM, 664 nM, 64 nM and 249 nM, respectively. The candidate compounds had a marginal >2-fold selectivity towards malaria parasites but did not show cross resistance, with resistance indices of >120.

In conclusion, *in silico* docking using software programs could be utilised as a potential tool for rapidly identifying feasible target-based antimalarial compounds while avoiding high throughput screening. Other possible target sites on the mitochondrion can be used to design new chemotypes. All the designed compounds showed significant antimalarial activity against the asexual stages tested on 3D7 strain with a significant resistance index. However, these compounds showed minimal activity on the gametocyte stage. Finally, compound EE5 showed to be the most potent, more selective and with higher resistance index, hence this can be further optimised for preclinical studies.

TABLE OF CONTENT

ACKNOWLEDGEMENTS i

DECLARATION OF ORIGINALITY ii

CONFERENCE PROCEEDINGS iii

SUMMARY iv

TABLE OF CONTENT vi

LIST OF ABBREVIATIONS ix

LIST OF FIGURES xii

LIST OF TABLES xiv

CHAPTER 1 15

LITERATURE REVIEW 15

INTRODUCTION 15

1.1 Global burden of malaria 15

1.2 The life cycle of *Plasmodium falciparum* 16

1.3 Current malaria controls strategies 18

1.3.1 Integrated vector management 18

1.3.2 Vaccine development 19

1.3.3 Current antimalarial therapies 20

1.4 Antimalarial drug discovery and developmental processes 22

1.5 Antimalarial Drug Development 24

1.5.1 The mitochondrial electron transport chain of *P. falciparum* as a potential drug target 26

1.5.3 2,6-Dimethyl-3-phenylpyridin-4(1H)-ones with potential antimalarial activity 31

1.6 Research question 34

1.7 Aim of study 34
1.8 Study objectives 35
1.9 Project outline 36
CHAPTER 2 37
MATERIALS AND METHOD 37
2.1 Computer-Aided Drug Design (CADD) 37
2.1.1 Software and computer system 37
2.1.2 Homology modeling *Plasmodium falciparum* cytochrome bc_1 38
2.1.3 Molecular dynamics 38
2.1.4 Docking Methodology 39
2.2 Materials 39
2.2.1 Reagents preparation 40
2.3 Collection of blood 42
2.4 Cultivation of malaria parasite (asexual stages) 42
2.4.1 Thawing and maintenance of parasites 42
2.4.2 Sorbitol synchronization 43
2.5 Effects of the candidate compounds on *Plasmodium falciparum* viability 43
2.6 Exposure of the candidate compounds to *P. falciparum* parasites 44
2.7 Culture of the HepG2 hepatocarcinoma cell line and toxicity assessment 46
2.7.1 Reagent preparation 46
2.8 Culture of the HepG2 hepatocarcinoma cell line 47
2.9 Effect of candidate compounds on HepG2 hepatocarcinoma cells 48
2.10 Stage-specificity of the candidate compounds 49
2.11 Speed of action analysis of candidate compounds 50
2.12 *In vitro P. falciparum* gametocyte culturing 50

CHAPTER 3 54
RESULTS 54
3.1 Computer-aided drug design 54
3.1.1 Homology modeling, molecular dynamics, and docking 54
3.2 Culturing of asexual and sexual stage of the *P. falciparum* parasites 64
3.3.1 IC_{50} determination 67
3.4 Inhibition of sexual stage (gametocytes) viability of *P. falciparum* parasites 70
3.5 Speed of action and stage specificity analysis 72
CHAPTER 4 78
DISCUSSION 78
5.1 Concluding remarks 84
5.2 Recommendations 84
References 86
Appendix I: Ethics approval letter 99
Appendix II: Ethics approval extension letter 100

LIST OF ABBREVIATIONS

3D7	Chloroquine-sensitive *P. falciparum* strain
ACT	Artemisinin combination therapies
ADME	Absorption, Distribution, Metabolism, Elimination
ADP	Adenosine diphosphate
ANOVA	Analysis of variance
ATCC	American Type Culture Collection
CDC	Centres for Disease Control and Prevention of USA
CM	Culture media
CoQ	Ubiquinone
$CoQH_2$	Ubiquinol
CQ	Chloroquine
DDT	Dichlorodiphenyltrichloroethane
DHFR	Dihydrofolate reductase
DHPS	Dihydropteroate synthetase
DMSO	Dimethyl sulfoxide
DNA	Deoxyribonucleic acid
EMEM	Eagle's Minimum Essential Medium
FCS	Foetal calf serum
G^-	Glucose negative media
G^+	Glucose enriched media
HCT	Haematocrit
HEPES	4-(2-Hydroxyethyl)-1-piperazine ethane sulfonic acid
HepG2	Human hepatocellular carcinoma (ATCC® HB-8065)
IC_{50}	Drug concentration resulting in 50% growth inhibition
IEC	Intra-erythrocytic life-cycle
IRS	Indoor residual spraying
ITN	Insecticides treated bed nets
K1	Multidrug-resistant *P. falciparum* strain

LogP	Octanol/water partition coefficient
MDR	Multidrug resistance
MMV	Medicines for Malaria Venture
MR4	Malaria Research and Reference Reagent Resource Centre
MSF	Malaria SYBR Green-1 based fluorescence assay
mtETC	Mitochondrial electron transport chain
NAG	N-acetyl glucosamine
NADH	Nicotinamide adenine dinucleotide
NMR	Nuclear Magnetic Resonance
PABA	p-amino-benzoic acid
PBS	Phosphate buffered saline
P*f*CRT	*P. falciparum* chloroquine-resistance transporter
P*f*MDR1	*P. falciparum* multidrug resistant protein 1
PMF	Proton Motive Force
PV	Parasitophorous vacuole
QED	Quantitative Estimate of drug-likeness
QSAR	Quantitative structure-activity relationship
RBC	Red blood cells
RBM	Roll Black Malaria
RI	Resistance index
RMSD	Root mean square deviation
ROS	Reactive Oxygen Species
RPMI 1640	Roswell Park Memorial Institute-1640 culture medium
SDS	Sodium dodecyl sulphate
SEM	Standard error of the mean
SI	Selectivity Index
SOP	Standard operating procedure
SRB	Sulforhodamine B
TCA	Trichloroacetic acid

TCP	Target Candidate Profile
TPP	Target Product Profile
Tris	Tris(hydroxymethyl)aminomethane
WHO	World Health Organisation

LIST OF FIGURES

Chapter 1

Figure 1.1: *Plasmodium falciparum* life cycle. 17

Figure 1.2: Different antimalarial drugs targeting the different stages of the *P. falciparum* life cycle. 21

Figure 1.3: Mitochondrial electron transport chain. 27

Figure 1.4: Cytochrome bc_1 of the mitochondrial electron transport chain 28

Figure 1.5: 2,6-Dimethyl-3-phenylpyridin-4(1H)-one mitochondrial membrane transport mechanism 30

Figure 1.6: Cytochrome bc1 Qi-site 4(1H)-pyridone inhibitors from which the common 2,6-Dimethyl3-phenylpyridin-4(1H)-one scaffold was derived from chemical cluster 87. 32

Chapter 2

Figure 2.1*:* Plate outlined for the exposure of the candidate compounds to the *P. falciparum* parasites. 45

Figure 2.2: Schematic representation of rings and schizonts stages of *P. falciparum* parasites production. 49

Figure 2.3: Schematic representation of the different stages of gametocytes parasites culture. 51

Chapter 3

Figure 3.1: Amino acid sequence alignment *P. falciparum* cytochrome bc_1 with *Bos taurus* (chain C of 4d6t), *Gallus gallus* (chain C of 3bcc), *Saccharomyces cerevisiae* (cghain c of 2ibz) and *Homo sapiens* (GenBank: AKN23372.1). 55

Figure 3.2: Interactions between ligand GW844520 and *P. falciparum* cytochrome bc_1. 56

Figure 3.3: Correlation between Autodock Vina free binding energy and experimentally determined IC_{50} inhibition against 3D7 malaria parasites. 57

Figure 3.4: Chemical structures generated from the interactions between ligand GW844520 and *P. falciparum* cytochrome bc_1. A. 2,6-Dimethyl-3phenylpyridin-4(1H)-one moiety B. Chemical structures generated from ligands docking. 58

Figure 3.5: Microscopic images are highlighting the characteristics of the different stages of the asexual cycle of the *P. falciparum* stained with Giemsa stain. 64

Figure 3.6: Light microscopy photography of the different stages of sexual development stained with Giemsa stain. 65

Figure 3.7: Dual point screening of potential antimalarial drugs on asexual stage. 66

Figure 3.8: The percentage parasite growth inhibition of *P. falciparum* cells and HepG2 hepatocarcinoma cells exposed to *in silico* designed compound EE1, EE3, EE5, and EE7. 67

Figure 3.9: Dual point screening of potential antimalarial drugs in early gametocytes. 70

Figure 3.10: Dual point screening of potential antimalarial drugs in late gametocyte 71

Figure 3.11: IC_{50} speed assay (3D7) synchronized cultures. 72

Figure 3.12: Stage-dependent effects of candidates' compounds. 73

Figure 3.13: Stage-dependent effects of candidate compounds on synchronous cultures of *P. falciparum* strain 3D7. 75

LIST OF TABLES

Chapter 1

Table 1.1: Overview of Target Candidate Profile and Target Product Profile Criteria 24

Chapter 2

Table 2.1*:* Different *Plasmodium falciparum* strain use in the experiment 59

Chapter 3

Table 3.1: Structure, QED score, binding energy and *in vitro* activity of synthesized compounds. 59

Table 3.2: 2,6-Dimethyl-3-phenylpyridin-4(1H)-one chemical backbone showing the halogen and phenoxyside chains to form the 6 candidate compounds. 61

Table 3.3: The Quantitative Estimate of Drug-likeness calculated for the candidate compounds series. 62

Table 3.4: IC_{50} values of *in silico* compounds after 96 h on different *Plasmodium* parasite strain and HepG2 cell 68

Table 3.5: Data summary of IC_{50} values for speed assay analysis 74

Table 3.6: Data summary of IC_{50} speed assay and stage specificity analysis. 76

CHAPTER 1
LITERATURE REVIEW

INTRODUCTION

1.1 Global burden of malaria

Malaria is a global parasitic disease and is one of the leading causes of mortality and morbidity, particularly in children. The 2016 World Health Organization report,(1) estimated the occurrence of 212 million cases of malaria with 429 000 deaths in 2015.(2) Children below the age of five accounted for 306 000 deaths. The African continent is more susceptible to malaria accounting for 90% of all reported malaria cases in 2015. The incidence of malaria in Africa is due to optimal climatic conditions that are favourable of the *Anopheles* mosquito that is the transmission vector for malaria parasite. Overpopulation, cultural practices, and poor socioeconomic conditions also contribute to the incidence of malaria. Most of the tropical and sub-tropical countries in Africa are malaria endemic, including Kenya, Uganda, Chad, Mali, Congo, Cameroon, Gambia, Sierra Leone, Ghana, Gabon, Nigeria.(3, 4) The global malaria eradication agenda has significantly decreased the malaria incidence by 41%, and mortality rates by 62% since 2000. Nevertheless, there is still a necessity for effective treatment and vector control strategies to be implemented in endemic malaria countries.(5)

Malaria is a mosquito-borne disease caused by the *Plasmodium* parasite which belongs to the phylum Apicomplexan.(6) Five species of the *Plasmodium* parasite have been identified as causing malaria in humans. These include *Plasmodium falciparum, P. malariae, P. ovale, P. vivax and P. Knowlesi.*(7) *P. falciparum* is the most dominant species in Africa and is responsible for the highest number of malaria deaths annually.(8) *Plasmodium* parasites are transmitted to human hosts,(9) through the bite of infected female *Anopheles* mosquitoes. *Anopheles arabiensis*, *Anopheles gambiae,* and *Anopheles funestus* are the most common parasite- transmitting vectors in Africa.(9) Upon infection with malaria, the disease manifests as an acute febrile illness with flu-like symptoms such as fever, headache, chills, and vomiting.(2)

P. falciparum is reported to cause the most severe form of malaria. This parasite's pathogenesis is associated with adhesion proteins that are expressed on the surface of infected red blood cells that aid in cytoadhesion, immune evasion, and sequestration.(10, 11) During cytoadherence, parasites sequester from the peripheral circulatory system and adhere to deep microvasculature of various organs such as the heart, brain, and lungs.(8, 10, 12)

1.2 The life cycle of *Plasmodium falciparum*

The *P. falciparum* parasite has a complex life cycle which uses both human and female *Anopheles* mosquito as hosts.(13) The multi-stage life cycle of *P. falciparum* is shown in Figure 1.2.(3) Human infection with malaria begins when sporozoites from the salivary glands of an infected female *Anopheles* mosquito are injected into the bloodstream of a human host during blood feeding (Figure 1.2: 1A). These sporozoites migrate through the blood vessels to the liver where they invade hepatocytes within an hour of the bite (Figure 1.2: 1B).(14, 15)

During the exoerythrocytic development cycle, the sporozoites remain in hepatocytes for 9 –16 days where they undergo asexual replication and divide mitotically into thousands of liver merozoites (Figure 1.2: 1B).(8) When the infected liver cells rupture, liver merozoites are released into the bloodstream of the human where they infect erythrocytes. This initiates the intra-erythrocytic cycle where the parasite multiplies asexually. Single merozoites bind to specific surface receptors on erythrocyte membranes within 2 minutes of release and form a tight junction then induce membrane invagination, resulting in merozoite invasion of the erythrocytes into a parasitophorous vacuole (PV) that is formed within the erythrocyte without compromising the erythrocyte membrane.(10) Once the merozoites enter the erythrocytes, they begin to develop into early trophozoites (Figure 1.2: 1D),(12, 16) also referred to as the "ring" stage of the parasite due to their morphology.(17) The ring stage develops into a trophozoite at

approximately 32 h after invasion during which time haemoglobin is digested, and the core haem group is converted into haemozoin crystals. At about 42 h the trophozoite starts to divide through a process of schizogony to form up to 32 new mature merozoites. When the merozoites are fully developed, the erythrocyte ruptures, releasing the newly formed merozoites into the blood that each may invade a new erythrocyte. The reinvasion of the erythrocytes by the merozoites reinitiates a new cycle of the blood-stage replicative cycle (Figure 1.2: 1D), (12) resulting in a rapid increased in blood parasitaemia.

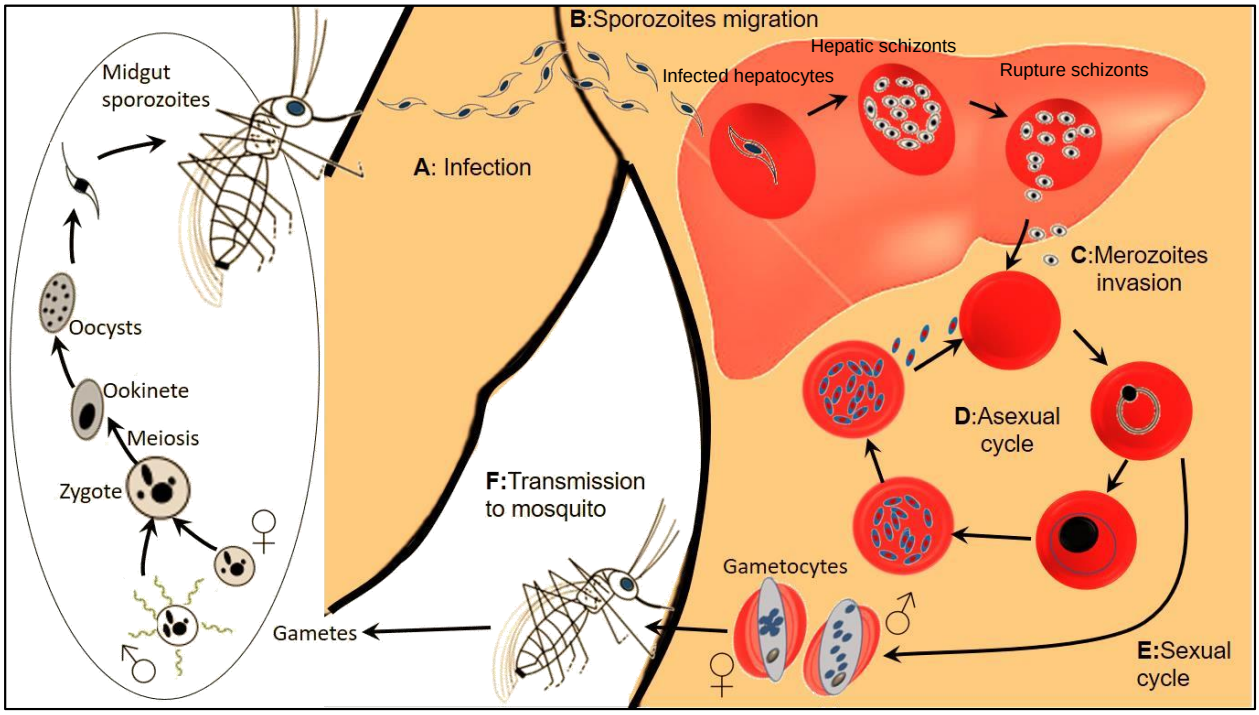

Figure 1.1: *Plasmodium falciparum* life cycle. (A) infection of the human host by the release of sporozoites during a bite from an infected female *Anopheles* mosquito (B) sporozoites migrate through the bloodstream and enter hepatocytes. (C) maturation and schizogony occur, and multiple merozoites are released into the bloodstream where they invade erythrocytes. (D) The intraerythrocytic asexual cycle progresses from the ring- to trophozoite- to schizont-stage parasite maturation. (E) Some trophozoites develop into male and female gametocytes during the sexual cycle. (F) Gametocytes are transferred to a mosquito when biting an infected human host. And through meiosis ultimately develop into oocysts. New sporozoites are then formed in the midgut of the mosquito, and the cycle repeats itself. The schematic was drawn using smartdraw and conceptdraw software and assembled using Microsoft PowerPoint.

During the intraerythrocytic asexual cycle, some of the trophozoites differentiate into male or female gametocytes (Figure 1.2: 1E). Gametocytogenesis occurs in the bone marrow(18) and can be divided into five distinct morphological stages,(19) early stage gametocytes

(stages I – III) and late stage gametocytes (stages IV – V).(18, 20) When the mosquito bites an infected person, it ingests only mature stage V gametocytes (Figure 1.2: 1F),(21) and then undergoes fertilisation; gametogenesis occurs in the *Anopheles* mosquito's gut lining where the gametes develop into the zygotes, ookinetes and finally oocysts, from which multiple sporozoites are released. These sporozoites accumulate in the mosquito's salivary gland, from where the life cycle may again be initiated during a blood meal from a human.(21, 22) The development of the parasite through its multi-stage life-cycle is vital for the survival and transmission of malaria.

1.3 Current malaria controls strategies

1.3.1 Integrated vector management

In the absence of effective antimalarial compounds, controlling the vector responsible for the spread of malaria can be used to reduce the prevalence. The Centers for Disease Control and Prevention (CDC)(23) has established various malaria vector control strategies that have been described as:

Indoor residual spraying (IRS) uses insecticidal spray that is used to coat the indoor walls and surfaces of the houses with an insecticide, commonly dichloro phenyltrichloromethane (DDT) in southern Africa. DDT is usually applied at a very high concentration (>80%) and remains effective for several months. The insecticide kills insects that settle on the wall and prevents the transmission of malaria.(24)

Insecticide-treated bed nets (ITNs) where mosquito bed nets are treated with a pyrethroid insecticide which kills mosquitoes and other insects.(23) This insecticide is selective for insects and poses very low health risks for humans. Recent data however suggested a rise in pyrethroid resistance by mosquitoes and a decrease in the effectiveness of ITNs.(25)

Another form of vector control includes fogging and area spraying which is usually utilized in cases of emergency, for example in a malaria epidemic area. The synthetic pyrethroid insecticide is used in the mosquito fogging spray. Fogging and spraying involve spraying fine droplets of insecticides that can kill only insects and targets mosquitoes with no adverse effects on people who are occasionally get exposed to the fog. The challenges with this method are; it is difficult for the insecticides to reach the crevices, it is costly and can result in insecticide overuse.(23)

1.3.2 Vaccine development

P. falciparum parasites has a complex life cycle yet adapts very quickly and well to their surroundings. The complexity of its life cycle has led to the development of parasite resistance to a wide range of antimalarial therapies. Malaria vaccine development has been proven to be a challenge due to a vast array of active defences employed by the parasite, including extensive antigenic variation and a poor understanding of the interaction between *P. falciparum* parasites and the human immune system.(26) Pre-erythrocytic stage vaccines are the main focus in malaria vaccine development, and its purpose is to prevent blood-stage re-infection. The pre-erythrocytic stage is usually the symptomatic phase, and the vaccine is reputed to protect against early disease onset. These vaccines prevent the establishment of infection by targeting the sporozoites or the schizont-infected hepatocytes so that exo-erythrocytic schizogony is halted. This means that no merozoites will be released to infect erythrocytes in the bloodstream.(27) Asexual stage vaccines are designed to reduce the severity of the disease symptoms,(28) where sexual stage vaccines induce antibodies which prevent infection of mosquitoes with the sexual forms of the parasite during a blood meal.(29) Numerous challenges have been encountered to successfully develop an antimalarial vaccine due to antigenic variation, the adaptable nature of the parasite and finally lack of knowledge regarding its immunological interaction between human antibodies and *P. falciparum* parasites.(4)

Recently, vaccine development approaches have redirected their focus to the preerythrocytic stage to prevent disease progression.(30) The RTS, S/AS01 vaccine is a pre-erythrocytic stage vaccine and is the furthest in clinical trial. The mechanism of action of RTS, S/AS01 is to induce an immune response against the *Pf* circumsporozoite protein that is present on the sporozoite surface.(31) RTS, S, a pre-erythrocytic vaccine was developed for the prevention of clinical *Plasmodium* malaria in children and is the first vaccine to complete a Phase III clinical trial. RTS, S/AS01 reduced clinical malaria by ~50% in children aged 5 -17 months and showed a ~30% reduction in infants aged 6-12 weeks.(32) While the vaccine may contribute to antimalarial control efforts in high transmission areas, improved vaccine efficacy is still required.(27) There are currently 25 ongoing malaria vaccine projects globally, where four are in Phase IIb or III clinical trials. Various other blood-stage and transmission blocking vaccination strategies are currently being investigated that may potentially lead to the development of a vaccine that successfully prevents malaria infection and transmission.(33)

1.3.3 Current antimalarial therapies

Acquired resistance to current antimalarial treatments by the *Plasmodium* parasite has led to the therapeutic challenge of producing new and effective antimalarial compounds. Uncomplicated malaria usually presents without severe signs and symptoms or evidence of vital organs dysfunction. The progressive increase of *Plasmodium* resistance to antimalarial compounds has become a major concern.(34) At present, *P. falciparum* has shown resistance to many currently available antimalarial treatments with artemisinin resistance being reported in south east Asia. This parasite resistance to drugs may result from genetic mutations that are known to confer drug resistance.(35) There is a high demand to design new antimalarial drug which is less susceptible to developing resistance. Antimalarial drugs are known to target different stages of the *P. falciparum* life cycle (Figure 1.2) with some of them (atovaquone and artemisinin) targeting more than one stages.

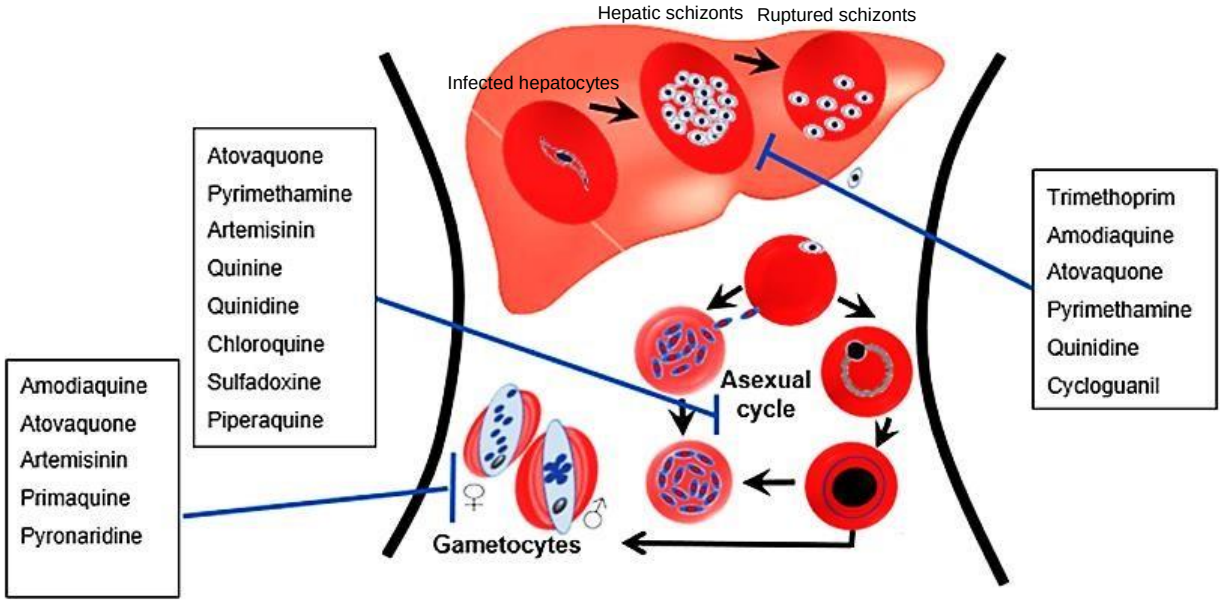

Figure 1.2: **Different antimalarial drugs targeting the different stages of the *Plasmodium falciparum* life cycle.** Some of the antimalarial drugs target more than one stages of the parasite life cycle. The schematic was drawn using smartdraw and conceptdraw software and assembled using Microsoft PowerPoint.

Artemisinin is currently the one of the effective antimalarial drugs against *P. falciparum.* The endoperoxide antimalarials referred to as artemisinin and its derivatives, have a potent and rapid action against *Plasmodium* parasites.(36) (Artemisinin has proven efficacy against various life stages of the parasite (trophozoites, schizonts, and young ring-form parasites) by inhibiting metabolic processes such as glycolysis, nucleic acid and protein synthesis.(37, 38) The artemisinin derivatives which include dihydroartemisinin, artemether and artesunate have higher antimalarial activity and are more soluble than artemisinin.(39)

As of 2006, ACT-resistant strains were reported at the borders of Thai-Cambodia and Thai-Myanmar in Southeast Asia.(35) This artemisinin resistance was found to be associated with a genetic mutation in a molecular marker known as ‘Kelch’ 13 protein’ (K13), and located in the propeller domain.(38, 40) K13 has several propeller domains acting as protein binding sites that are needed for ubiquitination-regulated protein

degradation and oxidative stress responses.(41) Although the evidence is not yet compelling, artemisinin should no longer be used as a monotherapy.

Due to the development of resistance to the majority of the antimalarial monotherapy, the WHO recommends the use of ACT (Artemisinin Combinations Therapy) in malaria endemic countries. The first-line treatment for uncomplicated malaria in South Africa is artemether-lumefantrine.(42) The five other antimalarial combinations drugs exist, which are also currently recommended are artemether-lumefantrine, artesunate-amodiaquine, artesunate-mefloquine, artesunatesulfadoxine-pyrimethamine and dihydroartemisinin-piperaquine.(42) The rapid development of drug resistant form of malaria demands an urgency for constant innovative strategies to develop new antimalarial drug with new potential target.(35)

1.4 Antimalarial drug discovery and developmental processes

Given the inevitability of global drug-resistance against current antimalarial therapies, novel classes of antimalarial medicines with alternative modes of action are urgently needed.(11, 43) Various novel scaffolds with different mechanisms of action have undergone clinical development in recent years, including clinical candidates OZ439, KAE609, MMV390, KAF156 and DSM265.(44) Specific characteristics must be present in novel antimalarial targets. These characteristics include the importance of the target in the parasite's life cycle progression, significant variation from the biological process in the human host, low probability for resistance and the parasite must not be able to evade the target with an alternate pathway.(1, 45, 46)

With the intention of eliminating malaria, various organizations such as the Medicine for Malaria Venture (MMV) and Roll Back Malaria (RBM) convened by the WHO and the Bill and Melinda Gates Foundation have established guidelines that new potential antimalarial compounds must followed. To adequately treat malaria, drugs must be fast

acting, highly potent against the asexual blood stages, minimally toxicity and affordable to residents of endemic regions.(45, 47) Additionally, the antimalarial should prevent the relapse of dormant forms of the parasite (hypnozoites, specifically in *P. vivax* and *P. ovale*).(43) Antimalarial compounds to be used as combination therapies should suppress or completely block gametocyte formation and the subsequent transmission to the mosquito vector, thereby halting the infection cycle.

Targeting malaria transmission at the gametocyte stage is a new focus of the TCP expected by the MMV. *P. falciparum* gametocytes are the longer-living form of the parasite, which makes transmission stage of the *P. falciparum* blocking challenging. *P. falciparum* gametocyte development involves various poorly understood genetic and metabolic changes that in turn alter the sensitivity of mature gametocytes to current antimalarial agents.(48, 49) Various antimalarial agents have been shown to lack activity against mature gametocyte stages, and this may be attributed to the loss of metabolic activity by the parasite, which then leads to increased resistance to antimalarial and metabolic inhibitors.(48) New compounds with gametocytocidal activity are needed in the drug discovery pipeline to add significant value to the antimalarial treatment options.

Successful drug discovery involves starting with a clear idea of what characteristics the final product should ideally have, and this is described as the target product profile (TPP). In the case of drug combinations, the TPP summarizes the properties of the combined profile.(50) For further drug development, a product can be obtained, which contains two or more active candidates, and most importantly the appropriate formulation. The newly defined TPP guidelines are strategic tools used to give guidance during drug discovery and development. During *in vitro* screening against *Plasmodium* parasites, it is essential for the test compounds to be assessed according to the malaria. Target Candidate Profile (TCP) guidelines as described by Burrow's et al., (2017).(51) TPP-1 requires the use of a combination of two or more molecules with TCP1, TCP-3, and TCP-5.(Table1.1) Also, TPP-1 requires the use of a single, fast-acting TCP-1 administered via the parenteral

route. TPP-2 defines chemoprophylaxis for travellers in combination with a TCP-4 and TCP-1 to blocking emerging infections.(Table 1.1)(51)

Table 1.1: Overview of Target Candidate Profile and Target Product Profile criteria(51)

Candidate molecule	Usage	Profile drugs	
TCPs		TPP-1	TPP-2
TCP-1	Asexual stage clearance	✔	✔
TCP-2	Profile Retired		
TCP-3	Active against hypnozoites	✔	
TCP-4	Active against hepatic schizonts		✔
TCP-5	Active against gametocyte (BT)	✔	
TCP-6	Active against insect vector (BT)		

BT; Block Transmission, ✔; the tick mark represents the candidate molecule present in the different target profile.

1.5 Antimalarial Drug Development

Antimalarial drug discovery has focused on identifying potential drugs with new target sites to combat the current drug resistant-prone *Plasmodium* species.(52, 53) Drug discovery techniques have been used as a time saving tool for the design of potential new drugs and is separated into two main categories being: target-based and phenotypic-based drug discovery approaches.(52)

Target-based drug discovery uses molecular tools such as forward and reverse genetics, cheminformatics, proteomic and genomic profiles to investigate specific molecular properties of a target site or molecular pathway.(54, 55) The identification of a unique target, preferably present in both the asexual and sexual stages is essential(45) and this makes the process of target validation complicated but is associated with a high degree of uncertainty.(54)

Phenotypic-based drug discovery assesses the effect of various compounds or compound combinations without prior design or knowledge of the candidate compound's

molecular mechanism of action.(52, 53) Phenotypic screening involves primary high throughput screening against *P. falciparum* infected erythrocytes to identify hits in a broad array of compounds. The benefit of this approach is that large numbers of compounds can be pre-screened at a lower cost to identify compounds that decrease parasite numbers *in vitro.* Additionally, specific active groups of compounds may be identified to define possible structure-activity relationships.(56)

A recent article published by Eder et al. (2014)(57) summarises the two different drug discovery approaches used to determine new molecular entities. In this study, from the 113 first-in-class drugs approved by the US Food and Drug Administration (FDA) from 1999 to 2013, the majority (70%) were discovered via the target-based approach route.(57) With this being considered, target-based drug discovery was used for the purpose of this research.

Target-based drug discovery efforts focus on a single gene or gene product, where a library of compounds is initially screened against a protein using software programs that calculate binding efficiencies. The compound that best fits the activation or catalytic site is identified as having a high probability of showing activity. The target sites are validated by modulation of the desired target using homology modelling(58) and the potential compounds structurally modified to optimise the drug likeness by altering the potency or pharmacokinetic properties.(58, 59) There is a need to produce a new generation of antimalarial compounds that can counteract the most drug-resistant forms of the malaria parasite. For this study, a target-based drug discovery approach was used to develop antagonistic compounds to target the cytochrome bc_1 of the *P. falciparum* mitochondrial electron transport chain.(52-54)

1.5.1 The mitochondrial electron transport chain of *P. falciparum* as a potential drug target

It has been proposed that cytochrome bc_1 of the *Plasmodium* mitochondrial electron transport chain (mtETC) is a potential biological target for establishing a potent multi-stage antimalarial therapy. This is because targeting cytochrome bc_1 provides an approach for a single dose drugs, reducing treatment cost, increase effectiveness and improve compliance with antimalarial treatment.(60) The emergence of resistance to atovaquone, which targets the Q_o site of the Cyt bc_1 complex, provides a warning about the long-term efficacy of drugs targeting this protein.(61, 62) Therefore, many aspects of any potential mitochondrion selective drug need to be investigated to assess their suitability as new emerging drugs.

The endosymbiotic theory states that the mitochondrion is a bacterial cell living within eukaryotic cells.(63) The *Plasmodium* mitochondrion consist of a double membrane and is located in the cytoplasm.(64) ATP(Adenosine Triphosphate) synthesis requires the generation of an electrochemical gradient across the inner membrane of the mitochondria. For the mitochondria to attain its electrochemical gradient potential, the electrons are transported through the chain four essential transporter complexes that sequentially export protons into the intramembrane space of the mitochondrion.(65) These complexes include NADH-coenzyme Q oxidoreductase (Complex I), succinate coenzyme Q oxidoreductase (Complex II), coenzyme Q-cytochrome c oxidoreductase (Complex III or cytochrome bc_1), and the cytochrome *c* oxidase (Complex IV). A diagram illustrating the complexes and the energy sources are represented in Figure 1.3.(66) Complex I passes electrons from NADH (Nicotinamide adenine dinucleotide) to coenzyme Q, and Complex II transfers the electrons to CoQ. Complex III then passes the electrons from the reduced CoQ to cytochrome c. Finally, Complex IV catalyses the synthesis of ATP using ATP synthetase.(65, 66) The mtETC is a good target because it is required in all the parasites developmental stages for energy requirements.(60) An important argument on inhibiting the mitochondrial electron transport chain is that if either

Complex I or II are blocked there is a possibility of by-passing these two complexes and still produce the proton gradient through Complex III.

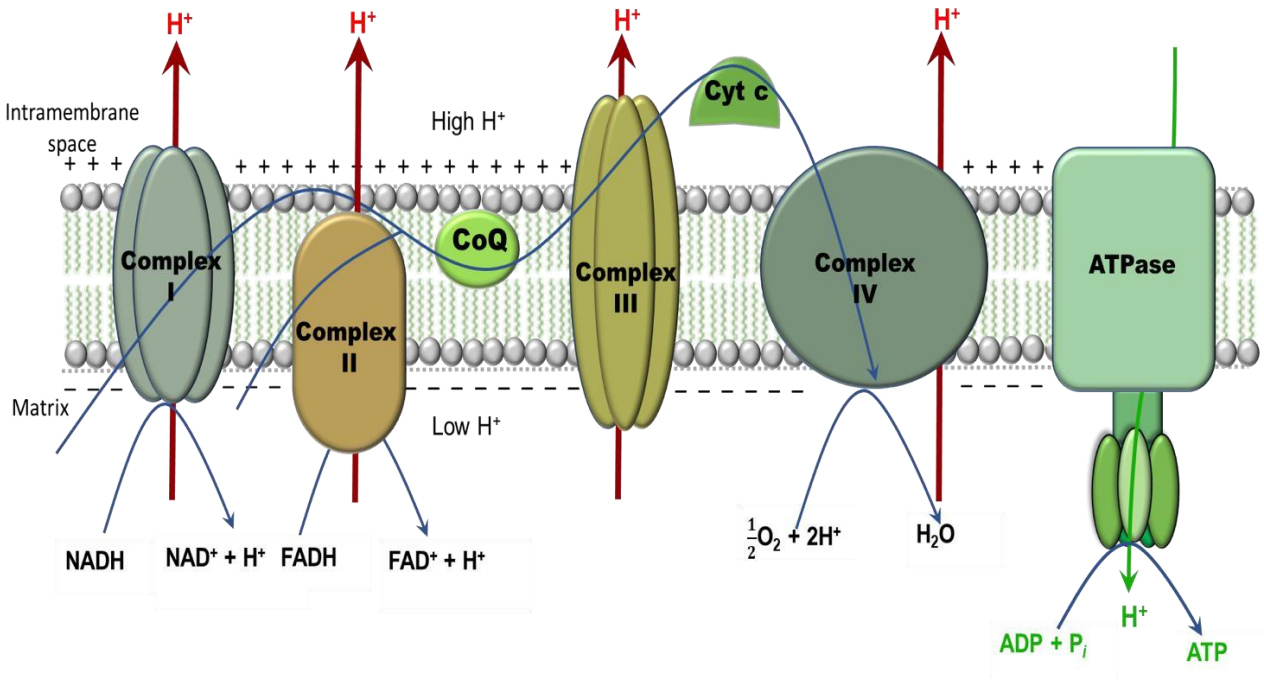

Figure 1.3: Mitochondrial electron transport chain.(67) This schematic indicates the pathway of electron transfer(blue) and proton translocation (red). Electrons flow through Complex I and III by the membrane-soluble coenzyme Q (CoQ) and between complexes III and IV by cytochrome c. Complex II transfers electrons from succinate to coenzyme Q. An electrochemical gradient accumulates in the intramembrane space which is used to catalyse the conversion of ADP to ATP.(66) The mtETC schematic was drawn using smartdraw software and assembled using Microsoft PowerPoint

The Rieske protein is a highly mobile component of Complex III that allows for the transfer of electrons to the haem group of cytochrome c_1. The Rieske protein mobility is a result of a shortened protein hinge segment, which allows for an easy conformational shift. The conformational shift allows the His182 found at the head of the Rieske protein to rotate, bridging the FeS cluster proximal to haem c.(68, 69) Inhibition of the Q_i site blocks the transfer of electrons from haem b_H (cyt b) to its oxidised form causing mitochondrial membrane potential arrest.(70)

The transmembrane of complex III contains three protein subunits each with a prosthetic group namely cytochrome *b*, cytochrome c_1 and the Rieske iron–sulphur protein (ISP) (Figure 1.4). Cytochrome *b* contains a relatively low potential b_L haem and higher potential b_H haem.(71) According to the standard model of the proton motive Q cycle,(72) $CoQH_2$ (ubiquinol) binds at the Q_o site located on the positively-charged (intermembrane) side (p-side) of the inner mitochondrial membrane (Figure 1.4).(68) This is followed by a single electron transfer to the high potential chain of the Rieske ISP cluster, resulting in the formation of a semiquinone ($Q^{\bullet-}$).(68) The low potential chain then oxidizes Q•− by donating a single electron to the relatively low potential b_L heme, resulting in the formation of CoQ (ubiquinone). Electrons donated to the high potential chain are transferred to cytochrome c_1 ultimately reducing cytochrome *c* (cyt *c*) to ferrocytochrome *c*.

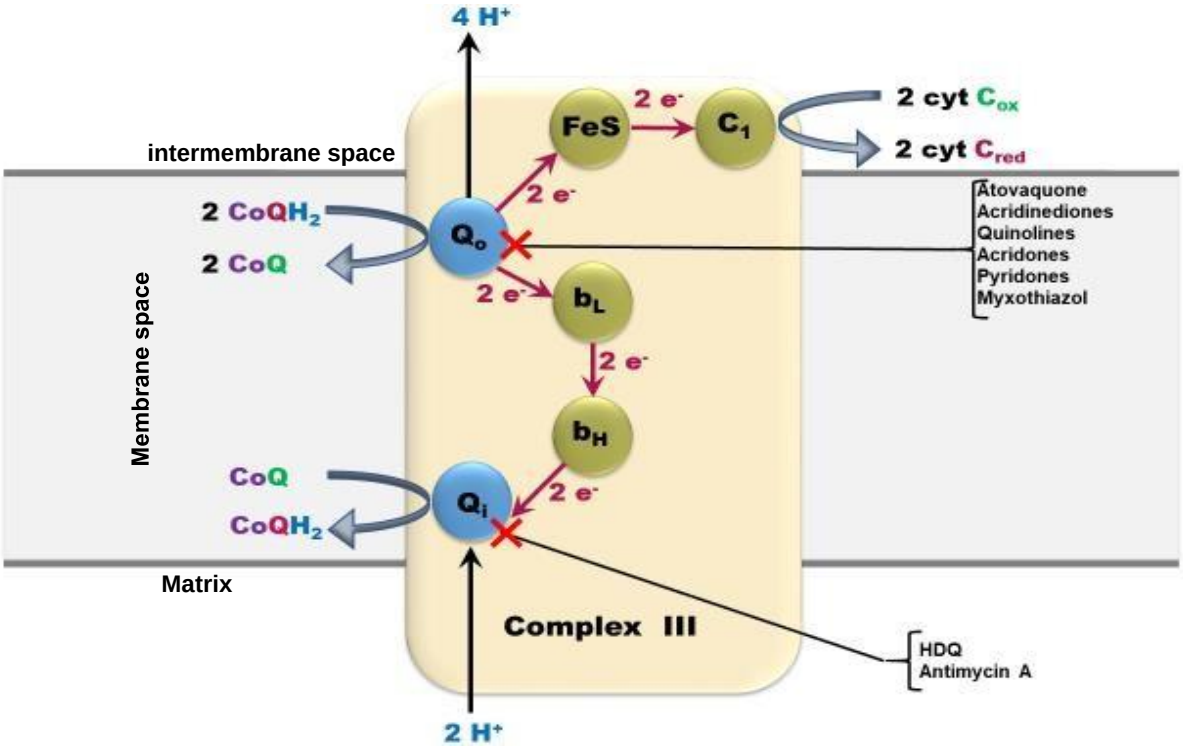

Figure 1.4: Cytochrome *bc₁* of the mitochondrial electron transport chain.(73) The grey area represents the inner mitochondrial membrane. CoQ: ubiquinone, $CoQH_2$: ubiquinol, Q_o: oxidation site and Q_i: reduction site. The Q cycle requires two separate binding sites for the reduction and oxidation of ubiquinol and ubiquinone. Q_o site for quinone reduction near the intermembrane space, and Q_i site for the reoxidation of quinol in the mitochondrial matrix. The schematic was drawn using smartdraw software and assembled using Microsoft PowerPoint.

Electrons donated to the low potential chain reduce the slightly higher potential b_H heme and are finally transferred to the Q_i site located on the negatively charged side (n-side or matrix) of the inner mitochondrial membrane (Figure 1.4).(74, 75) The low potential electron transfer reduces the $Q/Q^{\bullet-}$ couple bound at the Q_i site, resulting in the formation of $CoQH_2$, by the transfer of two protons from the matrix to one $CoQ^{\bullet-}$ molecule.(68) After two rounds of the efficient transfer of electrons from 2 $CoQH_2$ molecules at the Q_o site, two electrons are accumulated at the Q_i site to fully reduce 1 CoQ molecule to $CoQH_2$ which are transferred to 2 cytochrome *c* molecules.(66, 76, 77) Electron transfer at complex III is accompanied by the movement of 4 protons from the matrix across the inner mitochondrial membrane and reduction of 2 cyt *c* haem proteins for each $CoQH_2$, and contributes to both establishing the mitochondrial membrane potential and the proton gradient component of the proton motive force (PMF) ($2CoQH_2 + CoQ + 2cyt\ c^{3+} + 2H^+(matrix) \rightarrow CoQH_2 + 2CoQ + 2cyt\ c^{2+} + 4H^+$.(78) The PMF is used to drive the synthesis of adenosine triphosphate (ATP) from adenosine diphosphate (ADP) at Complex V. By inhibiting the Q_i site, the contribution of complex III's towards the PMF can be blocked thereby decreasing ATP production by complex V. Therefore, the killing of *P. falciparum* due to PMF disruption seems likely.

1.5.2 The mitochondrial membrane permeability of *P. falciparum* to potential antimalarial drugs

The outer mitochondrial membrane is freely permeable to ions and small molecules, while the inner mitochondrial membrane is impermeable to most of these molecules which properties needed to consider.(64, 79, 80)

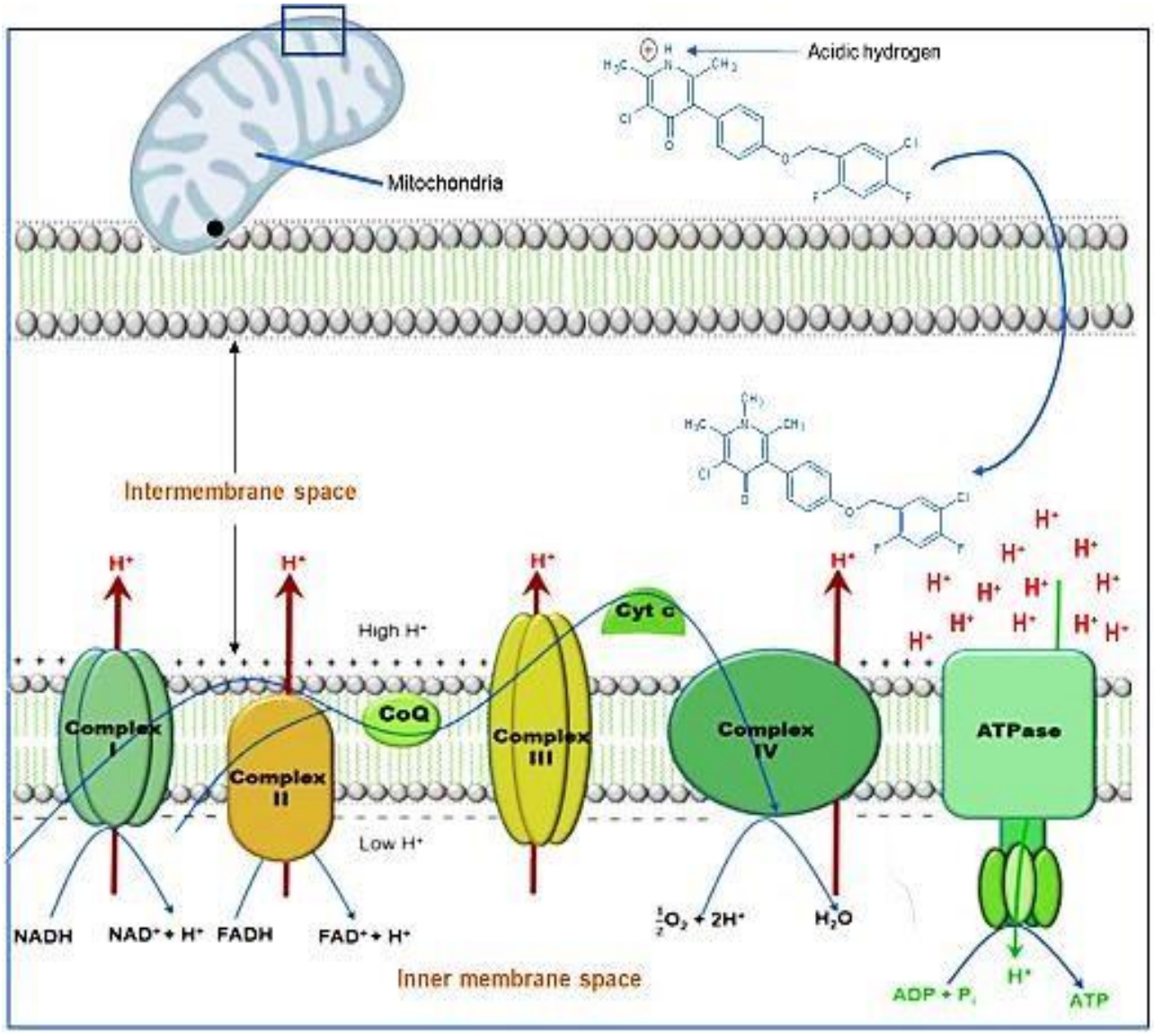

Figure 1.5: 2,6-Dimethyl-3-phenylpyridin-4(1H)-one mitochondrial membrane transport mechanism. The outer mitochondrial membrane is permeable to molecules with the help of transporters while the inner mitochondria membrane is impermeable except by the process of translocation. The schematic of the possible transport mechanism was drawn using smartdraw and conceptdraw software and assembled using Microsoft PowerPoint.

The intracellular membranes are composed of a bilayer of phospholipids, which has hydrophobic tail that produce a very hydrophobic environment in the middle of the lipid membrane bilayer. Molecules are transported through the inner mitochondrial membrane through two primary transport mechanisms by carriers or channel pumps.(64) These transporters either transport single specific molecules (uniporters) or transport two or more molecules at the same time (cotransporter). These transport mechanisms facilitate the permeability or diffusion of the membrane to compounds into the inner membrane space, improving the compounds susceptibility to the parasite.(79) Membrane permeability properties needs to be considered in the designed and synthesis of new antiplasmodial compounds. Membrane permeability can either be hydrophobic or hydrophilic, so the membrane properties can be considered when designing new antimalarial compounds.(64, 79)

1.5.3 2,6-Dimethyl-3-phenylpyridin-4(1H)-ones with potential antimalarial activity

Gamo and colleagues screened thousands of compounds for antimalarial activity.(81) For many of the compounds, the mechanism of action of the active compounds is not known. Activity against the 3D7 (chloroquine-sensitive) strain, Dd2 (chloroquine-resistant) strain, *P. falciparum* lactate dehydrogenase and human transformed liver HepG2 cells was reported at 10 mM. In order to identify promising chemical scaffolds from this list of compounds, all the compounds that showed less than 20% inhibition against human transformed liver HepG2 cells at 10 μM, and more than 80% inhibition against the Dd2 strain at 2 μM were considered. From this list, TCMDC-137587 from chemical cluster 87 was the most potent (5.29 nM against 3D7 cells, Figure 1.6A) and 72 compounds that meet the aforementioned criteria are also from chemical cluster 87. Many of these compounds contain the 2,6-Dimethyl-3-phenylpyridin-4(1H)-one core structure (Figure 1.6B). This core structure was then used as the chemical scaffold that was modified to design more potent antimalarial compounds.

In 2015, Capper identified the Q_i site as the target for 4(1H)-pyridones.(82) (Figure 1.6C). The GW844520 inhibitor was co-crystallised in complex with the *Bos Taurus* cytochrome *bc₁* (PDB code:4d6t).(82) This core structure provided the unique opportunity, using computer-aided drug design tools, to design new and more potent active site binding compounds that could target the Q_i site of the Cyt bc_1.(82) By targeting the Q_i site of the Cyt bc_1, parasite death can potentially be induced through three different mechanisms being ATP starvation due to decreased proton motive force; pyrimidine starvation; and lastly through excessive reactive oxygen species (ROS) production.(83)

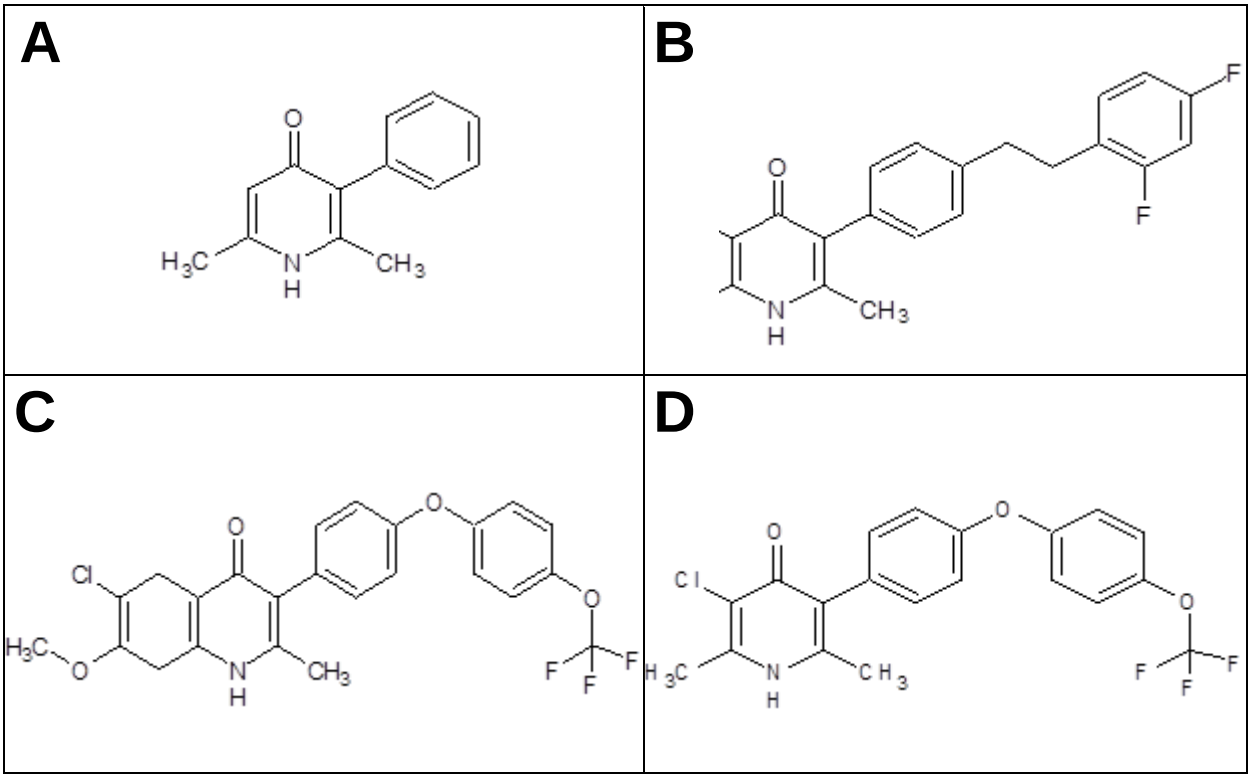

Figure 1.6: Cytochrome *bc₁* Q_i-site 4(1H)-pyridones inhibitors from which the common 2,6-Dimethyl3-phenylpyridin-4(1*H*)-one scaffold was derived from chemical cluster 87. A) The common 2,6 Dimethyl-3-phenylpyridin-4(1*H*)-one scaffold from chemical cluster 87 in Gamo et al., (2010). (81) B) Compound TCMDC-137587 from Gamo et al*.,* (2010)(81) with *in vitro* activity at 5 nM against 3D7 *P. falciparum* parasites**.** C) Cytochrome *bc₁* Q_i-site 4(1H)-pyridones inhibitor. D) ELQ300 compound with potent single-dose prophylactics, with remarkable multi-dose efficacy against blood-stage malaria parasites.

Painter *et al.,*(2007),(67) have showed that blood stage *P. falciparum* parasites maintain an active mitochondrial electron transport chain to regenerate ubiquinone. Ubiquinone is essential in the pyrimidine biosynthesis pathway by acting as an electron acceptor for dihydroorotate dehydrogenase (DHODH). The same mechanism of action for 4(1H)-pyridones was confirmed since these compounds are inactive against transgenic parasites expressing yeast DHODH.(82)

The final possible mechanism of action is via excessive ROS formation. Two components of the electron transport chain, Complex I and Complex III are primarily responsible for superoxide generation.(84) ROS are molecules with free, unpaired electrons. These include superoxide- ($O_2^{\bullet-}$), hydroxyperoxyl- ($^{\bullet}OH$), carbonate- ($CO_3^{\bullet-}$), peroxyl- ($RO_2^{\bullet-}$) and alkoxyl radicals. Superoxide is unstable and either undergoes a dismutation, resulting in the formation of hydrogen peroxide (H_2O_2) or forms peroxyl radicals, the conjugate acid of superoxide, by reacting with hydrogen ions. The dismutation reaction is catalysed by manganese superoxide dismutase (MnSOD) within the mitochondrial matrix, and intracellular superoxide is catalysed by copper-zinc superoxide dismutase (Cu/Zn-SOD).(85) Superoxide dismutation results in the formation of H_2O_2. Neither superoxide nor H_2O_2 are strong oxidizing molecules but are major sources for the downstream formation of ROS.(86) Superoxide converts ferric (Fe^{3+}) ions to ferrous (Fe^{2+}) ions ($Fe^{3+} + O_2^{\bullet-} \rightarrow Fe^{2+} + O_2$). Ferrous ions, in turn, react with H_2O_2 in the Fenton reaction, yielding the highly reactive hydroxyperoxyl radicals ($H_2O_2 + Fe^{2+} \rightarrow Fe^{3+} + {}^{\bullet}OH + OH^-$).(87) This process is called the Haber-Weiss reaction ($O2^{\bullet-} + H_2O_2 \rightarrow O_2 + {}^{\bullet}OH + OH^-$).(87) The H_2O_2 forms the majority of hydroxyperoxyl radicals generated *in vivo* during the Fenton reaction.(87) Hydroxyperoxyl radicals are highly reactive and cause oxidative damage to biomolecules, including nuclear and mitochondrial DNA, lipids and proteins.(88)

In humans, Complex I and Complex III are the primary sources of superoxide. At Complex III, two sites are considered to be major contributors to ROS production with the $CoQ^{\bullet-}$ intermediate being the electron donor for superoxide formation. (89) Historically, three

Complex III inhibitors have been used to determine the exact site of ROS production at Complex III being antimycin A, myxothiazole and stigmatellin.(89) Antimycin A interferes with the transfer of the second electron from cytochrome *b* to the relatively stable $CoQ^{\bullet-}$ at the Q_i site, causing the unstable $CoQ^{\bullet-}$ at the Q_o site to accumulate and increasing the chance of donating an electron to oxygen for superoxide formation.(89) Like antimycin A, 4(1H)-pyridones may act by increasing ROS production and ultimately cause cell death due to oxidative damage or activate pro-death signalling through redox sensitive signalling cascades. Interestingly, ELQ300 (another Q_i site inhibitor shows potent single-dose prophylactic activity, with remarkable multi-dose efficacy against blood-stage malaria parasites.(60) Also, combining ELQ300 with the Q_o inhibitor atovaquone shows promise as a treatment that can effectively prevent the emergence of drug resistant parasites.(90) Therefore, designing new and potent Q_i site inhibitors as a strategy to killing *Plasmodium falciparum* parasites and to overcome parasite atovaquone resistance is justified and pursued in the present study.

1.6 Research question

Computer-Aided Drug Design (CADD) is used as a valuable tool for the design of drugs when the target protein is known, and preferably the proteins 3D structure is known from physical measurements using X-ray diffraction. Can new cytochrome bc_1 Qi site inhibitors be designed and synthesis as feasible target-based antiplasmodial compounds, with improved solubility and more potent activity against different *Plasmodium falciparum* strains?

1.7 Aim of study

The aim was to assess the efficacy of six potential antiplasmodial drugs designed *in silico* to specifically target the Q_i site of cytochrome bc_1 on both asexual blood-stage and gametocyte stage parasite.

1.8 Study objectives

To complete this aim, the following objectives were completed:

- Determine the drug-likeness parameters of six new *in silico* designed candidate compounds as potential antimalarial drugs.
- Perform initial fixed dose screening of the inhibition potential of the six candidate compounds and determining the IC_{50} of the most promising candidates on the chloroquine-sensitive *Plasmodium falciparum* 3D7 strain after 96 h exposure.
- To determine if the potential antimalarial candidates are also active against the multidrug-resistant *Plasmodium falciparum* K1 strain.
- To determine the candidate compounds selectivity towards *Plasmodium* parasites using HepG2 cells.
- To ascertain whether the effect of the most active antimalarial drug compounds is parasite stage-specific.
- To determine the kill rate and speed assay for the candidate compounds.
- To assess if the candidate compounds will be active against gametocyte stage parasite.

1.9 Project outline

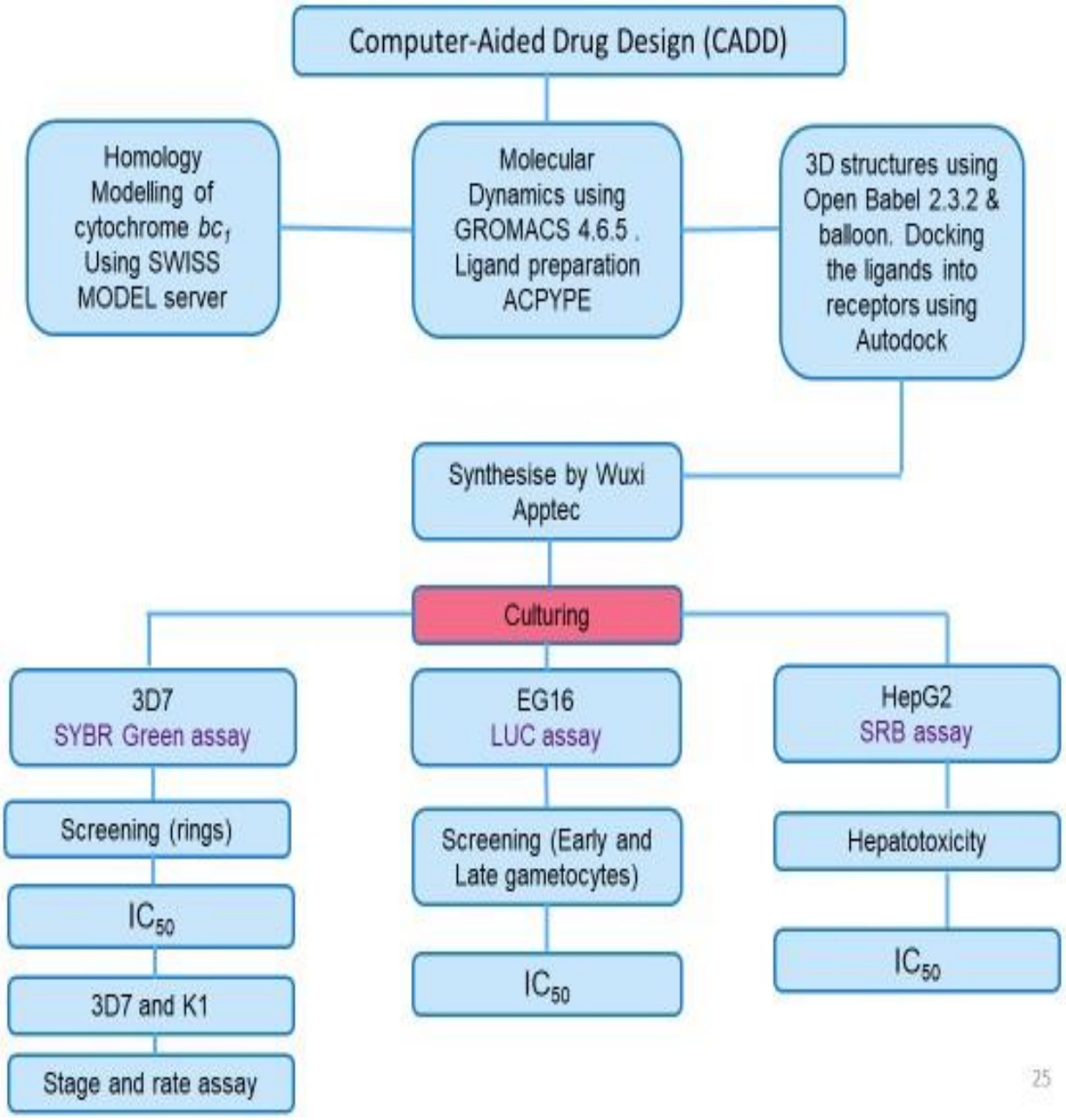

CHAPTER 2
MATERIALS AND METHOD

2.1 Computer-Aided Drug Design (CADD)

This component (Section 2.1) of the work reported in this study was completed by Dr. A Stander (Department of Physiology) and is included here for the sake of clarity and completeness in the context of the rest of the dissertation.

2.1.1 Software and computer system

The following software packages were used on an Ubuntu 14.04 LTS computer system with an Intel Core i7-5820K CPU and a GeForce GTX 980 GPU:
Chimera,(91)
Chemsketch,(92)
Open Babel 2.3.2,(93)
Balloon,(94, 95)
Autodock Vina,(96)
GROMACS 4.6.5,(97) the
AMBER99sb force field,(98)
The Stockholm lipids forcefield,(99)
CUDA 8.0,(100) ACPYPE(101) using antechamber from the AMBER 14 suite(102) and g_mmpbsa.(103) Molecular docking was performed using the Autodock Vina docking. Autodock Vina is a widely used docking program from the Molecular Graphics Lab of The Scripps Research Institute and is faster and as accurate as Autodock.(96) It is a grid based docking solution and is based on the X-Score scoring function.(96, 104) The scoring function is derived using the PDB bind data set, and the software implements an efficient, Iterated, Local Search global optimizer method to find the optimal docking pose. Autodock Vina is faster than Autodock and is also able to reproduce the crystal poses (root mean squared deviation (RMSD) < 2.0) in 78% of the tested protein-ligand complexes, 29% better than Autodock 4.(96)

2.1.2 Homology modelling *Plasmodium falciparum* cytochrome bc_1

The sequences of cytochrome bc_1 for *P. falciparum* (GenBank: AAC63391.1), *Bos taurus* (chain C of 4d6t), *Gallus gallus* (chain C of 3bcc), *Saccharomyces cerevisiae* (chain C of 2ibz) and *Homo sapiens* (GenBank: AKN23372.1) were used to investigate potential amino acid positions within the protein structure and active sites to target for compound docking selectivity. The cytochrome bc_1 chain C of 4d6t contained the 4(1H)-pyridones inhibitor and was used to generate *P. falciparum* cytochrome bc_1 homology models. The Swiss-PDB online server and Swiss-Pdb Viewer were used to produce a *P. falciparum* cytochrome bc_1 homology model.(105, 106)

2.1.3 Molecular dynamics

Molecular dynamics simulations were performed using GROMACS 4.6.5,(97) the AMBER99sb force field for proteins.(98) The nonbonded force calculations were accelerated through GPU acceleration using CUDA 8.0.(100) Ligands from the various template proteins were preserved in the homology models. The ligand topologies were prepared with ACPYPE(101) using *antechamber* from the AMBER 12 suite.(102) Haem parameters were generated using bond lengths, bond angles, dihedral angles and charges from Oda et al. (2005).(107) The protein was placed in a lipid membrane (80 x 80 Angstrom) by making use of the OPM server membrane protein alignment coordinates.

The system was prepared by heating it to 310 K (tau_t = 0.2) during a 500 ps constant volume simulation with 2 fs time step using the modified Berendsen thermostat (Vrescale) using velocity rescaling.(108) The pressure was equilibrated to 1 atm during a 1000 ps constant pressure simulation with a 2 fs time step using the Parrinello-Rahman parameters for pressure coupling.(109) In both simulations, all heavy atoms were position restrained with force constant of 1000 kJ/(mol.nm^2).

For the molecular dynamics run a temperature and pressure were maintained at 310 K and 1 atm using the Berendsen thermostat (V-rescale) and Parrinello–Rahman pressure coupling method. The short-range non-bonded interactions were computed for the atom pairs within the cut-off of 1 nm, and the long-range electrostatic interactions were calculated using particle-mesh-Ewald summation method with fourth-order cubic interpolation and 0.12 nm grid spacing.(110) The parallel Linear Constraint Solver (LINCS) method was used to constrain bonds.(111)

2.1.4 Docking Methodology

From the list of compounds identified by Gamo et al. (2010)(81) all compounds that had more than 20% inhibition against human transformed liver HepG2 cells at 10 μM and less than 80% inhibition at 2 μM against the DD2 strain were removed. From this list, compounds from chemical cluster 87 with the 2,6-Dimethyl-3-phenylpyridin-4(1H)-one moiety were converted to 3D structures using Open Babel 2.3.2(93) and Balloon.(94, 95) Autodock Vina(96) was used to dock the ligands into receptors. Autodock Vina exhaustiveness was set to 15 with the rest of the parameters set by default.(96)

2.2 Materials

All reagents were of highest chemical purity available and purchased from reputable international chemical vendors. The different malaria parasites strain was obtained from the Malaria Research and Reference Reagent Resource Centre (MR4) (Virginia, USA). The Fluoroskan Ascent FL microplate fluorometer was purchased from ThermoScientific (Waltham, Massachusetts, USA). The Promega luciferase assay reagents and the Glomax-Multi detection system was purchased from Promega (Madison, USA). The gas mixture of 5% CO_2, 5% O_2 and 90% N_2 was purchased from Afrox (Johannesburg, South Africa). C-28A centrifuge was purchased from BOECO (Hamburg, Germany). The ELX800 UV plate reader was purchased from Bio-Tek Instruments, Inc (Shanghai, China).

2.2.1 Reagents preparation

i. *In silico* candidate compounds preparation

WuxiApp Tec (Shanghai, China) synthesised and chemically characterised (NMR and mass spectrometry) the six best rated candidate compounds were under the contract from the Departments of Physiology and Pharmacology, University of Pretoria. These compounds were provided as chemically pure preparations of the *in silico* designed candidate compounds and coded as: EE1 (MM=454.69 g/mol), EE3 (MM=487.70 g/mol), EE4 (MM=464.15 g/mol), EE5 (MM=410.24 g/mol), EE7 (MM=443.25 g/mol), and EE8 (MM=419.70 g/mol), prepared in 100% (v/v) Dimethyl sulphoxide (DMSO). Chloroquine purchased from SigmaAldrich (St Louis, USA) was used as a positive control and reference and prepared in phosphate saline buffer (PBS). The compounds were filter sterilized using a 0.22 µm filter and aliquots of each compound were made and stored between at -20^{o}C for the duration of the study.

ii. Sorbitol

Sorbitol was purchased from Sigma Aldrich (St Louis, USA). A 5% solution was made by dissolving 25 g of sorbitol in 500 mL of distilled water and was stored at room temperature (25^{o} C).

iii. Phosphate-buffered saline (PBS)

Sodium chloride (NaCl), potassium chloride (KCl), sodium hydrogen phosphate (Na_2HPO_4), and potassium hydrogen phosphate (KH_2PO_4) were purchased from Merck (Darmstadt, Germany). The solution was prepared by dissolving 8 g of NaCl, 0.2 g of KCl, 1.44 g of NaH_2PO_4, and 0.24 g of KH_2PO_4 into 1L of distilled water and autoclaved. The solution was stored at room temperature (25^{o} C).

iv. Lysis buffer

Tris, EDTA (Ethylenediaminetetraacetic acid), Saponin, and Triton X-100 were purchased from Sigma-Aldrich (St Louis, USA). A solution was made by adding 2.42 g of Tris, 51.86 g of EDTA, 0.08 g of Saponin, and 800 g of Triton X-100 into 1L of distilled water and autoclaved. The solution was stored at room temperature (25^{o} C).

v. SYBR green lysis buffer

SYBR Green I fluorescence dye was purchased from Life Technologies (California, USA). A solution was prepared by adding 0.2 µL/mL; (Molecular Probes, Inc) in lysis buffer. The solution was stored at -20^{o} C.

vi. Incomplete culture media

RPMI 1640 medium, Gentamycin, HEPES (4-(2-hydroxyethyl)-1-piperazineethanesulfonic acid), Glucose, and Hypoxanthine were purchased from Sigma-Aldrich (St. Louis, USA). The powder of one glass bottle of RPMI 1640 (10.4 g) was slowly dissolved in 800 mL distilled water. In 50 mL distilled water 1.8 g $NaHCO_3$ was dissolved and added to the media. Also, sterile 20 mL of 1.25 M HEPES, 20% glucose, 80 mg/mL of gentamycin, and 80.8 mM of hypoxanthine was added. The volume was adjusted to 1 L with distilled water. The solution was filter sterilize using 0.2 µm filter and vacuum system into a sterile bottle and stored at 4^{o} C.

vii. Complete culture media

Albumax II was purchased from Life Technologies PTY (Johannesburg, South Africa). A solution was prepared by dissolving 5 g of albumax II into 40 mL of incomplete culture medium. The solution was made up to 1 L with incomplete media and filter sterilized with a 0.22 µm filter and stored at 4^{o} C.

viii. Thawing solution

Sodium chloride solution was purchased from Merck (Darmstadt, Germany). The thawing solution was prepared using 0.2 mL of 12% (w/v), 10 mL of 1.6% (w/v) and 10 mL of 0.9% (w/v) of NaCl was added into a 50 mL Falcon tube and stored at 4^{o} C.

2.3 Collection of blood

This study was performed under the guidelines of the Research Ethics Committee of the Faculty of Health Sciences of the University of Pretoria. Ethical clearance for the use of human erythrocytes for infectious agents and working with malaria parasites were obtained from the University of Pretoria, Faculty of Health Sciences Research Ethics Committee (Ethics Reference No: 383/2016) (see appendix II and III). A qualified nursing sister at the Student Health Services on Hatfield Campus, University of Pretoria performed the blood collection procedure. Different blood groups could be used as the culture media is supplemented with Albumax II (bovine serum supplement) and different students voluntarily donated blood for laboratory use. The blood was collected directly into a blood bag (Fenwal Primary container with 70 mL citrate phosphate adenine anticoagulant, for the collection of 500 mL of blood, Adcock Ingram). The blood was aseptically aliquoted into 50 mL falcon tubes and left overnight at 4ºC to allow the erythrocytes to separate from the serum. The serum and buffy coat were aspirated, and the erythrocytes were washed three times with phosphate-buffered saline (PBS; pH 7.2) before re-suspending the erythrocytes with an equal volume of incomplete culture medium to obtain a 50% haematocrit suspension. The blood was stored in a sterile environment at 4ºC. The red blood cells were used to culture malaria parasites in a sterile environment using a standardised protocol.(112)

2.4 Cultivation of malaria parasite (asexual stages)

The asexual blood stages of the 3D7 *P. falciparum* parasites strain was maintained under sterile conditions at 37ºC in human erythrocytes, suspended at a haematocrit of 5% in a complete culture medium and a gas mixture of 5% CO_2, 5% O_2 and 90% N_2.(113-115)

2.4.1 Thawing and maintenance of parasites

All culturing procedures were performed under sterile conditions. A stored cryotube containing viable frozen *P. falciparum* 3D7 and K1 parasite was thawed in a 37ºC water bath. The parasites were added to a falcon tube with 5 mL of thawing solution (NaCl

solution). Then, the tube was centrifuged at 600 x *g* for 5 minutes using a C-28A centrifuge and the supernatant decanted. The excess NaCl was removed by washing once with 5 mL incomplete media and then centrifuged at 600 x *g* for 5 minutes. The supernatant was decanted, and 6 mL of media was added to the final pellet and resuspended. The culture was transfer into 25 cm^2 culture flask and then was gased for 30 s with a gas mixture of 5% CO_2, 5% O_2 and 90% N_2. Finally, the culture was incubated in the shaking incubator at 37^oC overnight. For the culture maintenance, the falcon tube containing the parasite was centrifuged at 600 x *g* for 5 minutes, and the supernatant removed. Then 1 mL of fresh Red Blood Cells (RBC) (50% haematocrit) and 10 mL of complete culture media was added to obtained 5% haematocrit. The parasite culture was poured into a 25 cm^2 flask, gased for 30 s and incubated at 37^oC.

2.4.2 Sorbitol synchronization

Parasites at a 10% parasitaemia and with more than 90% in the ring stage were centrifuged at 600 x *g* for 3 mins. To the pellet 15 mL of 5% sorbitol was added, and the parasites were incubated for 15 mins in a warm water bath. Synchronisation was achieved using a sorbitol solution that lyses erythrocytes infected with mature stages of the parasite (trophozoites) but does not affect erythrocytes infected with ring-forms or uninfected erythrocytes. The culture was centrifuged at 600 x *g* for 3 mins and was diluted to 5% haematocrit. The parasites were treated with 5% sorbitol once every week to keep the parasites synchronised within a reasonably narrow window.(116) (117)

2.5 Effects of the candidate compounds on *Plasmodium falciparum* viability

The effect of the *in silico* designed candidate compounds on the *Plasmodium* parasite proliferation was determined using the Malaria SYBR Green-1® based fluorescence (MSF) assay according to methods previously described by Smilkstein et al., (2004)(118) and modified by and Niemand et al., (2013)(119). SYBR Green I is a cyanine dye which penetrates the cell membrane and binds with high-affinity to double-stranded DNA of the

Plasmodium parasites. The antimalarial activities of the candidate compounds were tested on three different strains as shown in Table 2.1.

Table 2.1: Different *Plasmodium falciparum* strain used in the experiments.

Strain	Characteristics	Description
3D7	Chloroquine-sensitive	Cloned from the NF54 isolate (MRA-1000)
K1	Multidrug-resistant (resistant to Chloroquine, Pyrimethamine, Mefloquine, and Cycloguanil)	Carries mutations in genes *pfmdr1, pfcrt, pfdhfr, pfdhps*
EG16pfs16-GFP-Luc	Expresses the pfs16 promoter which is expressed 10-fold more in gametocytes than asexual stages. (120)	Genetically modified from NF54 strain

pfmdr, *Plasmodium falciparum* multidrug resistant, pfcrt *Plasmodium falciparum* chloroquine-resistant, pfdhfr *Plasmodium falciparum* dihydrofolate resistant, pfdhps *Plasmodium falciparum* dihydropteroate

2.6 Exposure of the candidate compounds to *P. falciparum* parasites

In a 96 well plate, the outer wells of the plate were filled with 200 µL of PBS to avoid edge effects and obtaining false positive results. In the remaining wells, 100 µL of parasite suspension (1% parasitemia and 1% haematocrit) was pipetted. Different treatments were added to the parasites. To the positive control wells, 100 µL 0.5 µM chloroquine disulphate was added to serve as a blank for background effects. The positive control wells received 100 µL complete culture media. The rest of the wells were dosed with the 100 µl candidate compounds into the successive well in a 2-fold serial dilution for 3D7 and K1 (Figure 2.1).

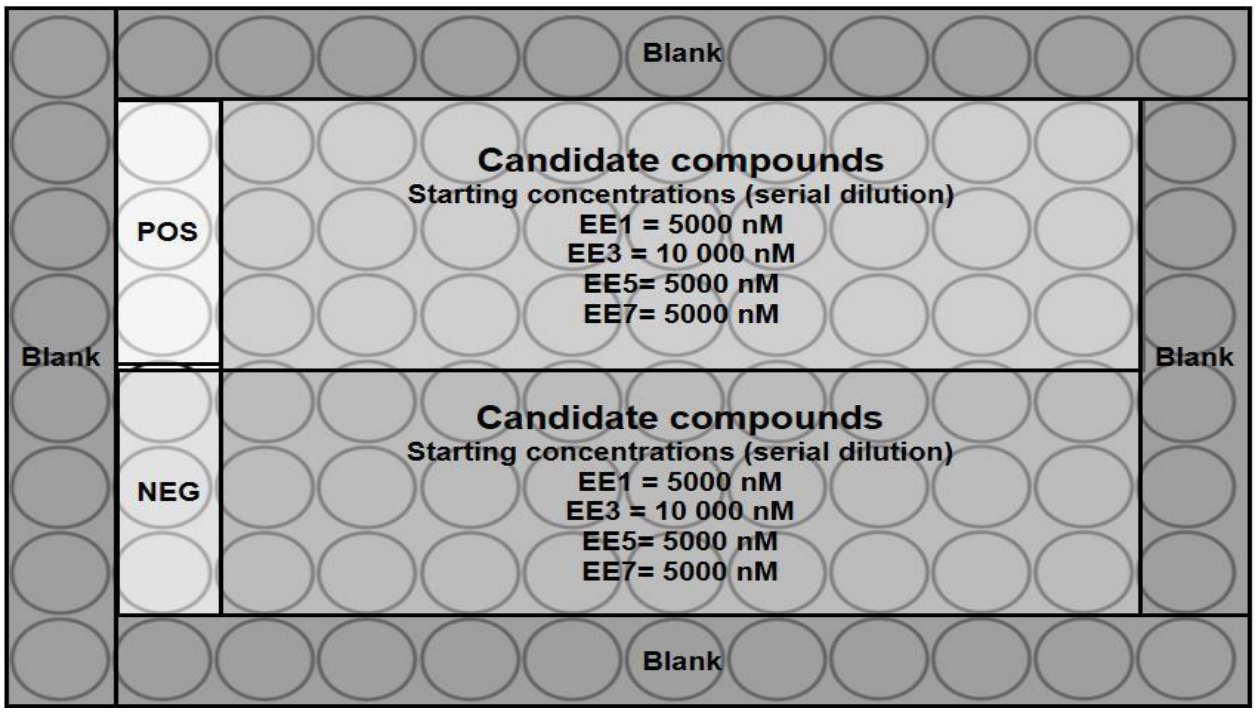

Figure 2.1*: Plate outlined for the exposure of the candidate compounds to the P. falciparum* parasites. Two candidate compounds were assessed per plate at the following starting concentration and the respective controls were plated as shown.

After dosing the parasites, the plates were placed in the gas chamber and were gassed with a gas mixture containing 5% CO_2, 5% O_2 and 90% N_2 for 3 mins. The plates were incubated in a stationary incubator for 96 h at 37^{o}C. Then the plates were frozen overnight to enable red blood cells lysis. After that, the plates were allowed to thaw, and the content resuspended. To a clear plate 100 µL of SYBR Green I lysis buffer was added and 100 µL of the resuspended parasites was transferred to a corresponding well on a new plate. The fluorescence intensity was measured using the Glomax-Multi+Detection System with Instinct Software (Promega. Sunnyvale, USA) with an excitation wavelength (λ_{ex}) at 485 nm and emission wavelength (λ_{em}) at 538 nm. All the values were blank-adjusted, and the data represented as a percentage of the untreated control to determine the parasite proliferation.

$$Parasite\ proliferation\ (\%\ relative\ to\ negative\ control) = \frac{Fsample}{Fnegative} \times 100$$

where, F_{sample} = blank-adjusted fluorescence of the sample, and $F_{negative}$ = blank-adjusted average of the untreated negative control.

2.7 Culture of the HepG2 hepatocarcinoma cell line and toxicity assessment

2.7.1 Reagent preparation

i. Eagles Minimum Essential Medium

EMEM and sodium bicarbonate were purchased from Sigma-Aldrich (St Louis, USA). A 1.2% solution of EMEM was prepared by dissolving 57.61 g of the medium powder and 13.20 g of sodium bicarbonate in 5 L of deionised water. The solution was filter-sterilized twice with 0.22 µm cellulose acetate and supplemented with 1% penicillin/streptomycin mixture and stored at 4^{o}C in 1 L bottles. The media was supplemented with 10% FCS, when needed by adding 100 mL FCS per 900 mL EMEM.

ii. Penicillin/streptomycin

Penicillin/streptomycin was purchased from Bio Whittaker (Walkersville, USA) at 10 000 units penicillin and 10 000 µg streptomycin per 1 mL

iii. Foetal calf serum

FCS was purchased from The Scientific group (Gauteng, RSA). The solutions were inactivated through heating at 56^{o}C for 45 min and stored at -20^{o}C.

iv. Sulforhodamine B

Sulforhodamine B (SRB) was purchased from Sigma-Aldrich (St. Louis, USA). A 0.057% solution was prepared by dissolving 171 mg per 300 mL acetic acid (1%). The solution was stored at 4^{o}C.

v. Trichloroacetic acid

Trichloroacetic acid (TCA) was purchased from Merck Chemicals (Johannesburg, South Africa). A 50% TCA was prepared by dissolving 50 g crystals per 100 mL distilled water and stored at 4^{o}C.

vi. Tris-base buffer

Tris(hydroxylmethyl) aminomethane was purchased from Sigma-Aldrich (St. Louis, USA) in powder form. A 10 mM solution was prepared by dissolving 242.2 mg per 200 mL distilled water and the pH was adjusted to 10.5 using sodium hydroxide. The solution was stored at room temperature(25^{o}C).

vii. Dimethyl sulfoxide

Dimethyl sulfoxide (DMSO) was purchased from Merck Chemicals (Johannesburg, South Africa). A 0.1% DMSO was prepared by adding 9.6 µl of DMSO in 9590.4 µl of distilled water and stored at room temperature(25^{o}C).

.

2.8 Culture of the HepG2 hepatocarcinoma cell line

HepG2 (ATCC® HB-8065™ or the American Type Culture Collection) cells were cultured using in-house protocols of the Department of Pharmacology, University of Pretoria. The cells were maintained in EMEM supplemented with 10% FCS, 100 µg/mL penicillin, and 100 µg/mL streptomycin. Cells were cultured at 37^{o}C, in a 5% CO_2 atmosphere in 75 cm^2 flask in a humidified incubator. Once a confluence of 80% was reached, cells were washed with sterilized PBS and detached from the flask using 0.25% trypsin solution. Dissociated cells were centrifuged at 200 x *g* for 5 min to concentrate the cellular pellet and resuspended in 1 mL EMEM. The cellular concentration was determined using the trypan blue exclusion assay (0.1% w/v) and a haemocytometer. The cell suspension was diluted to 2 x 10^5 cells/mL in 10% FCS-fortified EMEM.

2.9 Effect of candidate compounds on HepG2 hepatocarcinoma cells

The SRB colorimetric assay was used to determine the effect of the *in silico* designed candidate compounds on the HepG2 cell density according to the methods of Vichai and Kirtikara., (2006).(121) The SRB assay quantifies proteins as it binds to basic amino-acid residues under acidic conditions. The dye is released and solubilized under basic conditions. The number of viable cells is directly proportional to the intensity of staining.(121, 122)

To the 96-well plate, 100 µL of cell suspension was pipetted (2 x 10^5 cells/mL), and the cells were incubated for 24 h to allow for cellular attachment. To the cell suspensions were added either 100 µL negative control (EMEM), vehicle control (0.1% DMSO), positive control (50 µM doxorubicin) for cytotoxicity, half-log dilution of 4000 µM chloroquine as reference standard and individual *in silico* compounds (half-log dilutions of 2 mM) for 72 h. Blanks containing 200 µL 5% FCS-supplemented EMEM alone were used to account for sterility and background noise. The plates were incubated in a stationary incubator for 72 h at 37^{o}C.

After incubation, the cells were fixed by addition of 50 µL cold 50% (w/v) TCA overnight. To remove excess TCA, plates were gently washed four times under running water then stained with 0.057% (w/v) SRB solution for 30 min in the dark. Plates were rinsed four times with 1% (v/v) acetic acid and allowed to dry at 40^{o}C. Two hundred microliters 10 mM Tris base solution (pH 10) was added to each well of the dry plate to solubilise bound dye. The absorbance value of each well was determined spectrophotometrically (ELX800 UV plate reader, Bio-Tek Instruments, Inc.) at 510 nm (with a reference reading at 630 nm). All values were blank-adjusted, and the percentage cell density relative to the negative control was determined as follows;

$$Cell\ density\ (\%\ relative\ to\ negative\ control) = \frac{Asample}{Anegative} \times 100$$

where, A_{sample} = blank-adjusted absorbance of the sample, and $A_{negative}$ = blank- an adjusted average of the negative control.

2.10 Stage-specificity of the candidate compounds

The asexual stage-specificity of the *in silico* designed candidate compounds on both the rings and schizonts were assessed over 48 h. The method outlined by Le Manach et al., (2013)(123) was followed as recommended by MMV. The methodology followed is illustrated in Figure 2.2. Asexual 3D7 parasites were first synchronised as described in Section 2.4.2. The 3D7 cultures were synchronised twice with 5% D-sorbitol. The first treatment with sorbitol was done 9 h after the preliminary treatment, to obtain a synchronous ring culture. The second treatment was performed at 31 h on late rings to get schizonts.

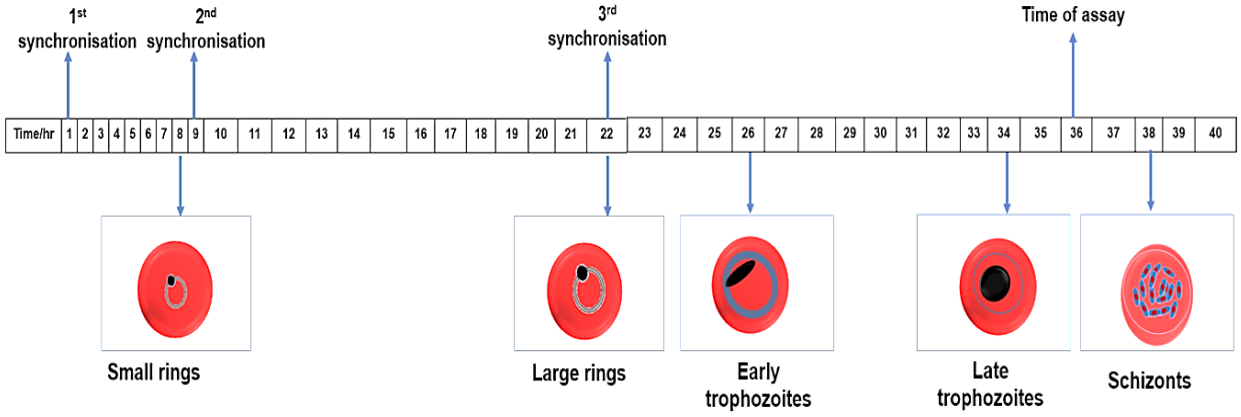

Figure 2.2: Schematic representation of ring and schizont stage parasite production previously synchronised parasites. Time of assay represents the time the assay was done on schizonts. This was summarised according to the method proposed by Le Manach et al., (2014).(123)

Ring (≥ 95%) and schizont (≥ 80%) cultures at 1% parasitaemia and a 1% haematocrit were treated with 100 x IC_{50} of each *in silico* candidate compounds (IC_{50} values obtained from data obtained in section 2.6), 230 nM CQ (positive control) or remained untreated

(negative control). The parasites cultures were treated at starting concentration (CQ=4000 nM, EE1=12200 nM, EE3=49800 nM EE5=12800 nM, and EE7=132800 nM) 2fold serial dilution at 8 different concentrations. In a 96-well microtiter plate, the synchronous stages were incubated for a further 48 h in the presence of the candidate compounds. SYBR Green-1 based fluorescence assay was performed as described in Section 2.6 to assess the viability of the candidate compounds on both the rings and schizonts.

2.11 Speed of action analysis of candidate compounds

Asexual 3D7 parasites were synchronised as described in Section 2.4.2. Synchronous ring stage parasites were added to wells of a 96-well microtitre plate. The parasites cultures were treated at starting concentration (CQ=400 nM, EE1 & EE5=600 nM, EE3=10 000 nM and EE7=3200 nM) 2-fold serial dilution at 8 concentrations. The treated parasites culture was incubated at different time points (48, 72, and 96 h) in separate plates. SYBR Green-1 based fluorescence assay was performed as described in Section 2.6 to assess the viability of the candidate compounds on the synchronised ring culture. From the IC_{50} values the rate of action of the candidate compounds was determined by obtaining the ratio of IC_{50} 48 h/IC_{50} 72 h.

2.12 *In vitro P. falciparum* gametocyte culturing

Gametocytes were generated using the EG16-pfs16-GFP-Luc protocol described by (Carter et al., 1993)(124) was used with modifications described by Reader et al., (2015). (125) The methodology used for gametocytes growth is explained on the schematic below; Figure 2.3. Asexual parasites in ring stage were initially synchronised twice, two days apart on Day -7 and Day -5, as described in Section 2.4.2. The parasite cultures were maintained at a 7-10% parasitaemia and used to initiate gametocytogenesis, with a starting haematocrit of 6% and a parasitaemia of 0.5% in negative glucose CM. On the day of initiation (day -3) cultures were maintained without shaking. Glucose-free CM was replaced 48 h later (Day -1) and every 24 h thereafter. On Day 0, the culture's haematocrit

was reduced to 4% using negative glucose media. Glucose starvation and reduction in haematocrit cause parasites to become stressed.(125, 126). Glucose positive (G^+) CM enriched with 50 mM N-acetylglucosamine (NAG, Sigma-Aldrich) was added and replaced daily on Days 1-3 and Days 4-7 for early and late stage gametocyte cultures, respectively.

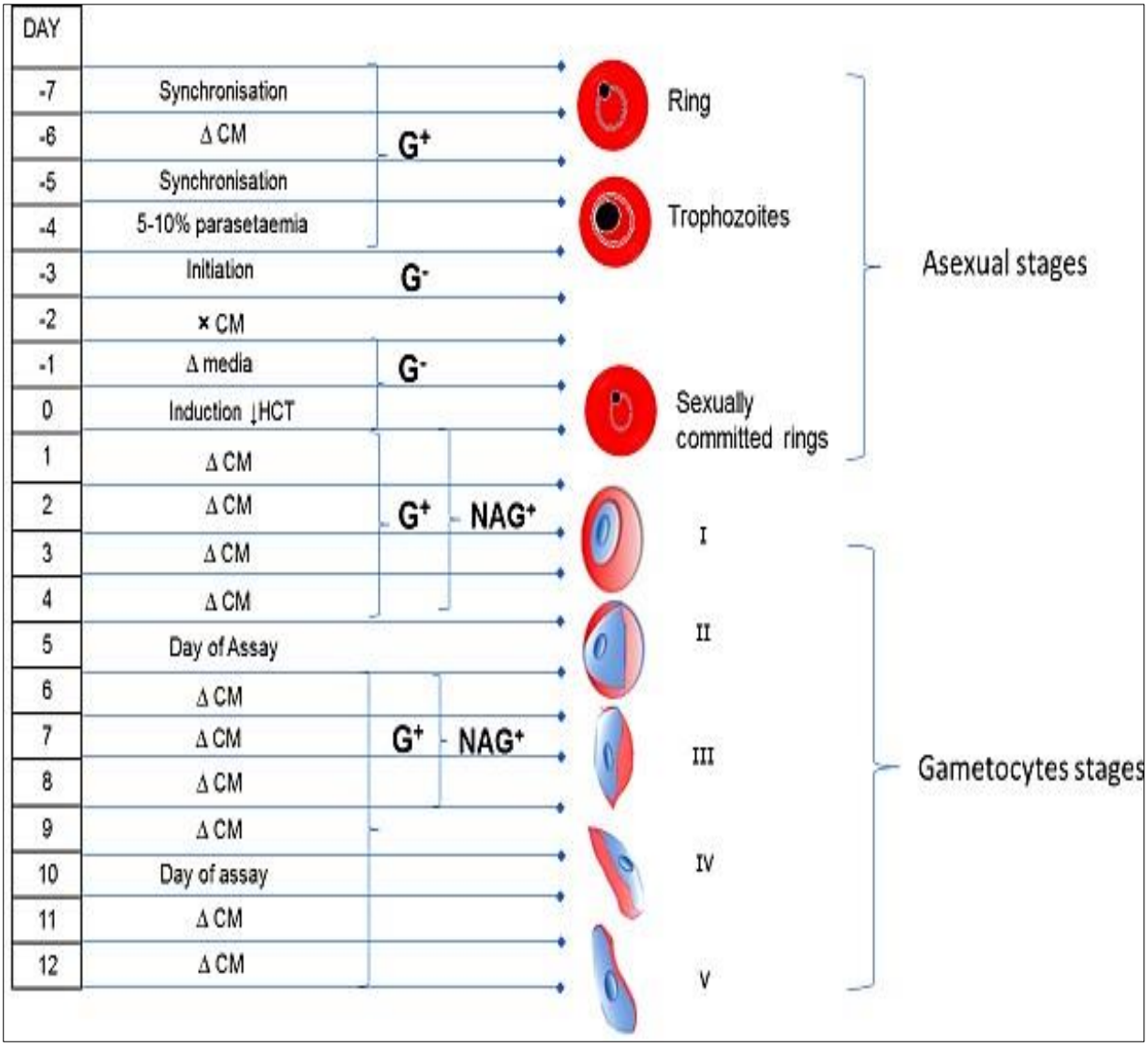

Figure 2.3: Schematic representation of the production of different stages of gametocytes parasites culture. CM; culture media, G^+ glucose enriched media, G^- glucose negative media, NAG^+ NAG enriched media, Δ change media culture, ↓HCT drop in haematocrit.

Following the cessation of NAG treatment, gametocytes were cultured with G^+ CM until the assays were performed. From approximately Day 3, gametocytes were visible under the microscope. Experiments using early and late stage gametocytes were carried out on Day 5 and Day 10, respectively. NAG inhibits any further asexual parasite growth, since it blocks erythrocyte invasion by the parasite, without affecting gametocyte development.(127)

2.13 Effects of candidate compounds on *Plasmodium falciparum* gametocytes viability

The effect of the antimalarial drug compound on the gametocyte proliferation was determined using luciferase-based antimalarial assay according to Verlinden et al., (2015).(128) Early and late stage *P. falciparum* gametocyte cultures at 2% haematocrit and 5% gametocytemia were treated with candidate compounds at 1 and 5 µM for the dual-point screening of inhibitory activity as was initially performed for the asexual blood stage sensitivity testing. This serves as a primary indication of compound activity against the gametocyte parasite stages. The controls for this assay included Methylene blue (5 µM, positive control for inhibition) and complete RPMI 1640 media (negative control for inhibition).

The treated parasites were grown for 72 h at 37˚C, after which a proportion of the culture medium (70 µL) was replaced with complete RPMI 1640 media and the plates incubated for a further 72 h. The assay was initiated on Day 5 (early gametocyte) and Day 10 (late gametocyte stage) after induction of gametocytogenesis from synchronised parasites culture (ring stage). The drug assays were set up using 0.5% parasitaemia and 6% haematocrit. The cultures were exposed to the drug for 48 h under hypoxic conditions at 37^{o}C. Luciferase activity was determined by adding 50 µL of luciferin substrate (Promega Luciferase Assay System) to 20 µL parasites lysates at room temperature. The resulting bioluminescence was measured with an integration constant of 10 s with Glomax-Multi+ Detection System with Instinct Software (Promega, Sunnyvale, USA). The data was represented as a percentage of the treated control after background subtraction

(methylene blue-treated infected RBC samples in which parasite viability was completely inhibited), to determine the percentage inhibition for each compound.

CHAPTER 3
RESULTS

3.1 Computer-aided drug design

This component (Section 3.1.1) of the work reported in this study was completed by Dr. A Stander (Department of Physiology) and is included here for the sake of clarity and completeness in the context of the rest of the dissertation.

3.1.1 Homology modelling, molecular dynamics, and docking

A homology model of the *P. falciparum* cytochrome bc_1 proteins was generated using the SWISS-MODEL server. Initial preparations and simulations of the protein complexed with the haem ligand were performed by generating force field parameters of the haem ligand using ACPYPE. However, the simulations were unsuccessful since the iron of the haem ligands did not stay complexed to the ligand and drifted into the system. This meant that a new force field had to be designed to keep not only the iron complexed to the haem ligand but also preserve the correct haem configuration inside the cytochrome bc_1 protein. This is important since the haem ligand forms part of the binding pocket for Q_i-site inhibitors. The bond lengths, bond angles, dihedral angles and charges from Oda et al., (2005)(107) were used to describe a new force field that was incorporated into Gromacs for ease of use.(107) Cytochrome bc_1 is a membrane bound protein that is part of Complex III of the electron transport chain. Simulating the protein in a membrane was essential. However, only cytochrome bc_1 was included to speed up the simulations. After placing the protein in a 1-palmitoyl-2-oleoyl-sn-glycero-3-phosphoethanolamine (POPE) lipid membrane, the system was minimized, and a 100 ns simulation was performed while complexed with GW844520 and the haem ligands. Post-simulation analysis revealed that the haem ligands and iron remained complexed inside the protein, and the GW844520 ligand preserved significant interaction as observed in the 4d6t crystal structure. These include the hydrogen bond interactions between the nitrogen of the pyridone and histidine 192, as well as the oxygen of the pyridine and a complexed water molecule between ASP218 and the ligand (Figure 3.1 and 3.2).

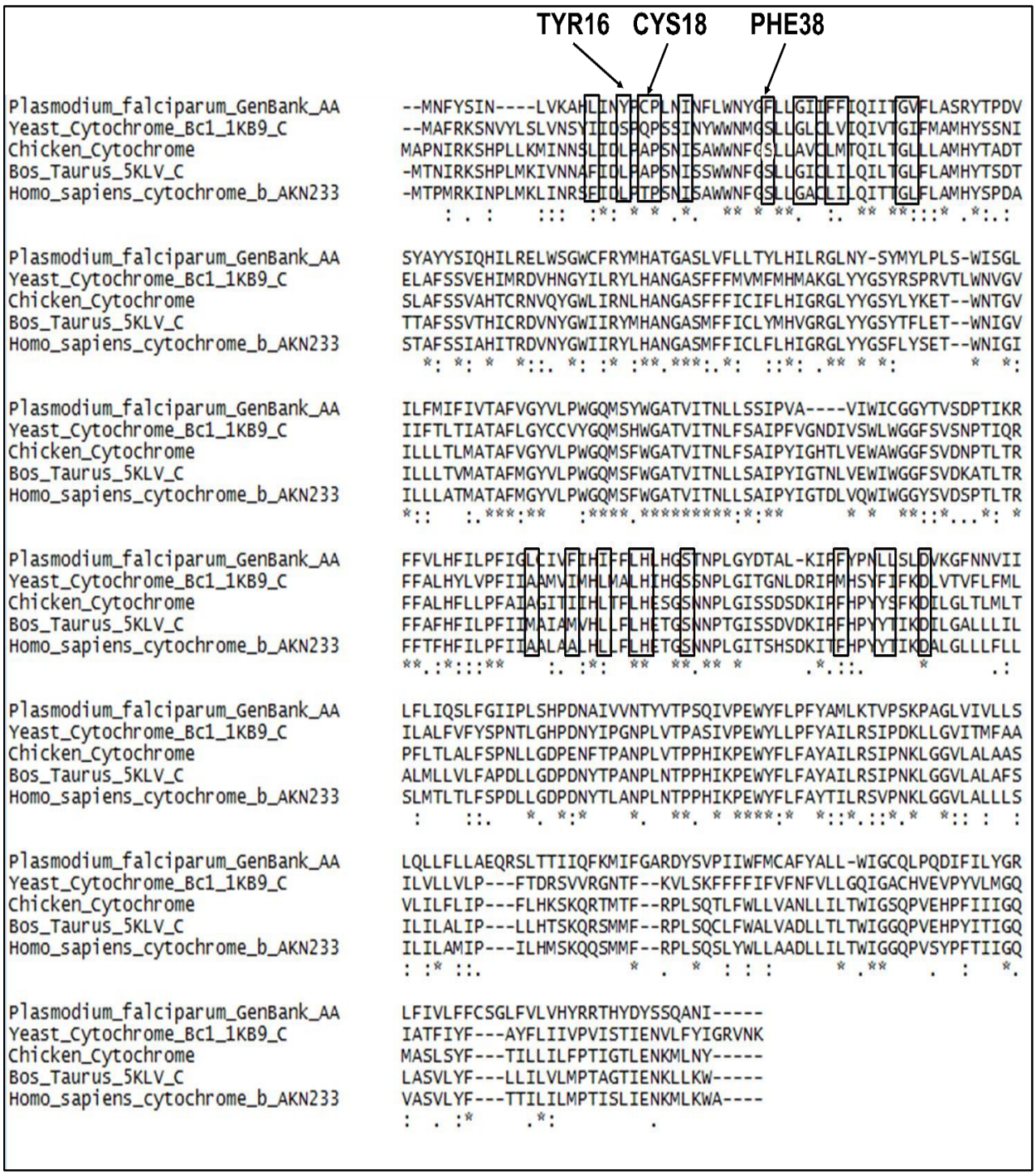

Figure 3.1: Amino acid sequence alignment of *P. falciparum* cytochrome bc_1 with *Bos taurus* (chain C of 4d6t), *Gallus gallus* (chain C of 3bcc), *Saccharomyces cerevisiae* (chain C of 2ibz) and *Homo sapiens* (GenBank: AKN23372.1). The black box indicates amino acids that interact with the ligand in the 4d6t structure. TYR16, CYS18 and PHE38 can be exploited to design species-specific inhibitors and are likely the reason this class of compounds shows relatively low potency against human cytochrome bc_1 proteins.

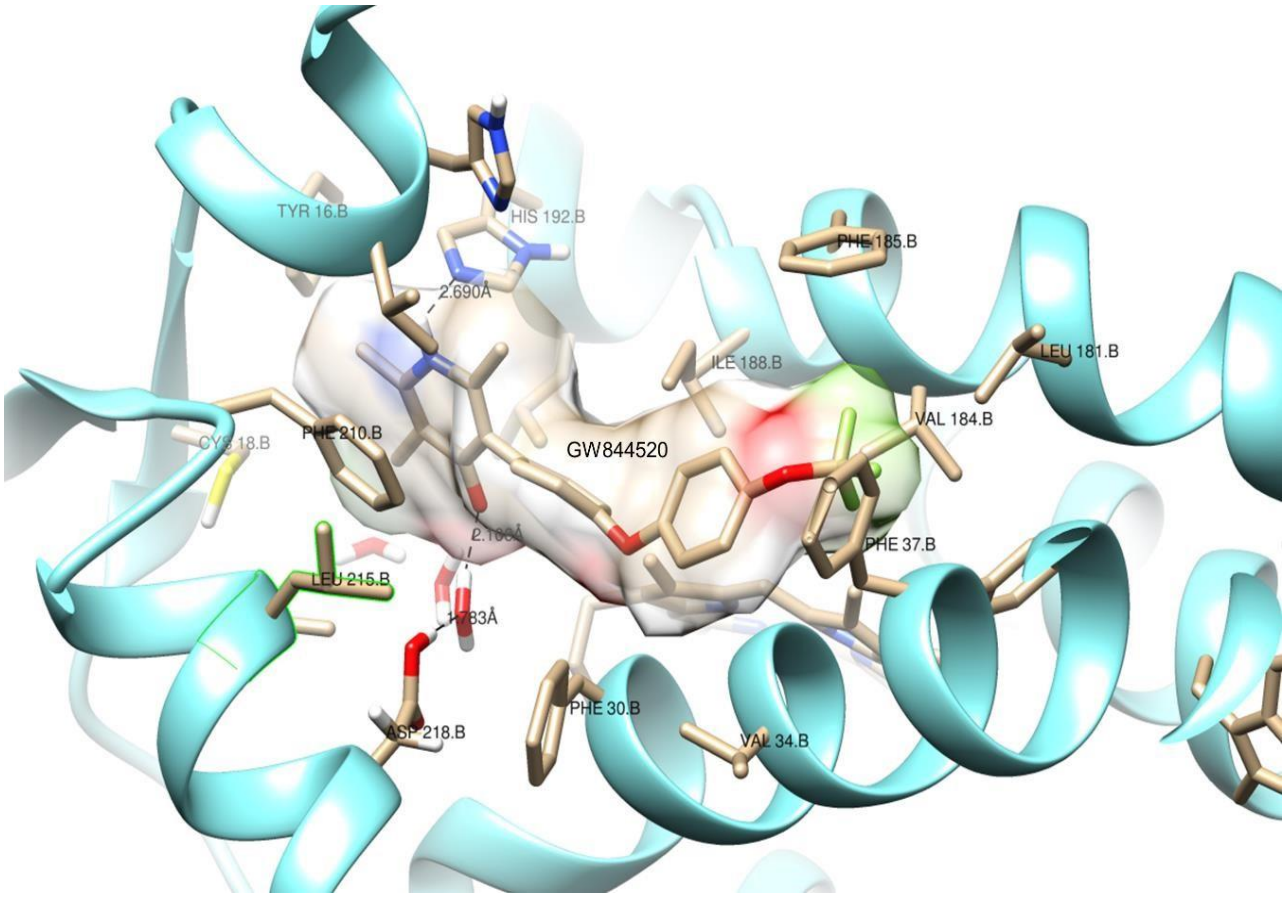

Figure 3.2: Interactions between ligand GW844520 and *P. falciparum* cytochrome bc_1.

After the simulation, structures after every 2 ns simulation were extracted and used as templates in an ensemble molecular docking study. A total of 50 receptors were used, and a total of 63 ligands were docked in each of these receptors. The average binding energy was calculated, and a coefficient of determination R^2=0.4792 between the Autodock Vina free binding energy and experimentally determined IC_{50} inhibition against 3D7 malaria parasites have been identified. Inspection of the structures of the chemical cluster 87 revealed that compounds with the core structure in Figure 3.2 showed overall high binding effect and selectivity (low activity against HepG2 cells at 10 μM) and would be relatively easy to synthesize. Group R^2 was modified according to three main criteria. Firstly, groups had to be chosen from a list of available chemical constituents that could be added. This list was available from the company, Wuxi AppTec (Shanghai, China) that synthesized the compounds, and was limited to this catalogue. This was a limiting factor

in choosing optimal groups. Secondly, the groups were chosen for their optimal drug likeness according to Lipinski and QED parameters.(129) Moreover, the groups had to perform well in docking against the ensemble of proteins from the molecular dynamics simulation. Average docking energy of less than -11.0 kcal/mol was considered sufficient for inclusion based on the correlation determined previously (Figure 3.3). An initial group of 12 compounds was identified, due to budget constraints only 6 could be synthesized, Compounds EE1, EE3, EE4, EE5, EE7 and EE8 (Table 3.1). The binding energies correlate well between the R^2 groups of the compounds and with the actual *in vitro* activity, demonstrating the usefulness of the docking to identify potential lead compounds (Figure 3.3).

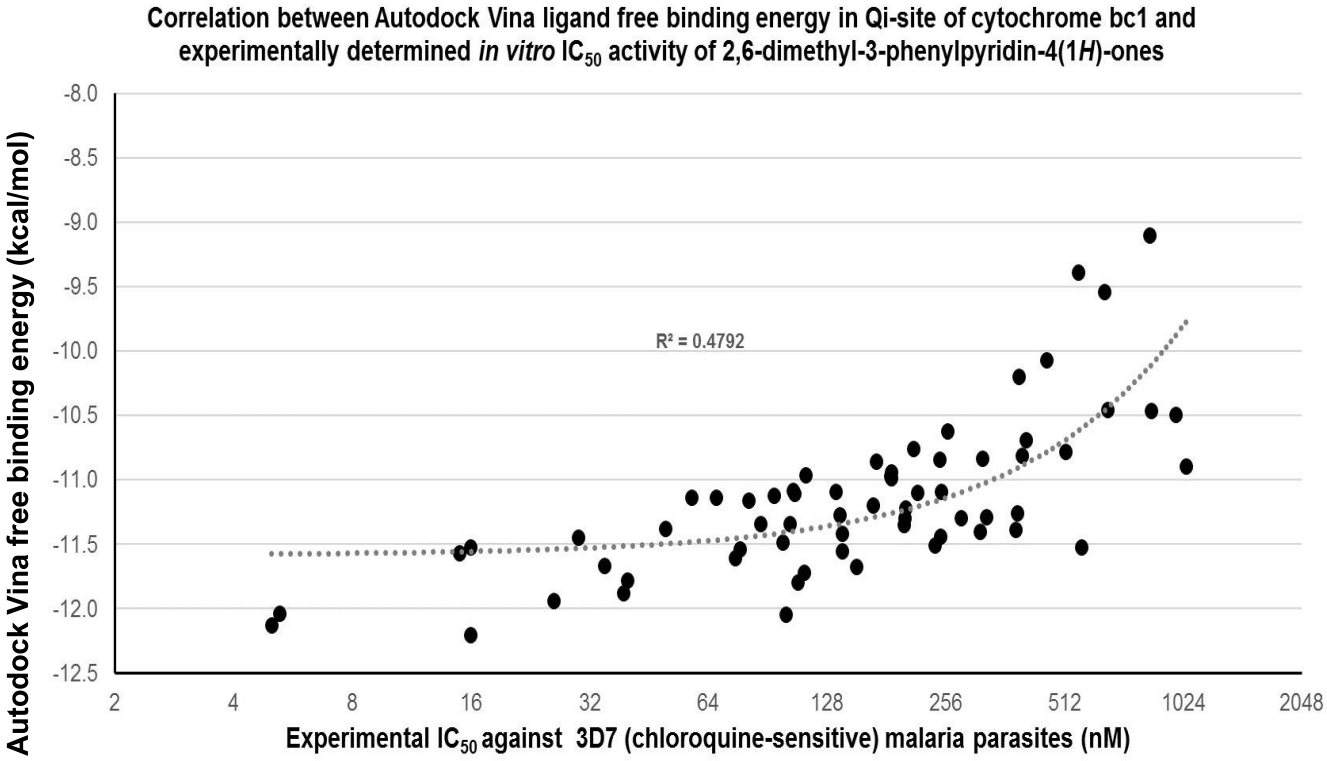

Figure 3.3: Correlation between Autodock Vina free binding energy and experimentally determined IC_{50} inhibition against 3D7 malaria parasites. A coefficient of determination (R^2) of 0.4792 between free binding energy and the IC_{50} was observed for docked ligands.

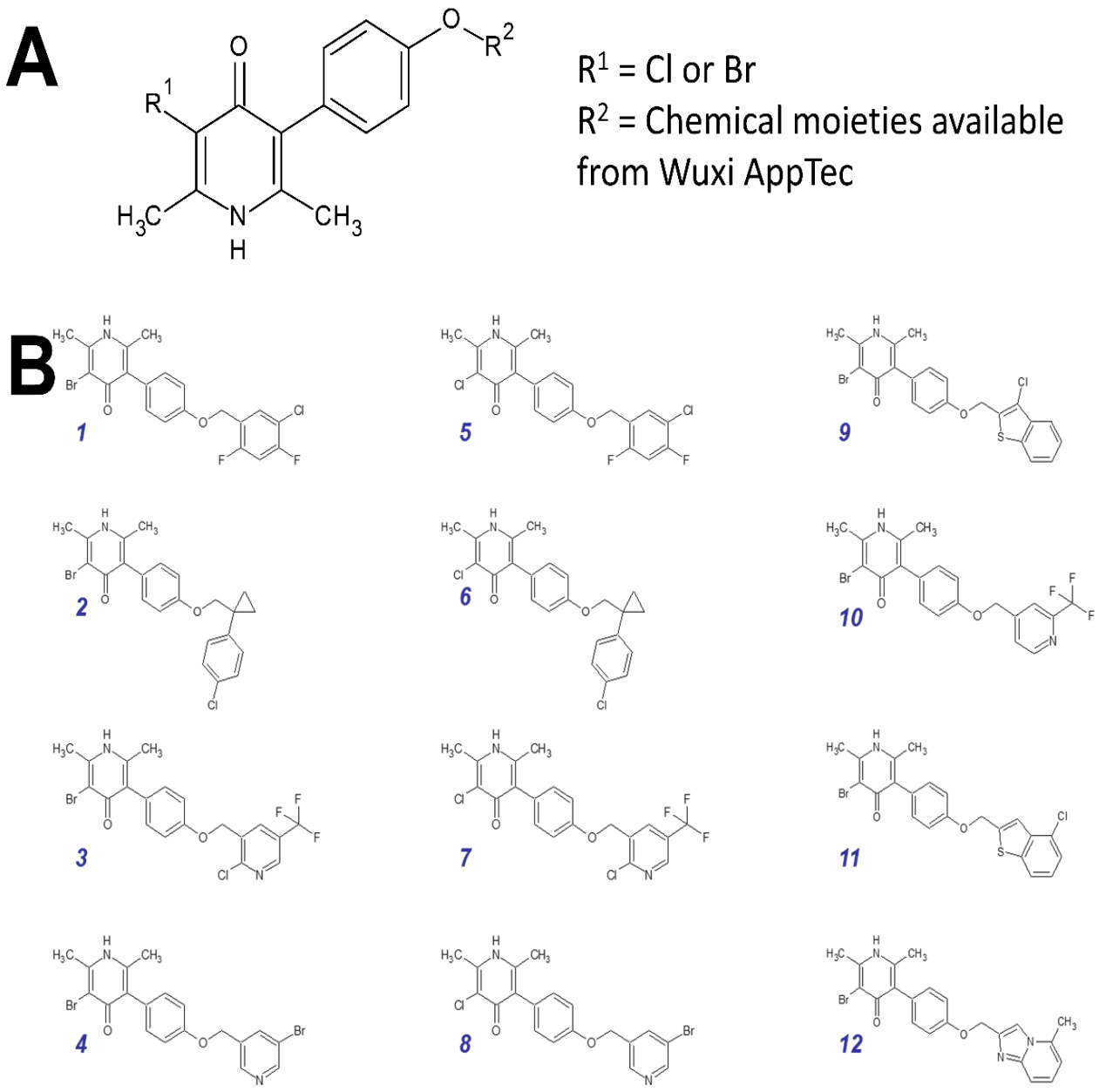

Figure 3.4: Chemical structures generated from optimisation of the interactions between ligand GW844520 and *P. falciparum* cytochrome *bc₁*. A. 2,6-Dimethyl-3-phenylpyridin-4(1*H*)-one moiety B. Chemical structures generated from ligands docking.

Table 3.1: Structure, QED score, binding energy and *in vitro* activity of synthesized compounds.

Compound	Structure	QED score	Binding energy (kcal/mol)	3D7 IC_{50} (nM)
EE1	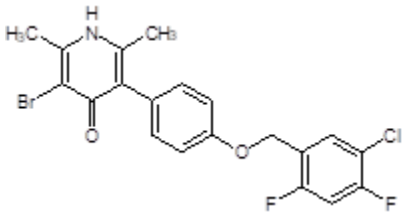	0.591	-12.03	76
EE5	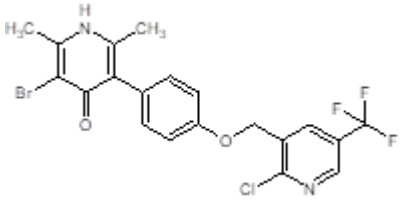	0.643	-12.10	62
EE3	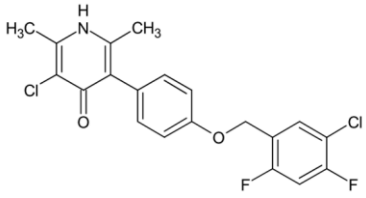	0.497	-11.93	592
EE7	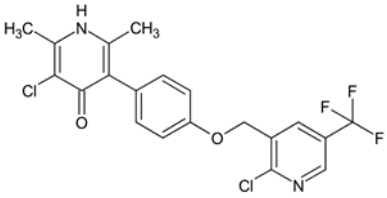	0.525	-11.99	263
EE4	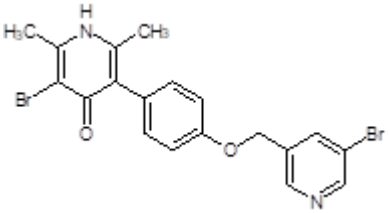	0.780	-11.00	N.D. (>800 nM)
EE8	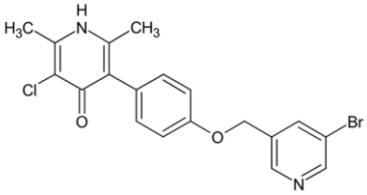	0.826	-11.15	N.D. (>800 nM)

EE1: 2-bromo-5-(4-[2-(5-chloro-2,4-difluorophenyl) ethoxy] phenyl)-2,6-Dimethylpyridin-4(1*H*)-one EE5: 3-chloro-5-{4-[2-(5-chloro-2,4-difluorophenyl) ethoxy] phenyl]-2,6-Dimethylpyridin-4(1*H*)-one EE3: 3-bromo-5-(4-[2-chloro-5-(trifluoromethyl) pyridin-3-yl] methoxy} phenyl)-2,6-Dimethylpyridin-4(1*H*)-one EE7: 3-chloro-5-(4-[2-chloro-5-(trifluoromethyl) pyridin-3-yl] methoxy} phenyl)-2,6-Dimethylpyridin-4(1*H*)-one EE4: 3-bromo-5-{4-[(5-bromopyridi-3-yl) methoxy] phenyl]-2,6-Dimethylpyridin-4(1*H*)-one EE8: 3-chloro-5-(4-[5-bromopyridi-3-yl) methoxy] phenyl]-2,6 Dimethylpyridin-4(1*H*)-one

Aparoy et al., (2012),(130) define QSAR (Quantitative structure-activity relationship) as a process of quantitatively correlating the structural molecular properties and functions in an attempt to find a relationship between the structure and the functions.(130) QSAR assumes that the molecular set of similar compounds all contain the features responsible for its biological, chemical and physical activity.(130, 131)

The 3-phenylpyridin-4(1H)-one pharmacophore core was altered by adding side chain modifications that were done either to improve binding affinity or solubility. The addition of a phenyl group to compound EE1, EE3 and EE5 were to enable the compounds to bind strongly to the hydrophobic pocket at the cytochrome bc_1 to form a bond between the halides and O-N on the backbones of the peptides. The halides (chloride and bromide) on the pharmacophore structure improves permeability through the intramembrane thereby increasing the bioavailability of the compounds in the parasite. The most active compounds (Compound EE1 and Compound EE5) have a 5-chloro-2,4difluorophenyl) ethoxy] phenyl group attached to the 2,6-Dimethyl-3-phenylpyridin-4(1H) one core structure.

Table 3.2: 2,6-Dimethyl-3-phenylpyridin-4(1H)-one chemical backbone showing the halogen and phenoxyside chains to form the 6 candidate compounds

	Chemical structure	
Core chemical structure	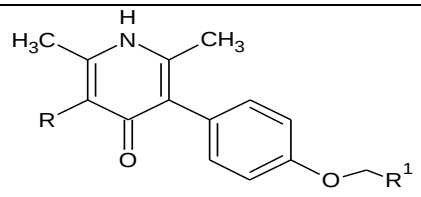	
	R	R^1
EE1	Br	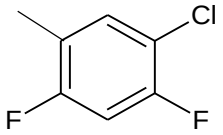
EE5	Cl	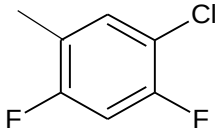
EE3	Br	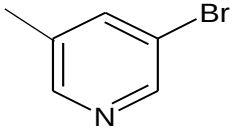
EE7	Cl	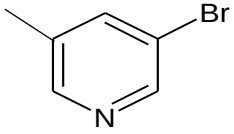
EE4	Br	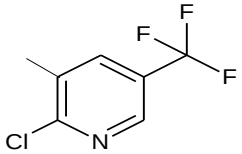
EE8	Cl	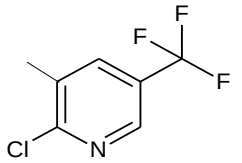

The position of the halide group on the different side chains affects the binding of the compounds to the target site and induce varying degrees of inhibition. Compound EE1 has a 5-bromo group, while compound EE5 which is the most active has a 5-chloro group.

Lipinski's rule of five (Ro5) implies that a compound is more likely to exhibit poor absorption or permeability if the compound violates 2 or more of the following parameters.(132)An ideal pharmacophore model should have the characteristics below;

i. A molecular weight of <500 g/mol
ii. <5 hydrogen bonds donors (HBD) or <10 hydrogen bonds acceptors (HBA)
iii. A calculate Log P (octanol/water partition coefficient) < 5

Data shown in Table 3.3 indicates that all the *in silico* designed compounds have less than 5 hydrogen bond donors, less than 10 hydrogen bond acceptors. Compared to the LogP value of chloroquine (4.4), Compound EE1, Compound EE5, and Compound EE3 have a higher logP value. Compound EE4 and Compound EE8 logP values were lower than that of the logP value of chloroquine. The molecular weights of all the *in silico* designed compounds are below 500 g/mol. Some of the *in silico* designed compounds (EE3, EE4, EE7 and EE8) comply with at least three of the Lipinski's rules.

Quantitative Estimate of Drug-likeness (QED) (Table 3.1) rank compounds according to their predicted drug-likeness and the compounds are ranked between zero (all properties unfavourable) and one (all properties favourable).(129)The predicted QED values for all six compounds range from 0.591 - 0.826. The range of values is very close to 1, which is associated with favourable properties for drug-likeness.

Table 3.3 The Quantitative Estimate of Drug-likeness calculated for the candidate compounds series

Properties	CQ	EE1	EE5	EE3	EE7	EE4	EE8
Molecular weight (<500 g/mol)	319.9	454.69	487.70	464.15	410.24	443.25	419.70
logP (<5)	4.4	5.36	5.20	4.57	4.40	3.88	3.71
HBD* (<5)	1	1	1	1	1	1	1
HBA* (<10)	3	3	3	4	4	4	4

HBD; Hydrogen bonds donors, HBA; Hydrogen Bonds Acceptor

The octanol-water partition coefficient (LogP) is an important parameter to determine the molecules hydrophobicity. Hydrophobicity is an essential parameter in the determination of drug absorption, bioavailability, hydrophobic drug-receptor interactions, metabolism of molecules as well as their toxicity.(133) LogP values are calculated using the formula below;

$$\text{Log P } ({}^{oct}/_{water}) = \text{Log } \frac{[Solute]\ unionized\ octanol}{[Solute]\ unionized\ water} \quad (134)$$

The LogP has been regarded as one of the critical properties to determine QSAR. All the candidate compounds showed a LogP value of higher than ±3.71/0.75, which is an indication of high lipophilicity (hydrophobic). In the hydrophobic compartment, there would be a wide distribution of lipophilic drugs.(134) Compounds with the Br group showed lower LogP values in comparison to compounds with the Cl group, thus improved lipophilicity of this chloro- compounds.

3.2 Culturing of asexual and sexual stage of the *P. falciparum* parasites

The *P. falciparum* 3D7 (chloroquine-sensitive), and K1 (multidrug resistant strain) were maintained in uninfected RBC at 5% haematocrit (hct) in complete culture medium. The different stages of the *P. falciparum* asexual cycle were obtained as follow;

Stages	Small Rings	Large rings	Early trophozoites	Late trophozoites	Schizonts
Morphology					
Time post invasion (h)	6-8	16-26	30-32	34-36	42-44
Features	Central vacuole surrounded by blue cytoplasm and contain no pigment	Contain a larger vacuole surrounded by a blue cytoplasm. The parasite reaches a diameter half that of an RBC	Dark cytoplasm, with a single nuclear region, and an enlarged cytoplasm	Spherical with a single irregular shaped nucleus. The cytoplasm stains strongly blue and is slightly amoeboid shaped	Nuclear division results in the production of merozoites. Cytoplasm is paler >5 nuclei

Figure 3.5: Microscopic images are highlighting the characteristics of the different stages of the asexual cycle of the 3D7 *P. falciparum* stained with Giemsa stain. Photographs were taken at 100x magnifications (Ostec 5 Mega Pixels USB Camera, 100x oil immersion lens).

The production of *P. falciparum* gametocytes was initiated by applying environmental stress to the asexual parasite culture (nutrient starvation and drop in haematocrit).(125, 135)

Stages	I	II	III	IV	V
Morphology					
Days after initiation	2-3	3-5	4-7	8-9	9-12
Features	Lightly stained or clear cytoplasm small rounded parasite containing no vacuole	One side of the parasites become extended giving half-moon shape with pointed ends. With one side smoothly rounded and the other straight	Pointed ends become bluntly rounded. The RBC becomes distorted along the length of the gametocyte	The parasite continues to elongate, and the two ends become pointed	Rounding off the ends of the gametocytes and the gametocytes body is curved at the ends

Figure 3.6: Light microscopy photography of the different stages *P. falciparum* EG16-pfs16-GFP-Luc sexual development stained with Giemsa stain. Photographs were taken at 100x magnifications (Ostec 5 Mega Pixels USB Camera, 100x oil immersion lens). The gametocytes differentiate during maturation into 5 distinct stages (I - V). The female ♀ (macrogametocytes) have closely aggregated chromatin and pigment granules at the centre of the parasite. The males ♂ (microgametocyte) chromatin and pigment granules are more dispersed.

3.3 Dual point evaluation of the inhibition of asexual stage of the *P. falciparum* proliferation

Initial screening of the candidate compounds was performed on the drug sensitive *P. falciparum* 3D7 strain that was treated with the 6 compounds at fixed doses of 1 and 5 µM for 96 h at 37ºC and the inhibition of parasite proliferation determined using SYBR green I fluorescence as described above (Section 2.3) and analysed using GraphPad Prism v5.0 or Microsoft Excel (Figure 3.7).

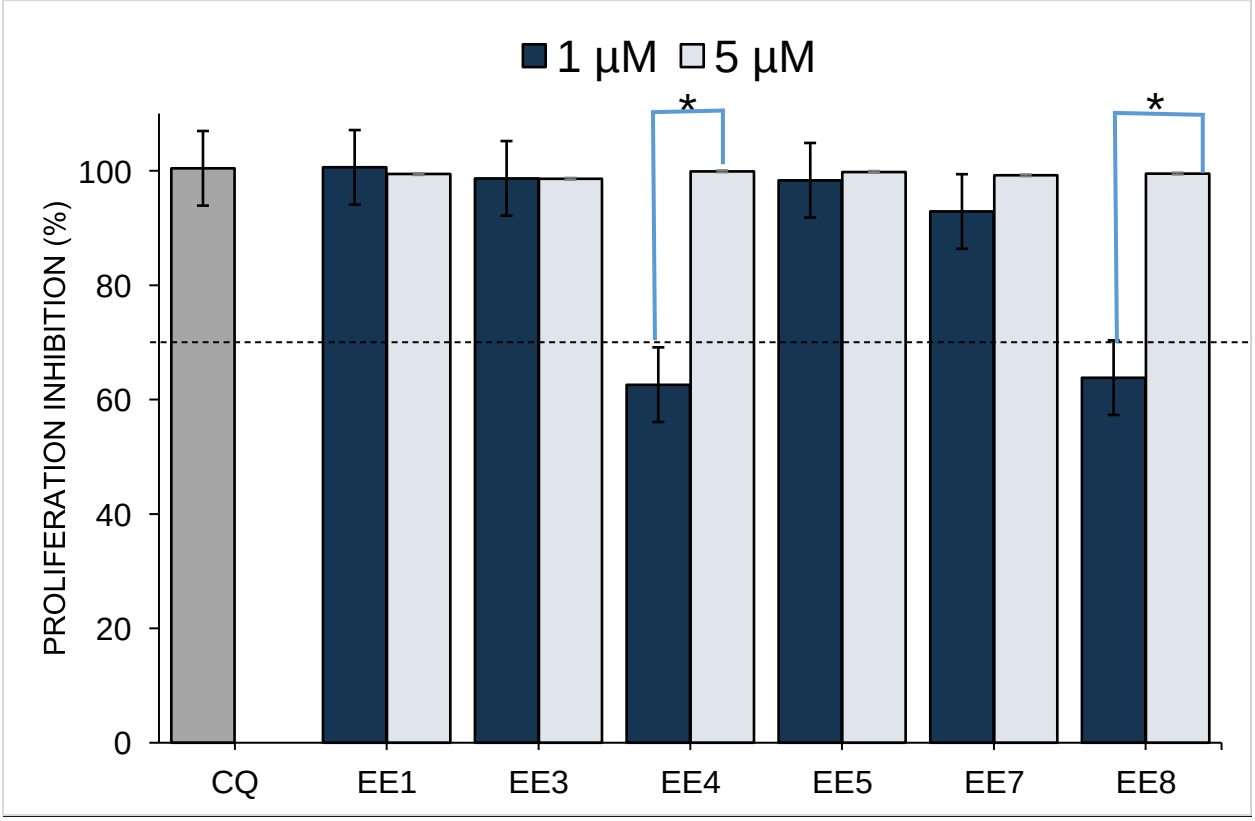

Figure 3.7: Dual point screening of potential antimalarial drugs in the asexual stage. The MSF assay was set up using synchronized ring stage *P. falciparum* parasite suspensions (1% parasitaemia at 1% haematocrit), which were treated with chloroquine (CQ=0.5 µM) and the candidate compounds (1 µM and 5 µM). The percentage proliferation inhibition was calculated for each compound relative to untreated controls. Data are the means of at least four independent experiments performed in triplicate ± S.E.M. Significance difference between chloroquine and the candidate compounds was calculated using two-tailed student *t*-test at **P*<0.05.

All 6 compounds prevented parasite proliferation at 5 µM, similarly to chloroquine. However, only compounds EE1, EE3, EE5 and EE8 maintained activity of >70% at 1 µM (P<0.05) as well and these were the compounds selected then for further dose-response evaluation.

3.2.1 IC_{50} determination

The four compounds prioritised for full dose-response evaluation were subsequently evaluated in triplicate for at least six independent biological replicates (Figure 3.8). For the dose-response curves, data were represented as a percentage of untreated control to determine cell viability. Sigmoidal dose-response curves (Figure 3.8), were plotted using GraphPad 5.0, from which the IC_{50} values were determined.

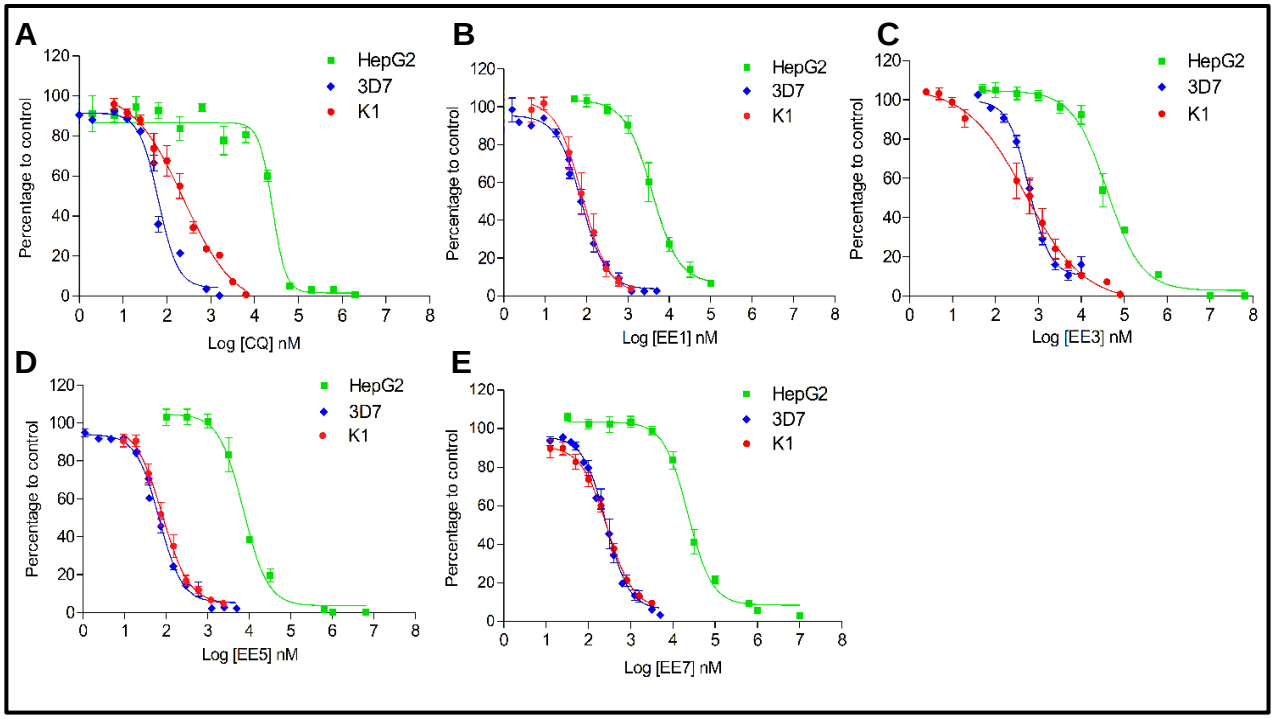

Figure 3.8: The percentage *P. falciparum* parasite growth and hepatocarcinoma cell inhibition exposed to in silico candidate compounds EE1, EE3, EE5, and EE7. HepG2 cells (green square) and *P. falciparum* strain 3D7 (blue triangle) and K1 (red circle) when exposed to compounds (A) CQ (B) EE1 (C) EE3 (D) EE5 and (E) EE7. The MSF assay was used to analyse the *P. falciparum* 3D7 strain and K1 strain to obtain the dose response curves above, from which the corresponding IC_{50} values were calculated. Data are the means of at least six independent experiments performed in triplicate ± S.E.M. Significant differences between CQ IC_{50} and the candidate compounds IC_{50} was assessed using two-tailed student t-test were shown as *** at P<0.001.

Sigmoidal dose response curve showing the antiplasmodial activity of the candidate compounds EE1, EE3, EE5 and EE7 are represented in Figure 3.8 above. From these

graphs, it is significantly clear how the candidate compound has increase efficacy to *Plasmodium* species (blue triangle and red circles) in comparison to the HepG2 (green square).

When assessing the dose-response curves obtained from K1 (blue triangle) and 3D7 (red circles), there was no significant IC_{50} curve shifts for all the candidate compounds. This suggest that the 3D7 strains are adequate for parasite stage specificity and speed assay analysis. The different IC_{50} values from the corresponding dose-response curves were summaries in the Table 3.4 below. Statistically significant difference (P<0.001) between the effect of the candidate compounds on the different strains was determined using two-tailed student t-test.

Table 3.4: IC_{50} values of *in silico* compounds after 96 h on different *Plasmodium* parasite strain and HepG2 cell. Resistance index (RI) and Selectivity Index (SI) values for candidate compounds relative to chloroquine

Compound	3D7	K1	HepG2	SI	RI
Chloroquine	64 ± 3.0	240 ± 6.0	4.5 x10^4 ± 115.1***	3	700
EE1	76 ± 1.4	80 ± 3.8	4.0 x10^3 ± 188.8***	1.1	52.8
EE3	592 ± 2.0	433 ± 7.0	4.1 x10^4 ± 111.0***	0.7	68.6
EE5	62 ± 2.3	95 ± 2.1	7.3 x10^3 ± 113.0***	1.2	117.1
EE7	264 ± 1.3	327 ± 1.1	2.5 x10^4 ± 119.0***	1.1	94.1

Data is reported in nM ± SEM, n=6. Statistically significant differences in IC_{50} values between the different strains of each candidate compound as compared to chloroquine is shown as ***P<0.001; as tested by the two-tailed student t-test. RI values are the ratio of IC_{50} of resistant strain/IC_{50} of a sensitive strain of *P. falciparum* parasites, and SI is the ratio of the IC_{50} of HepG2 cells/IC_{50} of a sensitive strain of *P. falciparum* parasites.

During this study, the IC_{50} values of chloroquine was determine as a reference to interpret results obtained from the candidate compound. The IC_{50} values for chloroquine on the 3D7

and HepG2 strain (Table 3.4) were 3 times higher than the IC_{50} values (23 nM and 640 nM, respectively) obtained by Delves et al., (2012).(136)This could be due to genetic shift in culture strain and diversity of the origin of the strain. From these results it is apparent that CQ has enhanced potency in comparison to all the other candidate compounds on both the 3D7 and K1 *P. falciparum* strain. Candidate compound EE5 showed to be the most potent on the 3D7 *P. falciparum* strain *(*approximately 4-fold lower than CQ) amongst all the other candidate compounds. Candidate compound EE3 was the least potent at concentration approximately 39-fold greater than CQ. Candidate compound EE1 and EE5 were the most potent against the K1 compared to the rest of candidate compounds and chloroquine.

The resistance index (RI) of the candidate compounds was established by obtaining the ratio of IC_{50} of resistant strain to the IC_{50} of a sensitive strain of *P. falciparum* parasites, and selectivity index (SI) which is the ratio of the IC_{50} of HepG2 cells to the IC_{50} of a sensitive strain of *P. falciparum* parasites (Table 3.4). Drugs with SI values of above 1000 have acceptable selective toxicity according to the MMV guidelines. But all candidate compounds including chloroquine had SI values of less than 1000. Good RI values should be less than 10, so far, all the candidate compounds had an SI value of less than 10.

Resistance index of these series of *in silico* compounds is significantly below the RI value calculated for chloroquine (Table 3.4). The compound with the highest resistance indices of the four *in silico* designed candidate compounds was compound EE5, followed by compound EE1 and EE7. Selectivity index is a significant parameter to evaluate for new derivatives in the drug discovery pipeline. This is because a compound should be more specific to the *Plasmodium* parasites rather than the human cells.(137) The selectivity index of the candidate compounds ranged from 11-fold to 53-fold. Of the four candidate compounds, compound EE5 was the most selective towards the *P. falciparum* parasites. The highest SI for this series of compounds was compound EE1 showing a 53-fold more selectivity towards *P. falciparum* parasites and 200-fold lower than the 1000 times required.

3.3 Inhibition of sexual stage (gametocytes) viability of *P. falciparum* parasites

For a compound to be classified as a good gametocidal drug that would act as a malaria transmission blocking agent, it needs to show activity against both the early and the late stages of the gametocytes. Early stage gametocytes of the *P. falciparum* EG16-pfs16-GFP-Luc strain that has been transfected to carry luciferase activity, were treated in three separate experiments with 6 candidate compounds at 1, and 5 µM for 48 h at 37^{o}C (Figure 3.9) and gametocyte viability assessed using luciferase reporter expression as described above (Section 2.13).

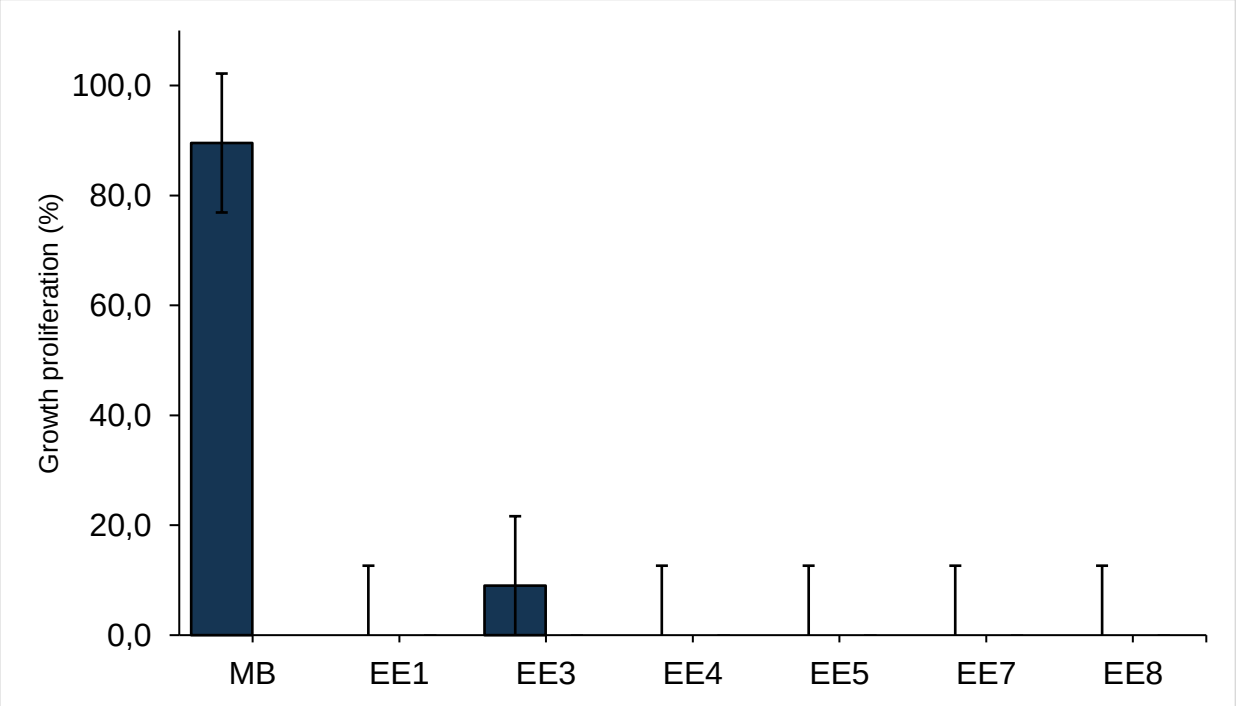

1 µM	89.5±5.1	0.0±0.0	0.0±0.0	0.0±0.0	0.0±0.0	0.0±1.2	0.0±0.0
5 µM		0.0±0.0	9.6±0.2	0.0±0.0	0.0±0.2	0.0±0.3	0.0±0.0

Figure 3.9: Dual point screening of potential antimalarial drugs in the early gametocytes. The luciferase assay was set up using *P. falciparum* EG16-pfs16-GFP-Luc early stage gametocytes on Day 5 at (2% parasitaemia and 4% haematocrit), which were treated with methylene blue (MB) at 5 µM and the candidate compounds at 1 µM and 5 µM. The 96-well plates were incubated at 5% O_2, 5% CO_2, and 90% N_2 in a stationary incubator at 37^{o}C for 96 h. The percentage inhibition was calculated for each treatment. Data are the means of at least three independent experiments performed in triplicate ± S.E.M. No significant difference between candidate compound activity at 1 µM and 5 µM was obtained as calculated using two-tailed student t-test.

As assessed by the two-tailed student t-test, none of the candidate compounds showed any significant inhibitory activity on the early gametocytes at 1 µM when compared to methylene blue (MB) as a positive control; only compound EE3 showed a marginal 9.6% inhibition of the early stage gametocytes at the higher test concentration of 5 µM.

Late stage gametocytes of the *P. falciparum* parasites (EG16-pfs16-GFP-Luc) were similarly evaluated for their ability of the 6 candidate compounds to inhibit their viability at 1 and 5 µM (Figure 3.10). However, only marginal (<20%) inhibition was observed for all the compounds, even at the highest concentration tested.

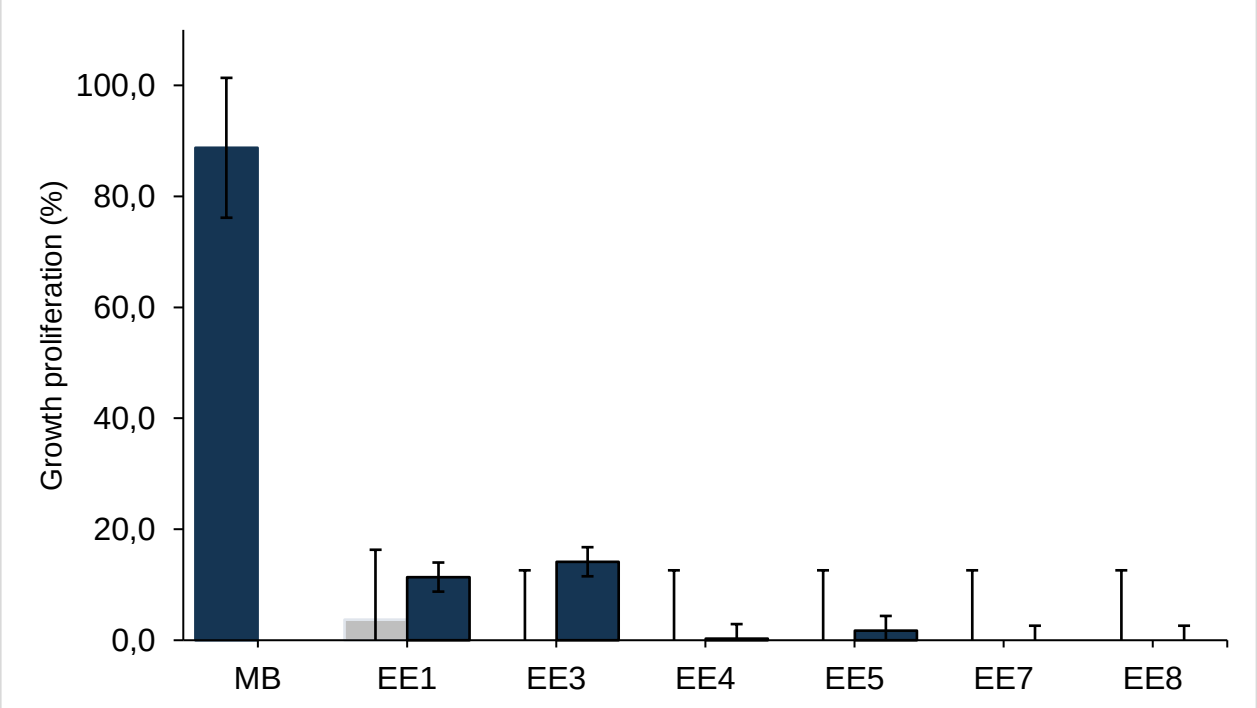

1 µM	88.7±4.1	3.7±4.0	0.0±0.0	0.0±0.0	0.0±0.0	0.0±1.2	0.0±0.0
5 µM		11.4±1.0	14.1±0.2	0.3±1.0	1.8±0.2	0.0±0.3	0.0±0.0

Figure 3.10: Dual point screening of potential antimalarial drugs in the late gametocytes. The luciferase assay was set up using *P. falciparum* EG16-pfs16-GFP-Luc late stage gametocytes on Day 10 at (2% parasitaemia and 4% haematocrit), which were treated with methylene blue (MB) at 5 µM and the candidate compounds at 1 µM and 5 µM. The 96-well plates were incubated at 5% O_2, 5% CO_2, and 90% N_2 in a stationary incubator at 37°C for 96 h. The percentage inhibition was calculated for each compound relative to the negative control. Data represent the means of at least three independent experiments performed in triplicate ± S.E.M. No significant difference was obtained as calculated using two-tailed student t-test.

3.4 Speed of action and stage specificity analysis

The speed assay was performed to determine whether the compounds are slow or fast acting and the compounds were tested against the different stages of *P. falciparum* parasites (rings and schizonts) according to Le Manach et al., (2013).(123) Sigmoidal dose response curves of the candidate compounds were obtained at different time periods; 48, 72 and 96 h incubations (Figure 1.11). Distinct dose-response curve were obtained from the different time periods and there was right shift in the IC_{50} curves between 48 and 72 h.(137, 138)

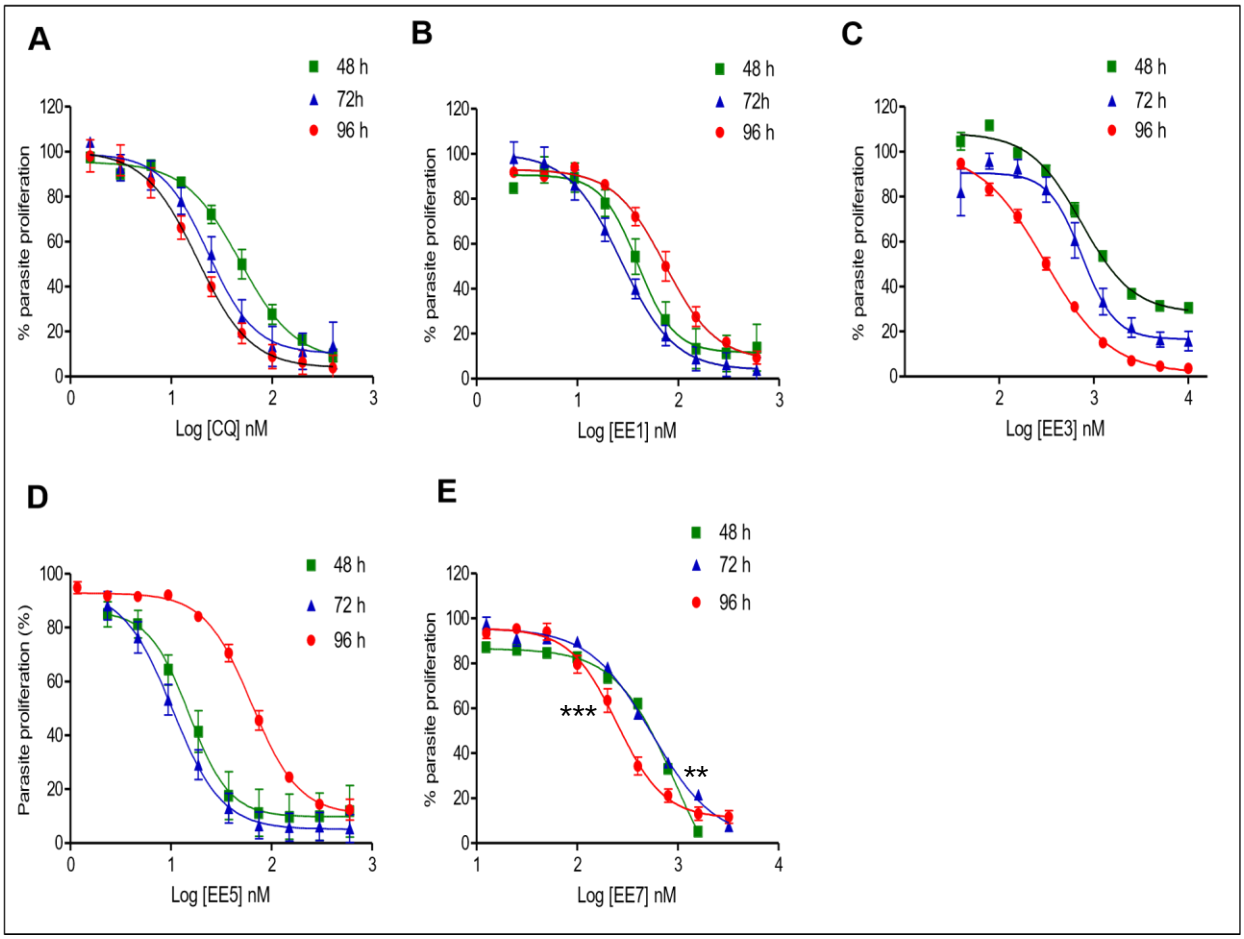

Figure 3.11: IC_{50} speed assay on 3D7 synchronized culture; The candidate compounds were screened against the drug sensitive *P. falciparum* 3D7 strain for 48, 72 and 96 h at 37°C and parasite proliferation was determined using fluorescence SYBR Green 1 assay. The graphs A) CQ, B) EE1 C) EE3 D) EE5 and E) EE7 represent the sigmoidal dose-response curves for the candidate compounds. Data are the means of at least four independent experiments performed in triplicate ± S.E.M. Significant difference (***P < 0.001 and **P < 0.01) was calculated using two-way ANOVA and tukey posthoc test to determine the significant difference between the different time periods.

The IC_{50} values of the candidate compounds at the different time periods (48, 72 and 96 h) were obtained from their corresponding dose-response curve (Figure 3.12) and summarised in Figure 3.12 below. Significant difference (*P*-value<0.05) was determined between the 48, 72 and 96 h for each candidate compounds EE1, EE5 and EE7 using the two-way ANOVA.

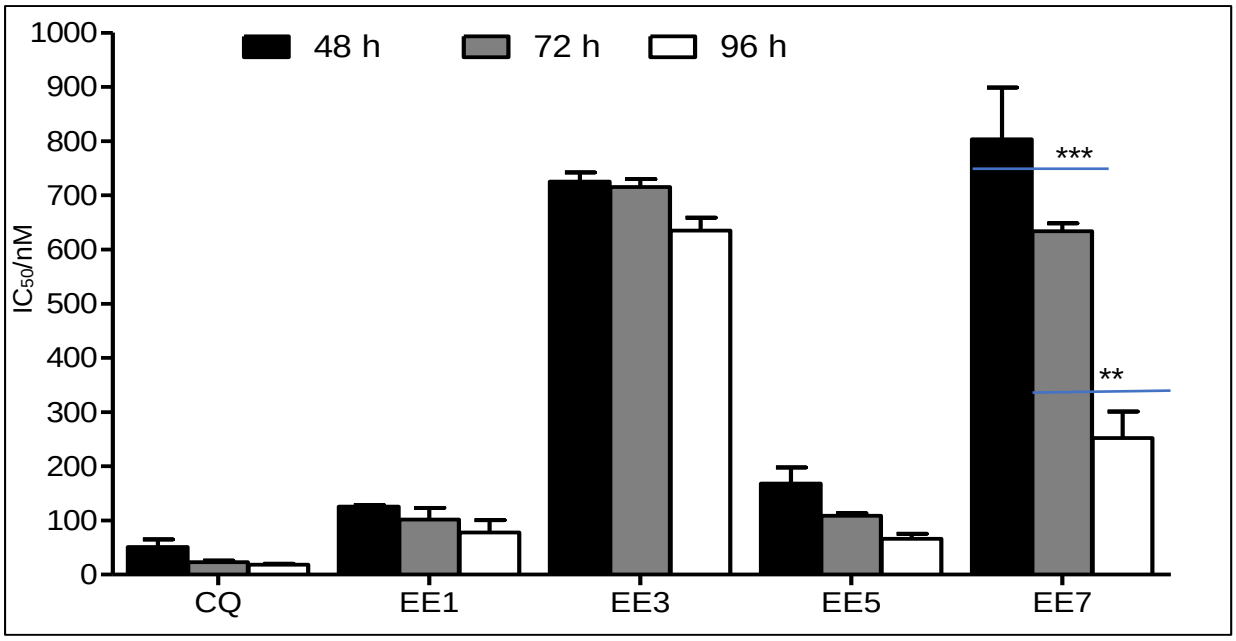

Figure 3.12: IC_{50} speed assay (3D7 synchronized culture; mean ± SEM n = 3 per assay). Candidate compounds, EE1, EE3, EE5, and EE7 treated for 48 h (black), 72 h (grey) and 96 h (white). Significant difference (****P* < 0.001 and ***P* < 0.01) was calculated using two-way ANOVA and tukey posthoc test to determine the significant difference between the different time periods.

.

Candidate compounds can either be classified as fast-acting or slow-acting by obtaining the ratio IC_{50} 48 h/ IC_{50} 72 h as described by method from Le Manach *et al.,* (2013).(123) (Table 3.5) According to this method, fast-acting compounds are considered to have a ratio of less than 1.5 and slow acting compounds are considered to have ratio of greater than 1.5. Candidate compounds EE1, EE3, and EE7 have a ratio of less than 1.5, however candidate compound EE5 had a ratio slightly higher.

Table 3.5: Data summary of IC_{50} values for speed assay analysis

Compounds	IC_{50} (nM)			Ratio IC_{50} 48 h/ IC_{50} 72 h
	48 h	72 h	96 h	
CQ	50.70 ± 4.19	22.94 ± 3.5	18.42 ± 2.0	1.1
EE1	125.60 ± 3.18	101.93 ± 2.2	77.91 ± 2.2	1.2
EE3	725.27 ± 5.22	715.60 ± 1.5	634.83 ± 2.1	1.0
EE5	168.33 ± 5.7	108.58 ± 2.3	66.30 ± 1.7	1.6
EE7	803.33 ± 2.5	634.00 ± 1.5	252.0 ± 2.1	1.3

The candidate compounds were tested against the different asexual stages (ring and schizonts) of the 3D7 *P. falciparum* parasite strain for a 48 h incubation period. Comparing the susceptibility of the candidate compounds on schizonts and rings using two-tailed student t-test. There was a significant difference at (*$P < 0.05$) between the activity of the candidate compounds on both the rings and the schizonts.

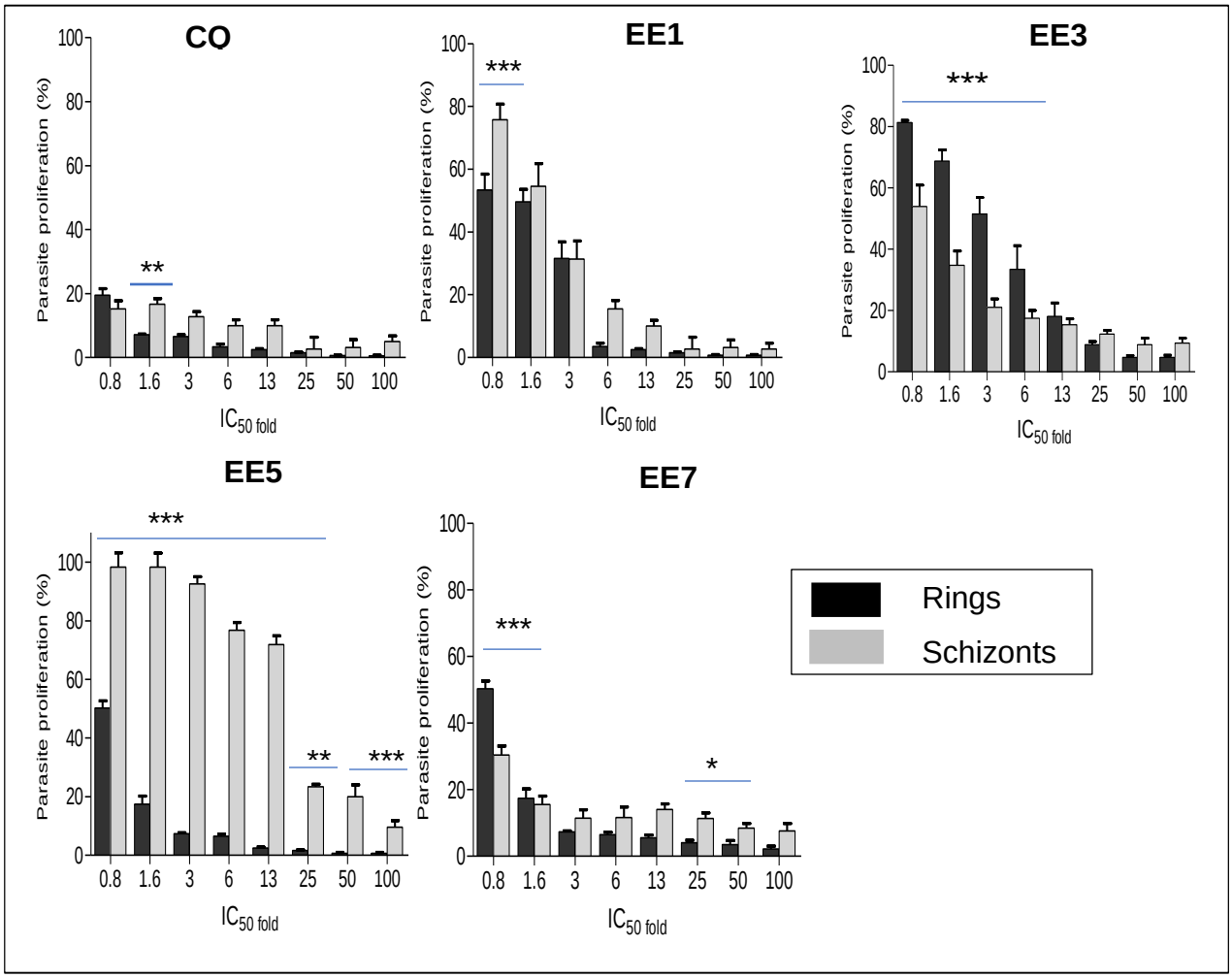

Figure 3.13: Stage-dependent effects of candidate compounds on synchronous cultures of *P. falciparum* strain 3D7. Cultures were exposed to 8 different concentrations of the compound for 48 h. The candidate compounds effects were assayed using the Malaria SYBR Green assay. The black bar and the grey bar represent the ring and schizont stage respectively. Each bar represents the mean ± SEM of n = 4 independent experiments. Significant difference (***$P < 0.001$, **$P < 0.01$ and *$P < 0.05$) was calculated using two-way ANOVA and tukey posthoc test to determine the significant difference between the schizonts and the rings.

For a candidate compound to be characterised as either slow-acting or fast-acting, is concluded from comparing both the speed assay and stage specificity analysis data (Table 3.6).

Table 3.6: Data summary of IC_{50} speed assay and stage specificity analysis

Compound	Speed assay	Conclusion	Stage assay	Conclusion	The speed of action
	[a]IC_{50} speed assay		[b]Action on different stages		
Chloroquine (positive control)	1.1	Fast	>95% on R >95% on S	Fast	Fast
EE1	1.2	Fast	>95% on R >85% on S	Fast	Fast
EE3	1.0	Fast	~65-95% on R ~80-90% on S	Fast	Fast
EE5	1.6	Fast	>95% on R ~25-90% on S	Slow	Fast/slow
EE7	1.3	Fast	>95% on R >90% on S	Fast	Fast

[a]IC_{50} speed assay (Ratio IC_{50} 48h/ IC_{50} 72h) and stage-specific analysis at 6-100x IC_{50} [b]S and R are synonyms for schizonts and ring stages, respectively [c] Ratios are means from ≥4 experimental repeats done using the chloroquine sensitive P. *falciparum* 3D7strain.

Chloroquine proved to be a fast-acting compound (Table 3.6) and showed a >95% activity on both the schizonts and the rings. These results confirm previous data obtained from Le Manach et al., (2013)(123), Sanz et al., (2012)(139) and Maerki et al., (2006).(123) The same effect was found for EE1, EE3, and EE7 which all showed fast acting potential and gave consistent results with both the rate and stage specificity assay, but candidate EE5 did not show the same effects. Compound EE1 showed a similar stage-specific and rate profile like chloroquine with predominantly strong action against the rings. Compound EE1 showed activity against the schizonts of <50% at 3x IC_{50} (95.3 nM - 762.5 nM) and >95% in the higher concentration range (1525 nM - 12200 nM).(139) Compound EE3 presented a similar stage specificity profile to that of atovaquone with a significant action on the schizonts but with limited activity against the ring stage that was <50% inhibition at concentrations up to 3x IC_{50} (194.5 nM-1556.3 nM) and >95% in the higher concentration range (3112.5 nM-49800 nM).(123)

Compound EE7 showed high activity against both asexual stages (>90% inhibition of both rings and schizonts in the 6-100x IC_{50} range, 8300 nM-132800 nM), which suggest it is a fast-acting compound, like the results obtained from the IC_{50} speed assay. The only molecule not showing fast acting results was compound EE5. The data from the IC_{50} speed assay suggests it is a fast-acting compound with a 1.6-fold IC_{50} 48 h/IC_{50} 72 h shift. However, the stage-specificity assay indicates a slow action on schizonts (<30% activity at concentrations up to 13x IC_{50} (50 nM – 1600 nM) and only ~75-90% inhibition at the three highest concentrations tested (1600 nM-12800 nM).

CHAPTER 4
DISCUSSION

Malaria is one of the prominent diseases affecting most of the developing countries in the world. The *Plasmodia* protozoan genus is the causative agent of malaria and is transmitted to the human host by the female *Anopheles* mosquitoes during a blood meal. According to recent WHO reports, about 212 million people are affected by malaria annually. Although there is progress in the development of new antimalarial treatments and avoidance strategies, continuous improvements in drug treatments are required to eradicate malaria completely. Several problems arise, due to the persistent development of resistance by the parasite to the currently available antimalarial drugs, which emphasises the need for continuous research to derive new antimalarial pharmacophores with a novel mechanism of action.

Thousands of compounds previously screened for antimalarial activity by Gamo et al. (2010),(81) reported showing activity against 3D7, Dd2 and HepG2 cells at 10 µM. From this list, compounds with a less than 20% proliferation inhibition against human transformed liver HepG2 at 10 µM, and more than 80% growth inhibition at 2 µM against DD2 were selected. Compound TCMDC-137587 was the most potent compound (5.29 nM) against 3D7 cells, and 72 other compounds from chemical cluster 87 of the compounds screened. From chemical cluster 87, 3 compounds (Figure 1.6) had the 2,6-Dimethyl-3-phenylpyridin-4(1H)-one core structure in common. This core chemical scaffold was then used to design more potent antimalarial compounds.

In 2015, Capper identified the Q_i-site as the target for 4(1H)-pyridones(82) (Figure 1.6C). The *Bos Taurus* cytochrome bc_1 (PDB code:4d6t) was crystallised together with the bound GW844520 inhibitor. This structure provided the unique opportunity to use computer-aided drug design tools to design new and more potent antimalarial drugs that specifically target the Q_i site of the mitochondrial cytochrome bc_1. By targeting the Q_i site, parasite death can potentially be induced through three different mechanisms.(83) The

potential mechanisms was via ATP starvation due to decreased proton motive force, via pyrimidine starvation and lastly via excessive reactive oxygen species (ROS) production.

From previous studies, the pyridines, which are derivatives of quinolones, are a multitarget pharmacophore model that has been suggested as an antimalarial drug.(140, 141) Following promising results from these candidate compounds, 2,6-Dimethyl-3-phenylpyridin-4(1H)-one derivatives were designed with improved pharmacokinetic parameters. There is increasing evidence that minor modification to a drug candidate can result in major changes in pharmacological properties The halogenation of a compound should allow for it to maintain or improve its essential pharmacokinetic and pharmacodynamic parameters.(142) Halogens are reported to be adequately similar in conformation and steric size when compared to the hydrogen and should fit into the catalytic site without any steric interference.(143) The halogens are reported as hydrogen bond acceptors, promoting hydrogen bond formation with the protein active site which increases binding energy.(144) The carbon-halides bond is strong and stable, making compounds more resistant to metabolic degradation. Six compounds with a 2,6-Dimethyl-3-phenylpyridin-4(1H)-one core structure was designed according to the binding efficiency at the active site of the *Plasmodium* homolog of the cytochrome bc_1 protein and adherence to the requirements for drug-likeness of a compound. These six compounds were synthesised under contract by chemical synthesis company and chemically characterised to confirm the structures and the purity of the compounds synthesised. The inclusion of the halide (either chloride or bromide) on the aromatic rings, as shown in Table 3.2, were tested for their contribution to drug-likeness of the final molecule.

The drug-likeness of compounds is used to predict the pharmacokinetics (ADME) of the compound within an organism, and which is influenced by rules such as Lipinski's Rule of Five.(66, 129, 145) Lipinski's rules state that a compound is more likely to show reduced permeability and metabolism when two parameters are out of range. The critical parameters are; a compound should not have a molecular weight of more than 500 g/mol, not more than five HBD or ten HBA and a LogP value of less than five.(134)

The LogP value refers to the lipophilicity of a compound and is essential for compound absorption, drug-membrane interactions, metabolism, and toxicity.(132) Regarding absorption from the gut wall into blood circulation, the predicted data ranges of the six newly synthesised *in silico* designed candidate compounds do not significantly differ from that of chloroquine. Compound EE1 and compound EE5 were more lipophilic than CQ. Increased lipophilicity refers to the improved ability of compounds to dissolve in fats, oils, lipids, bind to lipid-carrier plasma proteins and non-polar solvents. The increase in lipophilicity of the *in silico* designed compounds is due to the addition of the halides group to improve compound lipid solubility and the likelihood of therapeutic success.(146, 147) The mitochondrial inner membrane space is known to be an acidic environment, upon diffusion of the 3-phenylpyridin-4(1H)-one into the membrane space (Figure 1.5); this results in the oxidation of the candidate compounds. However, despite the efficacy of LogP, it is important to mention that LogP cannot be used to determine the probability for a compound to dissociate, giving several by-products.(133, 148)

A compound's aqueous solubility is very important for an efficient and effective delivery into an organism compartment. The aqueous solubility of a compound depends on a variety of factors such as the HBD and HBA properties of the molecule as well as the energy of solubilisation by disruption of molecule's crystal lattice.(134) When the number of HBD and HBA exceed recommended parameter, the compound becomes too polar, with the increase in polarity affecting the permeability of compounds across the lipid bilayer.(66, 134) Candidates compound EE3, compound EE4, compound EE7 and compound EE8 had four HBA and CQ had three, predicting that the compounds are more polar than CQ.

The QED value of compounds can range between zero and one. This range usually characterises compounds from all unfavourable properties for drug-likeness to all favourable properties for drug-likeness, respectively.(129) The QED value was used to show that the *in silico* designed compounds do have drug-likeness properties which might not correlate with the Lipinski rules of five yet comply with the Lipinski rules.(132) The

candidate compounds (EE1, EE3, EE5, and EE7) had QED values ranging from 0.497-0.643, which suggests that these compounds have a moderate favourability for drug-likeness(Table 3.1). This can also agree with the good potency determined for the IC_{50} results obtained on the drug-sensitive and drug resistant strains of *Plasmodium falciparum*.

The antiplasmodial activity of the *in silico* designed candidate compounds was assessed for several characteristics using *P. falciparum* strains with different drug sensitivity. The initial tests were done at fixed doses of 1 µM and 5 µM as a screening assay which already eliminated two of the candidate compounds (EE4 and EE8) due to low cytotoxicity (Figure 3.7). For the remaining four candidate compounds the IC_{50} values were determined using a range of different concentrations for each compound on both chloroquine-sensitive and chloroquine-resistant laboratory strains of *P. falciparum.* The IC_{50} values were in the nanomolar range and showed that there are no signs of cross-resistance and that the compounds are effective active against different parasite phenotypes. These results showed that compound EE1 and compound EE5 were the most potent compounds in this series. There is a relatively small correlation between the lower IC_{50} values and the higher binding efficiency of the compounds. This can be accounted for by the presence of a Br atom in the molecule that could aid in increase permeability and improve the potency of the compound *in vitro.*

Following the antiplasmodial activity results, the resistance index (Table 3.4) was calculated by dividing the IC_{50} value of the non-resistant strain (3D7) to the IC_{50} value of the resistant strain (K1). The resistance index represents the drugs' efficacy against resistant parasite versus the corresponding non-resistant parasite. The RI values of all *in silico* designed candidate compounds are less than that of CQ, which indicates a lower level of efficacy towards the resistant cell line and hints at a different mechanism of action. All the candidate compounds had a resistance index value ranging from 0.7-1.2, though compound EE5 had the highest resistance index of 1.2 (Table 3.4).

The therapeutic efficacy of most current antimalarial compounds is compromised due to either side effect toxicity or drug resistance by the parasite.(149) Due to the extremely high incidence of malaria in pregnant women and children below the age of five, antimalarial drugs need to act efficiently and effectively.(150) To further test for *in vitro* cytotoxicity against human cells the compounds were screened using HepG2 hepatocarcinoma cells (data in Table 3.4) as per the recommended protocols for cytotoxicity screening in human cells. Selectivity is a critical drug property to evaluate as non-selective cytotoxicity of drugs may results in serious side effects due to cytotoxicity of specific organ cells in the human patient. An ideal new drug should be efficacious and safe when administered to humans.(120) The calculated selectivity indices show that all four compounds tested against HepG2 cells are indeed more selective towards the parasites than mammalian cells (Table 3.4). From the selectivity index data compound EE5 had the highest selectivity index of 117-fold more selective towards parasite cells than mammalian cells but way below the 1000x recommended threshold. Not only is it the most selective compound but was also more effective against resistant strains than the other candidate compounds tested and shows the lowest IC_{50} value.

Fast-acting compounds are of great interest because they provide rapid parasitaemia clearance.(151) and decreasing the probability of occurrence of resistance mutations.(123) The mutations already found in the *P. falciparum* due to long term exposure to drugs might lead to the development of resistance to new drugs through similar mechanisms. In a clinical setting, fast-acting compounds provide rapid relief of symptoms for the patients.(152) Three of the designed candidate compounds (EE1, EE3, and EE7) were fast-acting while candidate compound EE5 was slow acting despite showing the most promising low IC_{50} value (Table 3.6).

For a compound to be classified as a good transmission blocking drug, it needs to show inhibitory activity against both the early and the late stages of the gametocytes. Suppressing the formation of gametocytes will prevent the subsequent transmission to the mosquito vector, thereby halting the infection cycle. Only candidate compound EE3

showed a 9.6% inhibition of the early stage gametocytes at 5 µM (Figure 3.9) and two compounds, EE3 (14.1%) and EE1 (11.4%) showed minor inhibitory activity against the late gametocyte at 5 µM (Figure 3.10) compared to the positive control used, methylene blue. These compounds accumulate in the mitochondrial membrane space, leading to decrease effectiveness.

The results obtained from this dissertation shows that chlorination of candidate compound EE1 and EE5 led to improved antiplasmodial activity to a lower nanomolar IC_{50} concentration range and improved selectivity. (Figure 1.5) All the candidate compounds showed minor gametocidal activity which is a major drawback for the compound to be characterised as a multi-stage and single dose efficacious compound. The low selectivity index value is also disadvantageous as the compounds has to show less toxicity to the mammalian cells. The Q_i site of the cytochrome bc_1 is not a good target as is located in the inner mitochondrial membrane which is impermeable to ions and small molecules. Further experiments should consist of optimising the candidate compounds to be efficient and more effective on the gametocytes.

CHAPTER 5

CONCLUDING DISCUSSION AND RECOMMENDATION

4.1 Concluding remarks

This study aimed to assess the efficacy of six potential antiplasmodial drugs designed *in silico* to specifically target the Q_i site of cytochrome bc_1. These candidate compounds possess low drug-likeness properties using *in silico* prediction models. The QSAR shows that the 2,6-Dimethyl-3-phenylpyridin-4(1H)-one provide structural properties good for antiplasmodial activity. This is the first series of compounds designed in South Africa to target the Q_i site of the cytochrome bc_1 and all the candidate compounds tested displayed broad antiplasmodial activity in the nanomolar range on the asexual stages of *Plasmodium* parasite. Two of the six candidate compounds didn't show significant activity against the *P. falciparum* parasite to warrant further testing. The candidate compound EE5 was the most potent and effective against all the asexual stages. All four candidate compounds tested against the HepG2 cells are more selective towards the parasites than the mammalian cells and more efficacious against the resistant parasite strain. The Q_i site of the cytochrome bc_1 is not a good target given the current malaria elimination agenda in South Africa, transmission blocking drugs are very important. But these candidate compounds can be further optimised to target the gametocytes and improved potency against the asexual stages.

4.2 Recommendations

Clinical experience has proven the value of a combination strategy to prolong the clinical use of new antimalarial drugs and to delay the emergence of drug resistance.(153) Drug combinations reduce the probability of *de novo* resistance selection; if a parasite that is resistant to one drug is involved the second drugs should kill it. The rationale behind the combination of drugs with different modes of action is that it decreases the risk of

resistance development against either of the partner drugs and protects each of the partner drugs.(60) Furthermore, when drugs with different modes of action are combined, each one can be used at its optimal dose with a decreased chance of unwanted side effects.(154) Thus, it is essential to assess the 3-phenylpyridin-4(1H)-one derivatives in combination with other antimalarial drugs.

Cross-resistance usually occurs when a single resistance mechanism results in resistance to an entire class of drug.(155) So, assessing the cross-resistance of 3-phenylpyridin-4(1H)-one derivatives against the atovaquone resistant strain TM902CB would be very important.(156) Also, to assess if prolonging treatment might result in a genetic mutation on the cytochrome bc_1.

In newly discovered drugs, it is crucial to determine the specific biochemical interaction through which the drug substance produces an effect. For this reason, it will be essential to determine if any other mechanisms of action are being induced by the 3-phenylpyridin4(1H)-one derivatives. From previous literature studies on quinolones, this might be as a result of ROS induction, glutathione reduction and a decrease in ATP production.(41) Assays to test each of these possible mechanisms needs to be established to assess these different parameters are in fact active mechanisms for these compounds.

Quinolones are known to be effective against the asexual stages which include liver stage (sporozoites). It is essential to determine the effectiveness of 3-phenylpyridin-4(1H)-one on the *Plasmodium falciparum* sporozoite. Additionally, the TCP-1 guidelines require compounds to be active against all the blood stages which include the sporozoites.(51)

References

1. Olliaro PL, Yuthavong Y. An overview of chemotherapeutic targets for antimalarial drug discovery. Pharmacol Ther. 1999;81(2):91-110.
2. WHO. World Malaria Report 2015. Available from [http://www.who.int/malaria/publications/world-malaria-report-2015/report/en/].
3. WHO. World Malaria Report 2016. Available from [http://apps.who.int/iris/bitstream/10665/252038/1/9789241511711-eng.pdf].
4. Alonso PL, Bassat Q, Binka F, Brewer T, Chandra R, Culpepper J, et al. A research agenda for malaria eradication: drugs. PLoS medicine. 2011;8(1):e1000402.
5. Alonso PL, Brown G, Arevalo-Herrera M, Binka F, Chitnis C, Collins F, et al. A research agenda to underpin malaria eradication. PLoS medicine. 2011;8(1):e1000406.
6. Mitchell P. Why the Donkey Did Not Go South: Disease as a Constraint on the Spread of Equus asinus into Southern Africa. African Archaeolog Rev. 2017;34(1):21-41.
7. Cox-Singh J, Davis T, Lee K-S, Shamsul S, Matusop A, Ratnam S, et al. Plasmodium knowlesi malaria in humans is widely distributed and potentially life threatening. Clin Infect Diseas. 2008;46(2):165-71.
8. Cowman A, Crabb B. Invasion of red blood cells by malaria parasites. Cell. 2006;124(4):755-66.
9. Sinka ME, Bangs MJ, Manguin S, Coetzee M, Mbogo CM, Hemingway J, et al. The dominant *Anopheles* vectors of human malaria in Africa, Europe and the Middle East: occurrence data, distribution maps and bionomic precis. Parasites & vectors. 2010;3:117.
10. Miller LH, Baruch DI, Marsh K, Doumbo OK. The pathogenic basis of malaria. Nature. 2002;415(6872):673-9.
11. Miller LH, Ackerman HC, Su XZ, Wellems TE. Malaria biology and disease pathogenesis: insights for new treatments. Nature Med. 2013;19(2):156-67.
12. Aikawa M, Miller LH, Johnson J, Rabbege J. Erythrocyte entry by malarial parasites. A moving junction between erythrocyte and parasite. The J of cell biolog. 1978;77(1):72-82.
13. Phillips R. Current status of malaria and potential for control. Clinical microbiolog reviews. 2001;14(1):208-26.
14. Tuteja R. Malaria− an overview. FEBS J. 2007;274(18):4670-9.

15. Shortt HE, Fairley NH, Covell G, Shute P, Garnham P. Pre-erythrocytic stage of *Plasmodium falciparum*. British Med J. 1949;2(4635):1006.

16. Glushakova S, Yin D, Li T, Zimmerberg J. Membrane transformation during malaria parasite release from human red blood cells. Current biolog. 2005;15(18):1645-50.

17. Bannister L, Mitchell G. The ins, outs and roundabouts of malaria. Trends in Parasitolog. 2003;19(5):209-13.

18. Talman AM, Domarle O, McKenzie FE, Ariey F, Robert V. Gametocytogenesis: the puberty of Plasmodium falciparum. Malaria J. 2004;3(1):24.

19. Sinden R. Gametocytogenesis of *Plasmodium falciparum in vitro*: an electron microscopic study. Parasitolog. 1982;84(01):1-11.

20. Dixon MW, Dearnley MK, Hanssen E, Gilberger T, Tilley L. Shape-shifting gametocytes: how and why does P. falciparum go banana-shaped? Trends in Parasitolog. 2012;28(11):471-8.

21. Ramasamy R. Molecular basis for evasion of host immunity and pathogenesis in malaria. Biochim et Biophys Acta (BBA)-Molecular Basis of Disease. 1998;1406(1):10-27.

22. Wipasa J, Elliott S, Xu H, Good MF. Immunity to asexual blood stage malaria and vaccine approaches. Immunolog and Cell Biolog. 2002;80(5):401.

23. CDC. How Can Malaria Cases and Deaths Be Reduced? [http://www.cdc.gov/malaria/malaria_worldwide/reduction/]. 2015 [updated September 22, 2015.

24. WHO. World Malaria Report, 2013. Available from [http://www.who.int/malaria/publications/world_malaria_report_2013/en/].

25. Farooq F, Bergmann-Leitner E. Malaria Prevention and Control. Introduction to Global Health Promotion. 2016:191.

26. Crompton P, Pierce S, Miller L. Advances and challenges in malaria vaccine development. J of Clin Investigat. 2010;120(12):4168-78.

27. Hemingway J, Shretta R, Wells TN, Bell D, Djimdé AA, Achee N, et al. Tools and Strategies for Malaria Control and Elimination: What Do We Need to Achieve a Grand Convergence in Malaria? PLoS Biology. 2016;14(3):e1002380.

28. Patarroyo ME, Amador R, Clavijo P, Moreno A, Guzman F, Romero P, et al. A synthetic vaccine protects humans against challenge with asexual blood stages of *Plasmodium falciparum* malaria. Nature. 1988;332(6160):158-61.
29. Miller LH, Howard RJ, Carter R, Good MF, Nussenzweig V, Nussenzweig RS. Research toward malaria vaccines. Science. 1986;234(4782):1349-56.
30. Harris H. Vaccines: a step change in malaria prevention? The Lancet. 2015;385(9978):1591-696.
31. Ballou WR, Arevalo-Herrera M, Carucci D, Richie TL, Corradin G, Diggs C, et al. Update on the clinical development of candidate malaria vaccines. The Ameri J of Trop Med and Hygien. 2004;71(2 Suppl):239-47.
32. Rts Clinical Trial Partnership. Efficacy and safety of RTS,S/AS01 malaria vaccine with or without a booster dose in infants and children in Africa: final results of a phase 3, individually randomised, controlled trial. Lancet. 2015;386(9988):31-45.
33. Epstein JE, Paolino KM, Richie TL, Sedegah M, Singer A, Ruben AJ, et al. Protection against Plasmodium falciparum malaria by PfSPZ Vaccine. JCI insight. 2017;2(1):e89154.
34. Le Bras J, Musset L, Clain J. [Antimalarial drug resistance]. Médecine et Maladies Infectieuses. 2006;36(8):401-5.
35. White N. Antimalarial drug resistance. J of Clin Investigat. 2004;113(8):1084.
36. Delfino R, Santos-Filho O, Figueroa-Villar J. Type 2 antifolates in the chemotherapy of falciparum malaria. J of the Brazilian Chem Society. 2002;13(6):727-41.
37. Terkuile F, White N, Holloway P, Pasvol G, Krishna S. Plasmodium falciparum: in vitro studies of the pharmacodynamic properties of drugs used for the treatment of severe malaria. Experiment Parasitolog. 1993;76(1):85-95.
38. Krishna S, Uhlemann A-C, Haynes R. Artemisinins: mechanisms of action and potential for resistance. Drug Resistance Updates. 2004;7(4):233-44.
39. Cui L, Su X-z. Discovery, mechanisms of action and combination therapy of artemisinin. Expert Rev of Anti-infective Therap. 2009;7(8):999-1013.
40. Winzeler E, Manary M. Drug resistance genomics of the antimalarial drug artemisinin. Genome Biolog. 2014;15(11):544.
41. Adams J, Kelso R, Cooley L. The kelch repeat superfamily of proteins: propellers of cell function. Trends in cell biolog. 2000;10(1):17-24.

42. Blumberg LH. Recommendations for the treatment and prevention of malaria: Update for the 2015 season in South Africa. South African Med J. 2015;105(3):175-8.
43. Burrows JN, Chibale K, Wells TN. The state of the art in anti-malarial drug discovery and development. Curr Top Med Chem. 2011;11(10):1226-54.
44. Wells TN, Hooft van Huijsduijnen R, Van Voorhis WC. Malaria medicines: a glass half full? Nat Rev Drug Discovery. 2015;14(6):424-42.
45. Burrows JN, Burlot E, Campo B, Cherbuin S, Jeanneret S, Leroy D, et al. Antimalarial drug discovery - the path towards eradication. Parasitolog. 2014;141(1):128-39.
46. Waksman SA. Humus. London: Bailliere, Tindall & Cox; 1938.
47. Rosenthal PJ. Antimalarial drug discovery: old and new approaches. J of Experiment Biolog. 2003;206(Pt 21):3735-44.
48. Peatey CL, Leroy D, Gardiner DL, Trenholme KR. Anti-malarial drugs: how effective are they against *Plasmodium falciparum* gametocytes? Malaria J. 2012;11:34.
49. Butterworth AS, Skinner-Adams TS, Gardiner DL, renholme KR. *Plasmodium falciparum* gametocytes: with a view to a kill. Parasitolog. 2013;140(14):1718-34.
50. Wells T, Alonso P, Gutteridge W. New medicines to improve control and contribute to the eradication of malaria. Nat Rev Drug Discovery. 2009;8(11):879-91.
51. Burrows J, Duparc S, Gutteridge W, van Huijsduijnen RH, Kaszubska W, Macintyre F, et al. New developments in anti-malarial target candidate and product profiles. Malaria J. 2017;16(1):26.
52. Swinney D. Phenotypic vs. target-based drug discovery for first-in-class medicines. Clin Pharmacol Ther. 2013;93(4):299-301.
53. Swinney D, Anthony J. How were new medicines discovered? Nat Rev Drug Discovery. 2011;10(7):507.
54. Sams-Dodd F. Target-based drug discovery: is something wrong? Drug discovery today. 2005;10(2):139-47.
55. Brown D. Unfinished business: target-based drug discovery. Drug Discovery Today. 2007;12(23):1007-12.
56. Lomize MA, Pogozheva ID, Joo H, Mosberg HI, Lomize AL. OPM database and PPM web server: resources for positioning of proteins in membranes. Nucleic Acids Research. 2012;40(D1):D370-D6.

57. Eder J, Sedrani R, Wiesmann C. The discovery of first-in-class drugs: origins and evolution. Nat Rev Drug Discovery. 2014;13(8):577.
58. Hughes J, Rees S, Kalindjian SB, Philpott K. Principles of early drug discovery. British J of Pharmacolog. 2011;162(6):1239-49.
59. G Wyatt P, H Gilbert I, D Read K, H Fairlamb A. Target validation: linking target and chemical properties to desired product profile. Current topics in med chem. 2011;11(10):1275-83.
60. Stickles A, Ting L-M, Morrisey J, Li Y, Mather M, Meermeier E, et al. Inhibition of Cytochrome bc1 as a Strategy for Single-Dose, Multi-Stage Antimalarial Therapy. The American J of Trop Med and Hyg. 2015;92(6):1195-201.
61. Goodman C, Buchanan H, McFadden G. Is the Mitochondrion a Good Malaria Drug Target? Trends in Parasitolog. 2016.
62. Korsinczky M, Chen N, Kotecka B, Saul A, Rieckmann K, Cheng Q. Mutations in Plasmodium falciparum Cytochrome b That Are Associated with Atovaquone Resistance Are Located at a Putative Drug-Binding Site. Antimicrobial Agents and Chemotherapy. 2000;44(8):2100-8.
63. Wallin IE. The mitochondria problem. The American Naturalist. 1923;57(650):255-61.
64. Cooper GM, Hausman RE. The cell: Sinauer Associates Sunderland; 2000.
65. Van Dooren G, Stimmler L, McFadden G. Metabolic maps and functions of the Plasmodium mitochondrion. FEMS Microbiology Reviews. 2006;30(4):596-630.
66. Voet D, Voet J, Pratt C. Principles of Biochemistry. 4th ed. WileyPlus2013. p. 596-600.
67. Painter H, Morrisey J, Mather M, Vaidya A. Specific role of mitochondrial electron transport in blood-stage Plasmodium falciparum. Nature. 2007;446(7131):88-91.
68. Crofts A, Lhee S, Crofts S, Cheng J, Rose S. Proton pumping in the bc1 complex: a new gating mechanism that prevents short circuits. Biochim Biophys Acta. 2006;1757(8):1019-34.
69. Moser CC, Farid TA, Chobot SE, Dutton PL. Electron tunneling chains of mitochondria. Biochimica et Biophysica Acta (BBA)-Bioenergetics. 2006;1757(9):1096-109.
70. Wikström M, Berden J. Oxidoreduction of cytochrome b in the presence of antimycin. Biochim et Biophys Acta (BBA)-Bioenergetics. 1972;283(3):403-20.

71. Berry E, Guergova-Kuras M, Huang L-s, Crofts A. Structure and function of cytochrome bc complexes. Ann Rev of Biochem. 2000;69(1):1005-75.
72. Hunte C, Palsdottir H, Trumpower B. Protonmotive pathways and mechanisms in the cytochrome bc 1 complex. FEBS Letters. 2003;545(1):39-46.
73. Biagini G, Viriyavejakul P, O'Neill P, Bray P, Ward S. Functional characterization and target validation of alternative complex I of Plasmodium falciparum mitochondria. Antimicrobial Agents and Chemotherapy. 2006;50(5):1841-51.
74. Gao X, Wen X, Esser L, Quinn B, Yu L, Yu C-A, et al. Structural basis for the quinone reduction in the bc 1 complex: a comparative analysis of crystal structures of mitochondrial cytochrome bc 1 with bound substrate and inhibitors at the Qi site. Biochemistry. 2003;42(30):9067-80.
75. Venditti P, Di Stefano L, Di Meo S. Mitochondrial metabolism of reactive oxygen species. Mitochondrion. 2013;13(2):71-82.
76. Di Rago J, Colson A. Molecular basis for resistance to antimycin and diuron, Q-cycle inhibitors acting at the Qi site in the mitochondrial ubiquinol-cytochrome c reductase in Saccharomyces cerevisiae. J of Biolog Chem. 1988;263(25):12564-70.
77. Trumpower B. A concerted, alternating sites mechanism of ubiquinol oxidation by the dimeric cytochrome bc 1 complex. Biochim et Biophys Acta (BBA)-Bioenergetics. 2002;1555(1):166-73.
78. Lodish H, Berk A, Zipursky SL, Matsudaira P, Baltimore D, Darnell J. Electron Transport and Oxidative Phosphorylation. 2000.
79. Herrmann JM, Riemer J. The intermembrane space of mitochondria. Antioxidants & redox signaling. 2010;13(9):1341-58.
80. Levin E, Johnson RM, Albert S. Mitochondrial changes associated with essential fatty acid deficiency in rats. J of Biolog Chem. 1957;228(1):15-21.
81. Gamo F-J, Sanz LM, Vidal J, de Cozar C, Alvarez E, Lavandera J-L, et al. Thousands of chemical starting points for antimalarial lead identification. Nature. 2010;465(7296):305-10.
82. Capper M, O'Neill P, Fisher N, Strange R, Moss D, Ward S, et al. Antimalarial 4 (1H)-pyridones bind to the Qi site of cytochrome bc1. Proceedings of the National Academy of Sciences. 2015;112(3):755-60.

83. Gregori-Puigjané E, Setola V, Hert J, Crews B, Irwin J, Lounkine E, et al. Identifying mechanism-of-action targets for drugs and probes. Proceedings of the National Academy of Sciences. 2012;109(28):11178-83.
84. Zorov D, Juhaszova M, Sollott S. Mitochondrial reactive oxygen species (ROS) and ROS-induced ROS release. Physiological Reviews. 2014;94(3):909-50.
85. Culotta VC, Yang M, O'Halloran T. Activation of superoxide dismutases: putting the metal to the pedal. Biochim et Biophys Acta (BBA)-Molecular Cell Research. 2006;1763(7):747-58.
86. Galaris D, Pantopoulos K. Oxidative stress and iron homeostasis: mechanistic and health aspects. Critical reviews in clinical laboratory sciences. 2008;45(1):1-23.
87. Liochev SI, Fridovich I. The Haber-Weiss cycle—70 years later: an alternative view. Redox Report. 2002;7(1):55-7.
88. Valko M, Rhodes C, Moncol J, Izakovic M, Mazur M. Free radicals, metals and antioxidants in oxidative stress-induced cancer. Chemico-biological interactions. 2006;160(1):1-40.
89. Adam-Vizi V. Production of reactive oxygen species in brain mitochondria: contribution by electron transport chain and non–electron transport chain sources. Antioxidants & redox signaling. 2005;7(9-10):1140-9.
90. Stickles AM, Smilkstein MJ, Morrisey JM, Li Y, Forquer IP, Kelly JX, et al. Atovaquone and ELQ-300 combination therapy as a novel dual-site cytochrome bc1 inhibition strategy for malaria. Antimicrobial Agents and Chemotherapy. 2016;60(8):4853-9.
91. Webb B, Sali A. Comparative protein structure modeling using Modeller. Curr prot in bioinform. 2014:5.6. 1-5.6. 32.
92. ACDLabs.com. Advanced Chemistry Development, Inc. ACD/Chemsketch 12.0 ed. Toronto, Canada2015.
93. OLBoyle NM, Banck M, James CA, Morley C, Vandermeersch T, Hutchison G. Open Babel: An open chemical toolbox. J of Cheminform. 2011;3:33.
94. Vainio MJ, Johnson MS. Generating conformer ensembles using a multiobjective genetic algorithm. The J of Chem Phys. 2007;47(6):2462-74.

95. Puranen JS, Vainio MJ, Johnson MS. Accurate conformation-dependent molecular electrostatic potentials for high-throughput in silico drug discovery. J of Computation Chem. 2010;31(8):1722-32.
96. Trott O, Olson AJ. AutoDock Vina: improving the speed and accuracy of docking with a new scoring function, efficient optimization, and multithreading. J of Computation Chem. 2010;31(2):455-61.
97. Pronk S, Páll S, Schulz R, Larsson P, Bjelkmar P, Apostolov R, et al. GROMACS 4.5: a high-throughput and highly parallel open source molecular simulation toolkit. Bioinformatics. 2013:btt055.
98. Lindorff-Larsen K, Piana S, Palmo K, Maragakis P, Klepeis JL, Dror RO, et al. Improved side-chain torsion potentials for the Amber ff99SB protein force field. Proteins: Structure, Function, and Bioinformatics. 2010;78(8):1950-8.
99. Jämbeck JP, Lyubartsev AP. An extension and further validation of an all-atomistic force field for biological membranes. J of Chem Theory and Computat. 2012;8(8):2938-48.
100. Nickolls J, Buck I, Garland M, Skadron K. Scalable parallel programming with CUDA. Queue. 2008;6(2):40-53.
101. da Silva AWS, Vranken W. ACPYPE-Antechamber python parser interface. BioMed Central Research Notes. 2012;5(1):367.
102. Jämbeck JP, Lyubartsev AP. Update to the General Amber Force Field for small solutes with an emphasis on free energies of hydration. The J of Phys Chem B. 2014;118(14):3793-804.
103. Kumari R, Kumar R, Lynn A. g_mmpbsa□ A GROMACS Tool for High-Throughput MM-PBSA Calculations. J of Chem Information and Modeling. 2014;54(7):1951-62.
104. Wang R, Lai L, Wang S. Further development and validation of empirical scoring functions for structure-based binding affinity prediction. Journal of Computer-Aided Molecular Design. 2002;16(1):11-26.
105. Guex N, Peitsch MC, Schwede T. Automated comparative protein structure modeling with SWISS-MODEL and Swiss-PdbViewer: A historical perspective. Electrophoresis. 2009;30(S1).

106. Arnold K, Bordoli L, Kopp J, Schwede T. The SWISS-MODEL workspace: a web-based environment for protein structure homology modelling. Bioinformatics. 2006;22(2):195-201.
107. Oda A, Yamaotsu N, Hirono S. New AMBER force field parameters of heme iron for cytochrome P450s determined by quantum chemical calculations of simplified models. J of Computation Chem. 2005;26(8):818-26.
108. Berendsen H, Postma J, van Gunsteren W, DiNola A, Haak J. Mole dynam with coupling to an external bath. The J of Chem Phys. 1984;81(8):3684-90.
109. Nosé S, Klein M. Constant pressure molecular dynamics for molecular systems. Molecular Physics. 1983;50(5):1055-76.
110. Darden T, York D, Pedersen L. Particle mesh Ewald: An N· log (N) method for Ewald sums in large systems. The J of Chem Phys. 1993;98(12):10089-92.
111. Hess B. P-LINCS: A parallel linear constraint solver for molecular simulation. J of Chem Theory and Computation. 2008;4(1):116-22.
112. Ljungström I, Moll K, Perlmann H, Scherf A, Wahlgren M. Methods in malaria research: MR4/ATCC; 2008.
113. Cranmer S, Magowan C, Liang J, Coppel R, Cooke B. An alternative to serum for cultivation of Plasmodium falciparum in vitro. Transactions of the royal society of tropical medicine and hygiene. 1997;91(3):363-5.
114. Trager W, Jensen JB. Human malaria parasites in continuous culture. J of Parasitolog. 2005;91(3):484-6.
115. Trager W, Jensen JB. Human malaria parasites in continuous culture. Science. 1976;193(4254):673-5.
116. Lambros C, Vanderberg J. Synchronization of Plasmodium falciparum erythrocytic stages in culture. The J of Parasitolog. 1979:418-20.
117. Moll K, Ljungström I, Perlmann H, Scherf A, Wahlgren M. Methods in malaria research. Manassas, VA. 2008.
118. Smilkstein M, Sriwilaijaroen N, Kelly JX, Wilairat P, Riscoe M. Simple and inexpensive fluorescence-based technique for high-throughput antimalarial drug screening. Antimicrob Agents and Chemo. 2004;48(5):1803-6.

119. Niemand J, Burger P, Verlinden BK, Reader J, Joubert AM, Kaiser A, et al. Anthracene-polyamine conjugates inhibit in vitro proliferation of intraerythrocytic Plasmodium falciparum parasites. Antimicro Agents and Chemo. 2013:AAC. 00106-13.
120. Fidock DA, Rosenthal PJ, Croft SL, Brun R, Nwaka S. Antimalarial drug discovery: efficacy models for compound screening. Nat Rev Drug Discovery. 2004;3(6):509-20.
121. Vichai V, Kirtikara K. Sulforhodamine B colorimetric assay for cytotoxicity screening. Nat Protoc. 2006;1(3):1112-6.
122. Voigt W. Sulforhodamine B assay and chemosensitivity. Chemosensitivity: Springer; 2005. p. 39-48.
123. Le Manach C, Scheurer C, Sax S, Schleiferböck S, Cabrera D, Younis Y, et al. Fast in vitro methods to determine the speed of action and the stage-specificity of anti-malarials in Plasmodium falciparum. Malaria J. 2013;12(1):424.
124. Carter R, Ranford-Cartwright L, Alano P. The culture and preparation of gametocytes of Plasmodium falciparum for immunochemical, molecular, and mosquito infectivity studies. Protocols in Molecular Parasitolog. 1993:67-88.
125. Reader J, Botha M, Theron A, Lauterbach SB, Rossouw C, Engelbrecht D, et al. Nowhere to hide: interrogating different metabolic parameters of *Plasmodium falciparum* gametocytes in a transmission blocking drug discovery pipeline towards malaria elimination. Malaria J. 2015;14:213.
126. Christophers S, Fulton J. Experiments with isolated malaria parasites (Plasmodium knowlesi) free from red cells. Annals of Trop Med & Parasitolog. 1939;33(2):161-70.
127. Jungery M, Pasvol G, Newbold C, Weatherall D. A lectin-like receptor is involved in invasion of erythrocytes by Plasmodium falciparum. Proceedings of the National Academy of Sciences. 1983;80(4):1018-22.
128. Verlinden B, De Beer M, Pachaiyappan B, Besaans E, Andayi W, Reader J, et al. Interrogating alkyl and arylalkylpolyamino (bis) urea and (bis) thiourea isosteres as potent antimalarial chemotypes against multiple lifecycle forms of Plasmodium falciparum parasites. Bioorganic & Med Chem 2015;23(16):5131-43.
129. Bickerton G, Paolini G, Besnard J, Muresan S, Hopkins A. Quantifying the chemical beauty of drugs. Nat Chem. 2012;4(2):90-8.

130. Aparoy P, Kumar Reddy K, Reddanna P. Structure and ligand based drug design strategies in the development of novel 5-LOX inhibitors. Curr med chem. 2012;19(22):3763-78.
131. Costanzi S. Homology modeling of class ag protein-coupled receptors. Homology Modeling: Methods and Protocols. 2012:259-79.
132. Leeson P. Drug discovery: Chemical beauty contest. Nature. 2012;481(7382):455-6.
133. Benfenati E. Quantitative Structure-Activity Relationships (QSAR) for pesticide regulatory purposes: Elsevier; 2011.
134. Lipinski CA, Lombardo F, Dominy BW, Feeney PJ. Experimental and computational approaches to estimate solubility and permeability in drug discovery and development settings1. Advan Drug Delivery Rev. 2001;46(1-3):3-26.
135. Fivelman QL, McRobert L, Sharp S, Taylor CJ, Saeed M, Swales CA, et al. Improved synchronous production of *Plasmodium falciparum* gametocytes *in vitro*. Mol and Biochem Parasitolog. 2007;154(1):119-23.
136. Delves M, Plouffe D, Scheurer C, Meister S, Wittlin S, Winzeler E, et al. The activities of current antimalarial drugs on the life cycle stages of Plasmodium: a comparative study with human and rodent parasites. PLoS Medicine. 2012;9(2):e1001169.
137. Verlinden B, Niemand J, Snyman J, Sharma S, Beattie R, Woster P, et al. Discovery of novel alkylated (bis) urea and (bis) thiourea polyamine analogues with potent antimalarial activities. J of Med Chem. 2011;54(19):6624-33.
138. Bussi G, Donadio D, Parrinello M. Canonical sampling through velocity rescaling. The J of Chem Phys. 2007;126(1):014101.
139. Sanz L, Crespo B, De-Cózar C, Ding X, Llergo J, Burrows J, et al. P. falciparum in vitro killing rates allow to discriminate between different antimalarial mode-of-action. PloS One. 2012;7(2):e30949.
140. Beteck R, Smit F, Haynes R, D N'Da D. Recent progress in the development of anti-malarial quinolones. Malaria J. 2014;13(1):339.
141. Beteck R, Coertzen D, Smit F, Birkholtz L-M, Haynes R, N'Da D. Straightforward conversion of decoquinate into inexpensive tractable new derivatives with significant antimalarial activities. Bioorgan & Med Chem Lett. 2016;26(13):3006-9.

142. Morgan KF, Hollingsworth IA, Bull JA. Studies on the synthesis, stability and conformation of 2-sulfonyl-oxetane fragments. Organ & Biomol Chem. 2015;13(18):5265-72.
143. Silipo C, Vittoria A. Principles and Usage of Steric Parameters in Correlation Analysis of Pesticides: CRC Press: Boca Raton Florida; 1992.
144. Wilcken R, Zimmermann MO, Lange A, Joerger AC, Boeckler FM. Principles and applications of halogen bonding in medicinal chemistry and chemical biology. J of Med Chem. 2013;56(4):1363-88.
145. Vugmeyster Y, Xu X, Theil F-P, Khawli LA, Leach MW. Pharmacokinetics and toxicology of therapeutic proteins: advances and challenges. World J of Biolog Chem. 2012;3(4):73.
146. Arnott JA, Planey SL. The influence of lipophilicity in drug discovery and design. Expert Opinion on Drug Discovery. 2012;7(10):863-75.
147. Di L, Fish PV, Mano T. Bridging solubility between drug discovery and development. Drug Discovery Today. 2012;17(9):486-95.
148. Hein CD, Liu X-M, Wang D. Click chemistry, a powerful tool for pharmaceutical sciences. Pharmaceutical Research. 2008;25(10):2216-30.
149. Barnard B. Inhibition of lysine-specific demethylase 1 as an antimalarial target by polyamine analogues 2015.
150. Biamonte MA, Wanner J, Le Roch KG. Recent advances in malaria drug discovery. Bioorgan & Med Chem Lett. 2013;23(10):2829-43.
151. Hombhanje FW, Huang Q. Artemisinin-naphthoquine combination (ARCO®): an overview of the progress. Pharmaceuticals. 2010;3(12):3581-93.
152. Burrows JN, van Huijsduijnen RH, Möhrle JJ, Oeuvray C, Wells T. Designing the next generation of medicines for malaria control and eradication. Malaria J. 2013;12(187):10.1186.
153. Martinelli A, Moreira R, Cravo P. Malaria combination therapies: advantages and shortcomings. Mini Rev in Med Chem. 2008;8(3):201-12.
154. Beers MH, Berkow R. The merck manual. Merck Research Laboratories. 1999;17.
155. Verlinden B, Louw A, Birkholtz L-M. Resisting resistance: is there a solution for malaria? Expert Opinion on Drug Discovery. 2016;11(4):395-406.

156. Sanders C. Mechanisms responsible for cross-resistance and dichotomous resistance among the quinolones. Clin Infect Diseases. 2001;32(Supplement_1):S1-S8.

Appendix I: Ethics approval letter

The Research Ethics Committee, Faculty Health Sciences, University of Pretoria complies with ICH-GCP guidelines and has US Federal wide Assurance.
- FWA 00002567, Approved dd 22 May 2002 and Expires 28 August 2018.
- IRB 0000 2235 IORG0001762 Approved dd 22/04/2014 and Expires 22/04/2017.

UNIVERSITEIT VAN PRETORIA
UNIVERSITY OF PRETORIA
YUNIBESITHI YA PRETORIA

Faculty of Health Sciences Research Ethics Committee

9/11/2016

Approval Certificate
New Application

Ethics Reference No.: 383/2016

Title: Assessing the in vitro efficacy of in silico designed compounds targeting the malarial Qi site of cytochrome bc1

Dear Miss Laura Damadeu Kouemo

The **New Application** as supported by documents specified in your cover letter dated 24/10/2016 for your research received on the 24/10/2016, was approved by the Faculty of Health Sciences Research Ethics Committee on its quorate meeting of 23/11/2016.

Please note the following about your ethics approval:
- Ethics Approval is valid for 1 year
- Please remember to use your protocol number (**383/2016**) on any documents or correspondence with the Research Ethics Committee regarding your research.
- Please note that the Research Ethics Committee may ask further questions, seek additional information, require further modification, or monitor the conduct of your research.

Ethics approval is subject to the following:
- The ethics approval is conditional on the receipt of **6 monthly written Progress Reports**, and
- The ethics approval is conditional on the research being conducted as stipulated by the details of all documents submitted to the Committee. In the event that a further need arises to change who the investigators are, the methods or any other aspect, such changes must be submitted as an Amendment for approval by the Committee.

We wish you the best with your research.

Yours sincerely

Dr R Sommers; MBChB; MMed (Int); MPharMed,PhD
Deputy Chairperson of the Faculty of Health Sciences Research Ethics Committee, University of Pretoria

The Faculty of Health Sciences Research Ethics Committee complies with the SA National Act 61 of 2003 as it pertains to health research and the United States Code of Federal Regulations Title 45 and 46. This committee abides by the ethical norms and principles for research, established by the Declaration of Helsinki, the South African Medical Research Council Guidelines as well as the Guidelines for Ethical Research: Principles Structures and Processes, Second Edition 2015 (Department of Health).

012 356 3084 deepeka.behari@up.ac.za / fhsethics@up.ac.za http://www.up.ac.za/healthethics
Private Bag X323, Arcadia, 0007 - Tswelopele Building, Level 4, Room 60, Gezina, Pretoria

Appendix II: Ethics approval extension letter

UNIVERSITEIT VAN PRETORIA
UNIVERSITY OF PRETORIA
YUNIBESITHI YA PRETORIA

Faculty of Health Sciences Research Ethics Committee

29/03/2018

Miss Laura Damadeu Kouemo
Department of Pharmacology
University of Pretoria

Dear Miss Laura Damadeu Kouemo

RE.: 383/2016 – Letter dated 5 March 2018

383/2016 Damadeu Kouemo	
Protocol Title	Assessing the in vitro efficacy of in silico designed compounds targeting the malarial Qi site of cytochrome bc1
Principal Investigator	Miss Laura Damadeu Kouemo Tel: 073 124 2792 Email: lauradamadeu@yahoo.com Dept: Pharmacology

We hereby acknowledge receipt of the following document:

- Extension of study until the end of December 2020

which has been approved at 28 March 2018 meeting.

With regards

Dr R Sommers; MBChB, MMed (Int), MPharMed, PhD
Deputy Chairperson of the Faculty of Health Sciences Research Ethics Committee, University of Pretoria

☎ 012 356 3085 ✉ fhsethics.up.ac.za 🌐 http://www.up.ac.za/healthethics
✉ Private Bag X323, Arcadia, 0007 - Tswelopele Building, Level 4-59, Gezina, Pretoria